Dissertation

Origin of Measured Plasma Cardiac Troponin T in Skeletal Muscle Disease

submitted by

Dr.med.univ.

Johannes SCHMID

for the academic degree of

Doctor of Medical Science

(Dr.scient.med.)

at the

Medical University of Graz

Department of Internal Medicine, Division of Cardiology

under the supervision of

Assoz.Prof. Priv.Doz. Dr.med.univ. Dr.med.sci. Peter RAINER

2020

Declaration

I hereby declare that this thesis is my own original work and that I have fully acknowledged by name all of those individuals and organisations that have contributed to the research for this thesis. Due acknowledgement has been made in the text to all other material used. The main results of this thesis have been previously published, inherent similarities to these publications may occur.
Throughout this thesis and in all related publications I followed the "Standards of Good Scientific Practice and Ombuds Committee at the Medical University of Graz".

Graz, 02.06.2020 *Johannes Schmid e.h.*

DISCLOSURES

Part of this thesis has been published here:

Schmid J, Beer M, Berghold A, Stojakovic T, Scharnagl H, Dieplinger B, Quasthoff S, Binder JS, Rainer PP. Cardiac involvement in a cross-sectional cohort of myotonic dystrophies and other skeletal myopathies. ESC Heart Fail. 2020; (accepted manuscript)

Schmid J, Liesinger L, Birner-Gruenberger R, Stojakovic T, Scharnagl H, Dieplinger B, Asslaber M, Radl R, Beer M, Polacin M, Mair J, Szolar D, Berghold A, Quasthoff S, Binder JS, Rainer PP. Elevated Cardiac Troponin T in Patients With Skeletal Myopathies. J Am Coll Cardiol. 2018; 71(14): 1540-1549.

Schmid J, Kaufmann R, Grübler MR, Verheyen N, Weidemann F, Binder JS. Strain Analysis by Tissue Doppler Imaging: Comparison of Conventional Manual Measurement with a Semiautomated Approach. Echocardiography. 2016; 33(3):372-378.

List of other publications resulting from the thesis project:

Letters:

Schmid J, Birner-Grünberger R, Quasthoff S, Binder JS, Rainer PP. Reply: Elevated Cardiac Troponin T in Skeletal Myopathies: Skeletal TnT Cross-Reactivity and/or Cardiac TnT Expression? J Am Coll Cardiol. 2018; 72(3): 349-350.

Posters:

Schmid J, Birner-Gruenberger R, Liesinger L, Stojakovic T, Scharnagl H, Dieplinger B, Asslaber M, Quasthoff S, Binder JS, Rainer PP. Elevated measured cardiac troponin T in skeletal myopathies - Re-expression in skeletal muscle or assay cross-reaction? Frontiers in CardioVascular Biology; Apr 20-22, 2018; Vienna, Austria.

Schmid J, Birner-Gruenberger R, Liesinger L, Stojakovic T, Scharnagl H, Dieplinger B, Asslaber M, Radl R, Polacin M, Beer M, Szolar D, Quasthoff S, Binder JS, Rainer P. Elevated cardiac troponin T but not troponin I in patients with skeletal muscle disease.

European Heart Journal, Vol 38, Issue suppl 1, 1 Aug 2017, ehx502.P2612; ESC Congress; Aug 26-30, 2017; Barcelona, Spain.

Schmid J, Polacin M, Sagmeister F, Quasthoff S, Binder JS, Beer M. Altered cardiac function and ECG in patients with myotonic dystrophies. DOI: 10.1594/ecr2017/C-1281; ECR; March 1-5, 2017; Vienna, Austria.

Schmid J, Polacin M, Sagmeister F, Maderthaner R, Quasthoff S, Binder JS, Beer M. Changes in cardiac function and ECG in patients with myotonic dystrophies. 8. Deutsche Kardiodiagnostiktage 2016; Feb 18-20, 2016; Leipzig, Germany.

Schmid J, Kaufmann R, Grübler MR, Verheyen N, Weidemann F, Binder JS. Strain analysis by tissue doppler imaging: comparison of conventional manual measurement with a semi-automated approach. Eur Heart J Cardiovasc Imaging. 2015; 16(suppl2):S4-S11; EuroEcho-Imaging; Dec 2-5, 2015; Sevilla, Spain.

Schmid J, Kaufmann R, Grübler MR, Gaksch M, Verheyen N, Stojakovic T, Windpassinger C, Pilz S, Binder JS, Quasthoff S. Cardiac troponin T correlates with creatine kinase in patients with hereditary myopathies. Eur Heart J Acute Cardiovasc Care. 2014; 3(2):170-171; ACCA Congress; Oct 18-20, 2014; Geneva, Switzerland.

Original articles published during the doctoral program not related to the thesis project:

Schmid J, Stojakovic T, Zweiker D, Scharnagl H, Maderthaner RD, Scherr D, Maier R, Schmidt A, März W, Binder JS, Rainer PP. ST2 predicts survival in patients undergoing transcatheter aortic valve implantation. Int J Cardiol. 2017;244:87-92.

List of co-authors who actively contributed to the thesis and the publications resulting from the thesis project:

Peter P. Rainer (Medical University of Graz)

Josepha S. Binder (Medical University of Graz)

Laura Liesinger (Medical University of Graz)

Ruth Birner-Grünberger (Medical University of Graz)

Tatjana Stojakovic (Medical University of Graz)

Hubert Scharnagl (Medical University of Graz)

Stefan Quasthoff (Medical University of Graz)

Dieter Szolar (Medical University of Graz; Diagnostikum Graz Süd-West)

Andrea Berghold (Medical University of Graz)

Martin Asslaber (Medical University of Graz)

Benjamin Dieplinger (Konventhospital Barmherzige Brüder Linz)

Roman Radl (Medical University of Graz)

Meinrad Beer (University Hospital Ulm, Germany)

Malgorzata Polacin (University Hospital Ulm, Germany)

Johannes Mair (Medical University of Innsbruck)

Permission statements:

All authors have explicitly agreed to the use of their data in this thesis.

ACKNOWLEDGEMENTS

The present thesis is the result of the joint efforts of a number of people, whose contributions made this project possible.

First, I thank my supervisor Josepha Binder who initiated this study, organised the funding and performed echocardiography. She has energetically supported me in every respect throughout my work. I particularly thank Peter Rainer who took over supervision and who considerably contributed to the study success with his invaluable scientific experience and expertise. He ensured a high quality of the study and resulting publications.

I want to express my gratitude to Ruth Birner-Grünberger and Laura Liesinger for performing the crucial western blot and mass spectrometry experiments in a very positive and cooperative collaboration. I thank Stefan Quasthoff who was involved in study planning and patient recruitment and who shared his expertise on neuromuscular disorders. I am grateful for the contributions of Tatjana Stojakovic, Hubert Scharnagl and their team who carried out most laboratory measurements, and of Benjamin Dieplinger who kindly performed cardiac Troponin I measurements. Martin Asslaber and Johannes Mair provided tissue samples, Roman Radl performed skeletal muscle biopsies and Andrea Berghold advised in ethical and statistical matters. Meinrad Beer and Malgorzata Polacin analysed cardiac magnetic resonance images acquired by Dieter Szolar and his team who also performed cardiac computed tomography.

This study was funded by a generous research grant from Roche Diagnostics, that also kindly provided cardiac Troponin T and I antibodies.

The thesis was conducted at the Doctoral School for Translational Molecular and Cellular Biosciences.

Finally, I thank all patients that willingly participated in the study.

TABLE OF CONTENTS

ABBREVIATIONS

ALS	Amyotrophic lateral sclerosis
BLAST	Basic Local Alignment Search Tool
BMD	Becker muscular dystrophy
BMI	body mass index
Ca^{2+}	calcium
cCT	cardiac computed tomography
CK	creatine kinase
CK-MB	creatine kinase-muscle/brain
cMR	cardiac magnetic resonance imaging
cTnI	cardiac Troponin I
cTnT	cardiac Troponin T
CV	coefficient of variation
DM	myotonic dystrophy
DM1	myotonic dystrophy type 1
DM2	myotonic dystrophy type 2
DMD	Duchenne muscular dystrophy
ECG	electrocardiogram
EDV	end-diastolic volume
EF	ejection fraction
ESC	European society of cardiology
FSHD	facioscapulohumeral muscular dystrophy
fTnT	fast skeletal Troponin T
GLS	global longitudinal strain
IBM	Inclusion body myopathy
IQR	interquartile range
LAVi	left atrial volume index
LBBB	left bundle branch block
LC-MS/MS	liquid chromatography coupled to tandem mass spectrometry
LGE	late gadolinium enhancement

LGMD	limb girdle muscular dystrophy
LoB	limit of blank
LoD	lower limit of detection
LoQ	limit of quantitation
LV	left ventricle
LVMi	left ventricular mass index
MCTD	Mixed connective tissue disease
MRI	magnetic resonance imaging
NT-proBNP	N-terminal pro brain natriuretic peptide
RBBB	right bundle branch block
SBMA	Spinobulbar muscular atrophy
SD	standard deviation
SDS	sodium dodecyl sulfate
SMA	Spinal muscular atrophy
sTnT	slow skeletal Troponin T
TAPSE	tricuspid annular plane systolic excursion
TBS-T	Tris-buffered saline with Tween 20
TDI	tissue doppler imaging
Tn	Troponin
TnC	Troponin C
TnI	Troponin I
TnT	Troponin T
URL	upper reference limit
XMPMA	X-linked myopathy with postural muscle atrophy

ABSTRACT IN GERMAN

Kardiales Troponin T (cTnT) ist ein zentraler Laborparameter zur Diagnose eines Herzinfarkts. Bei Patienten mit Skelettmuskelerkrankungen ist cTnT häufig erhöht, was oft weitere, teils invasive Abklärung nach sich zieht. Es herrscht Unklarheit über den Ursprung des gemessenen cTnTs bei diesen Patienten. In der vorliegenden Studie soll zum einen die Prävalenz erhöhten cTnTs bestimmt werden, zum anderen mögliche Ursachen für diese Erhöhung untersucht werden, wie etwa kardiale Beteiligung im Rahmen der Myopathie, Re-Expression in erkranktem Skelettmuskel oder eine Kreuzreaktion mit Skelettmuskel-Proteinen. Dazu wurde eine prospektive Kohorte von 74 Patienten mit verschiedenen hereditären und erworbenen Skelettmuskelerkrankungen untersucht. Blutabnahmen wurden nach 3 Stunden und nach einem Jahr wiederholt und neben cTnT auch kardiales Troponin I (cTnI), beide mit sogenannten high-sensitive Assays, sowie Creatin-Kinase (CK) und Myoglobin bestimmt. Die Patienten wurden außerdem mit 12-Kanal- und 24-Stunden-EKG, 24-Stunden-Blutdruckmessung, Echokardiographie, kardialer Magnetresonanztomographie und computertomographischer Koronarangiographie untersucht. cTnT (Median 24,0 [11,0-247,0] ng/L) war bei 69% der Patienten erhöht, während cTnI (3,6 [2,4-22,1] ng/L) bei 4% erhöht war. Im Gegensatz zu cTnI korrelierte cTnT mit CK und Myoglobin ($r=0,679$, $p<0,001$; $r=0,786$, $p<0,001$). Ein schwacher Zusammenhang ($p=0.025$) bestand auch zwischen cTnT und dem Vorliegen von kardialen Auffälligkeiten (22,9%). Für Western-Blots von gesunden und erkrankten Skelettmuskelproben und Kontrollgewebe wurden die in den kommerziellen Immunoassays verwendeten Antikörper verwendet. Die cTnT-Antikörper detektierten Banden in gesundem und erkranktem Skelettmuskel, die mit skelettalen TnT Isoformen vereinbar sind. Diese wurden auch in der Flüssigkeitschromatographie-Tandem-Massenspektroskopie dieser Banden nachgewiesen. cTnT-Messungen in mit Skelettmuskel-Homogenaten versetztem Plasma ergaben erhöhte cTnT-Werte bei hohen Skelettmuskel-Konzentrationen. Die Kreuzreaktion mit rekombinantem slow TnT betrug 0,02%. Die Ergebnisse dieser Studie bestätigen die Berichte häufiger cTnT-Erhöhungen bei Patienten mit Skelettmuskelerkrankungen, was bei cTnI nicht beobachtet wird. Der Grund für diese Erhöhung scheint eine Kreuzreaktion mit skelettalen TnT-Isoformen zu sein, die bei Skelettmuskelerkrankungen in hohen Konzentrationen im Blut auftreten.

ABSTRACT IN ENGLISH

Cardiac Troponin T (cTnT) is a pivotal laboratory test for the diagnosis of acute myocardial infarction. In patients with skeletal muscle diseases cTnT is frequently elevated, which may result in further, often invasive, diagnostic workup to exclude myocardial infarction. The origin of measured cTnT in these patients remains unclear. This study systematically evaluated the prevalence of cTnT elevation in skeletal myopathies and explored possible causes, such as cardiac involvement in myopathy, re-expression in diseased skeletal muscle or cross-reaction.

A cohort of 74 patients with different hereditary and acquired skeletal muscle diseases was prospectively enrolled. Patients underwent blood-sampling at baseline, 3 hours and 1 year with determination of cTnT, cardiac Troponin I (cTnI), both with high sensitive assays, CK and Myoglobin. 12-lead and 24-hour ECG, ambulatory blood pressure monitoring, echocardiography, cardiac magnetic resonance imaging, and if at increased risk for coronary artery disease computed tomography coronary angiography were performed. cTnT (median 24.0 [11.0-247.0] ng/L) was elevated in 69%, while cTnI (3.6 [2.4-22.1] ng/L) was elevated in 4% of patients. cTnT correlated with markers of skeletal muscle damage CK and Myogloben ($r=0.679$, $p<0.001$; $r=0.786$, $p<0.001$), while cTnI did not. There was a weak association of cTnT levels ($p=0.025$) with the presence of cardiac abnormalities (22.9%).

Western blots with healthy and diseased skeletal muscle and control tissue was performed applying the capture and detection antibodies of the commercial immunoassays. Both cTnT antibodies detected bands in healthy and diseased skeletal muscle that are compatible with skeletal TnT isoforms, which were also identified in the spectra of additional liquid-chromatography-tandem-mass-spectrometry of these bands. cTnT measurements in plasma with added skeletal muscle homogenates resulted in elevated measurement at high input concentrations. Cross-reaction with recombinant slow TnT was 0.02%.

Our results confirm reports of frequent cTnT elevation in skeletal muscle diseases, which is not observed in cTnI. This seems to be caused by a small cross-reaction of the cTnT assay with skeletal TnT isoforms that are abundant in serum of patients with skeletal myopathies.

1 INTRODUCTION

In cardiac and skeletal muscle sarcomere the Troponin (Tn) complex is pivotally involved in the regulation of actin myosin interaction. It is bound to tropomyosin on the actin filament and consists of the three subunits TnT, TnI and TnC. While TnI inhibits actin myosin cross-bridging, TnT binds the complex to tropomyosin and TnC interacts with cytosolic Ca^{2+}. Ca^{2+}-binding leads to conformational changes of the complex and allows actin myosin interaction.[1,2] Thus the Tn complex links excitation induced sarcoplasmatic Ca^{2+}-influx to activation of actin myosin cross-bridge cycling and muscle contraction (**Figure 1**).

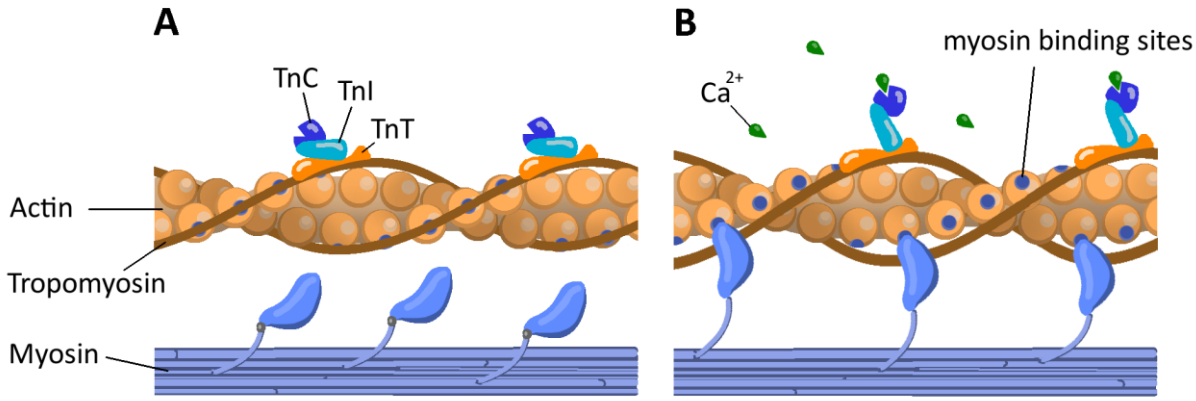

Figure 1: Schematic illustration of Ca^{2+} mediated regulation of actin myosin interaction via the Troponin complex during relaxation (**A**) and contraction (**B**). (Image created based on Fig.1 in Streng et al. [3])

To serve the different physiologic demands of the various types of muscle tissues, there are distinct cardiac and skeletal isoforms of TnT and TnI (i.e. cardiac, slow skeletal and fast skeletal TnT and TnI), which make these proteins excellent candidates for tissue-specific biomarkers. TnC does not exhibit these tissue specific isoforms.

Cardiac TnT (cTnT) (canonical isoform 1) consists of 298 amino acids and has a molecular weight of 36 kDa. Alternative splicing results in 12 known isoforms, of which isoform 6 predominates in adult heart, whereas isoforms 1, 7 and 8 are expressed in fetal heart. Numerous point mutations (approx. 24) have been described to be associated with hypertrophic or dilated cardiomyopathy.[4] Cardiac TnI (cTnI) is a 210 amino acid protein

with a molecular weight of 24 kDa. Similar to cTnT, mutations in cTnI cause different types of cardiomyopathies.[5]

Since measurement of cardiac Troponins (cTn) has entered clinical use in the 1990s they have evolved into a biochemical gold standard for the diagnosis of myocardial injury and necrosis. While in the past the diagnosis of myocardial infarction has been a question of equally combining the findings from electrocardiogram (ECG), clinical symptoms and unspecific cardiac enzymes, the advance of new, highly specific biomarkers for myocardial damage required a new and more precise definition of myocardial infarction. From the first redefinition in 2000[6] until the fourth universal definition of myocardial infarction in 2018[7] cTn assays increasingly form the cornerstone for the diagnosis of myocardial infarction. The current definition of acute myocardial infarction requires an elevation in serum cTn (above the 99th percentile of a healthy reference population) with a rise or fall pattern in combination with clinical symptoms, ECG findings or imaging evidence suggestive of myocardial infarction. Therefore, high sensitivity and specificity of these cTn assays are essential.

cTnT assays are produced solely by Roche Diagnostics due to patent rights, whereas cTnI assays are available from a number of different manufacturers. The first generation cTnT assay suffered from specificity problems especially in patients with renal failure or skeletal muscle diseases.[8–10] This was thought to be caused by insufficient specificity of the assay's capture antibody, which detected both the cardiac isoform and some fetal skeletal muscle TnT isoforms re-expressed in skeletal muscle in response to injury.[11] However, further development and better antibody specificity led to improved cTnT assays. The antibodies used in the cTnT assays since 1997 were shown to have a high specificity for cTnT[12], and several experimental studies concluded that cTnT had unique cardiac specificity that was equal to that of cTnI.[13,14] Conversely, some authors still questioned cTnT assay specificity even in the fourth generation assay.[15] A high precision of cTn tests is essential to confidently diagnose myocardial infarction and in 2007 the Joint ESC/ACCF/AHA/WHF Task Force for the Redefinition of Myocardial Infarction recommended a coefficient of variation (CV) of < 10% at the 99th percentile upper reference limit (URL) of cTn assays.[16] However, at that time no commercially available

assay actually met this criterion. Roche Diagnostics were the first to comply with this requirement with the introduction of their 5th generation so-called high sensitivity cTnT assay, which was a modification of the 4th generation assay.[17] Recently, other companies followed by introducing high sensitivity cTnI assays. Higher sensitivity, however, generally goes along with a decline in specificity and again concerns about the cardiac specificity of cTnT arose, especially in patients with skeletal muscle diseases.[18]

Several, mostly anecdotical reports on elevated cTnT measured with different assay generations in patients with different types of skeletal myopathies accumulated over the last decades.[19–28] The interpretation of elevated cTnT in skeletal muscle diseases is often challenging and in many cases elevated cTnT in combination with unclear clinical findings may necessitate further, sometimes invasive diagnostic workup in order to rule out acute myocardial injury.

Concerning the origin of elevated cTnT levels in patients with skeletal myopathies, two main hypotheses are conceivable. One explanation could be that cardiac manifestations of a systemic myopathy lead to subtle myocardial injury and thereby cause cTnT elevation, meaning that in this case cTnT plasma levels truly reflect myocardial damage in these patients. Alternatively, the cTnT assay might not detect cTnT derived from the myocardium but cTnT or a cross-reacting isoform that is (re-)expressed in diseased skeletal muscle. Whereas expression of the cardiac isoform would in principle conform with the cTnT assay's claimed high analytical accuracy, the presence of a cross-reacting isoform would mean false positive cTnT measurements and would fundamentally question the cardiac specificity of the assay. Although clarification of the origin of measured cTnT would have major implications on the interpretation of cTnT results and patient management, after almost two decades of scientific debate the causative mechanism behind cTnT elevations in skeletal myopathies is still unclear.

Binder et al. have described cardiac involvement in patients with mutations in the four-and-a-half-LIM-domain (FHL-1) gene, which causes X-linked myopathy with postural muscle atrophy (XMPMA) and found - besides a new form of spongious cardiomyopathy -

markedly raised cTnT levels using a fourth generation cTnT assay.[29] This finding triggered our study group's interest in the role of cTnT in skeletal muscle disease.

To elucidate the origin of elevated measured cTnT in skeletal muscle disease, we aimed to compare cTnT with cTnI levels in a range of different myopathies and to correlate cTn with cardiac abnormalities and with markers of skeletal muscle damage. Additionally, we thoroughly examined diseased skeletal muscle tissue with respect to the presence of cTnT or cross-reacting proteins.

2 METHODS

Patients with hereditary or acquired skeletal muscle diseases were asked to participate in this observational cohort study. In a baseline visit patients underwent a comprehensive cardiac examination, including blood sampling, electrocardiogram (ECG), 24-hour-ECG (24hECG), 24-hour ambulatory blood pressure monitoring (ABPM), echocardiography including strain analyses and cardiac magnetic resonance (cMR) with late gadolinium enhancement (LGE). After one year, blood sampling was repeated in a follow-up visit. Eligible patients were asked to undergo a skeletal muscle biopsy. Tissue samples were then analysed in vitro to detect and identify proteins reactive with cTnT and cTnI antibodies.

The study was approved by the ethics committee of the Medical University in Graz (26-282 ex 13/14) and conformed with all pertaining regulations and the principles of the declaration of Helsiniki.[30]

2.1 Patient population

92 patients of both sexes with the diagnosis of a congenital or acquired neuromuscular disease were included, who presented at the neuromuscular outpatient clinic of the Department of Neurology, Medical University of Graz or (one patient) at the Department of Internal Medicine, Medical University of Innsbruck. Myopathies comprised myotonic dystrophy types I and II (MD1, MD2), Becker and Duchenne muscular dystrophy (BMD, DMD), XMPMA, facio-scapulo-humeral muscular dystrophy (FSHD), limb girdle muscular dystrophies (LGMD), non-dystrophic myotonias, sporadic inclusion body myositis (IBM), inflammatory myopathies (e.g. dermatomyositis, polymyositis) and others. A subgroup consisted of patients that suffered from primarily neuronal diseases such as amyotrophic lateral sclerosis (ALS) or spinobulbar muscular atrophy (Kennedy's disease). Patients were older than 18 years and all gave written informed consent.

A subgroup of patients suffering from myotonic dystrophies were compared to anonymised data from healthy controls that were obtained from a previous study by Binder et al.[29]

2.2 Clinical and cardiac examinations

2.2.1 Laboratory parameters

Blood samples were taken at the first study visit at 0 and 3 hours and at a follow-up visit after one year. Among other routine laboratory parameters cTnT, myoglobin, creatine kinase (CK), creatine kinase-muscle/brain (CK-MB) and N-terminal pro brain natriuretic peptide (NT-proBNP) were determined immediately at each visit. From each sampling two serum aliquots were stored at -20°C to allow later analysis. cTnI was determined from frozen serum samples.

Both cTn tests are high sensitivity assays according to requirements of the Joint ESC/ACCF/AHA/WHF Task Force for the Redefinition of Myocardial Infarction demanding a coefficient of variation (CV) of < 10% at the 99th percentile upper reference limit (URL) which is used as a clinical cut-off.[16,31]

The cTnT assay (Troponin T hs, Roche Diagnostics) is an automated electochemiluminescence based immunoassay with a biotinylated capture antibody (5D8) and a Ruthenium labelled detection antibody (M7). 5D8 is a chimeric antibody derived from the M11.7 antibody that was used in western blots in this study. These antibodies form a sandwich complex together with the antigen (cTnT) which is then bound to streptavidin coated microparticles via biotin streptavidin interaction. These particles are then bound the electrode magnetically and the electrochemiluminescence reaction is induced by applying a voltage (**Figure 2**). Emitted light is measured with a photomultiplier. From this signal cTnT concentrations are determined via a calibration curve. The assay is reported to have a limit of blank (LoB) of 3 ng/L, a lower limit of detection (LoD) of 5 ng/L, a limit of quantitation (LoQ, lowest concentration with CV < 10%) of 13 ng/L and a measurement range of up to 10 000 ng/L. The URL defined as the 99th percentile of a reference population is 14 ng/L.[32]

The cTnI assay (STAT High Sensitive Troponin-I, Abbott Laboratories) is an automated chemiluminescence immunoassay that was used on an ARCHITECT $I2000_{SR}$ analyzer. Paramagnetic mircoparticles coated with the capture antibody (M3C7) are incubated with the analyte. After a washing step acridinium-labelled detection antibody (M19C7) is added and following another washing step trigger reagents are added to induce chemiluminescence. From the emitted light, cTnI concentrations are determined via a calibration curve. The manufacturer reports an LoB of 0.7-1.3 ng/L, lower LoD of 1.1-1.9 ng/L, LoQ of < 10.0 ng/L, a measurement range of up to 50 000 ng/L and an URL of 26.2 ng/L.[33]

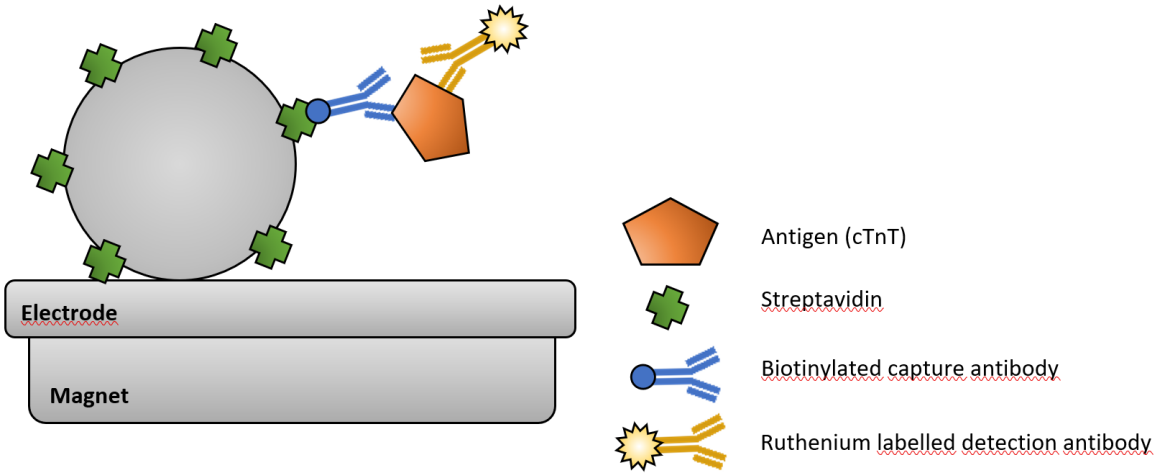

Figure 2: Schematic illustration of the cTnT electrochemiluminescence immunoassay. (Image created based on Fig.4 in Zhou et al.[34])

2.2.2 Electrocardiogram

Standard 12-lead ECG was acquired and patients underwent rhythm monitoring with 24-hour ECG. 24-hour ECGs were classified according to Lown (**Table 1**).

Table 1: Lown Classification, adapted from Lown et al.[35]
VPB ventricular premature beat, NSVT non-sustained ventricular tachycardia.

Grade	Observed
0	No VPB
1	Occasional isolated VPB
2	Frequent VPB (>30/h)
3	Multiform VPB
4	Repetitive VPB
a	Couplets
b	NSVT
5	Early VPB (R on T)

2.2.3 Echocardiography

Transthoracic echocardiography was performed with a Vivid 7 ultrasound scanner (GE Healthcare, Chicago, USA). A standard echocardiographic study for the evaluation of left and right heart dimensions and valvular heart disease was applied. Left atrial, LV end-diastolic, and end-systolic dimensions, as well as end-diastolic thickness of the posterior wall and septum, were measured from parasternal LV long-axis images. Left and right ventricular end-diastolic transverse diameters and septal thickness, end-systolic atrial longitudinal diameters were measured from the apical four-chamber view. Left atrial volume was be determined by the biplane method. Diastolic function was assessed as previously described[36] by pulse wave and tissue Doppler sonography (E wave velocity, A wave velocity, E/A ratio, e', E/e' ratio, and deceleration time). The velocity of early diastolic septal mitral annulus e' wave was measured from tissue doppler imaging (TDI) to assess early diastolic transmitral velocity/mitral annular velocity ratio (E/e'). Mean septal and lateral mitral annular plane systolic excursion (MAPSE) and tricuspid annular plane systolic excursion (TAPSE) were measured by M-mode from the apical 4-chamber view. In the presence of low grade tricuspid regurgitation pulmonary artery systolic pressure was assessed via tricuspid systolic gradient and estimated right atrial pressure.

2.2.4 Echocardiographic strain measurements

There are different approaches for measuring myocardial strain. Strain data can be extracted either from colour coded tissue doppler imaging (TDI) or by means of speckle tracking from B-mode grey scale loops. In this study a combined approach was chosen similar to the technique described by Ingul et al.[37] using primarily TDI information for strain data acquisition, but instead of manual placement of the region of interest and manual adjustment over the cardiac cycle, myocardial tracing is facilitated and automated by using speckle tracking. This method is a feature of the GE EchoPAC software (GE Healthcare, Chicago, USA), however, it has never been properly validated before. Therefore I have devoloped a standardized approach utilizing this function in GE EchoPAC and evaluated feasibility and comparability of the method in a cohort of healthy subjects and patients with FHL1-cardiomyopathy by a comparison to conventional TDI strain

measurements, which is described in detail in the Appendix and in Schmid et al.[38] One of the most important parameters of strain analysis is left ventricular global longitudinal strain (GLS), which reflects myocardial contractility in the longitudinal direction and thus is a marker of left ventricular systolic function.

2.2.5 Cardiac magnetic resonance imaging

All patients without contraindications for magnetic resonance imaging (MRI) (cardiac pacemakers or other MRI unsafe metal implants, chronic kidney disease with eGFR < 30 ml/min/1.73m², previous allergic reaction to MRI contrast medium, severe claustrophobia) underwent 1.5 Tesla ECG-gated cMR (Siemens Healthcare, Erlangen, Germany) with late gadolinium enhancement (LGE). The examination was performed in a single session lasting less than 40 min. CMR protocol was performed according to current guidelines.[39] Short axis images were used to quantify left ventricular global (EDV, ESV, SV, EF, LV myocardial mass) and regional (wall thickness and wall thickening) function by ARGUS software (Siemens Erlangen, Germany). Ten minutes after 0.4 ml/kg body-weight contrast agent (ProHance, Bracco Imaging, containing 279.3mg/ml Gadoteridol) application, single shot inversion-recovery steady state free precession image sequence with phase sensitive reconstruction (PSIR) were obtained to determine LGE images covering the entire heart in gapless short axes, 4-chamber, LV 2-chamber and 3-chamber slices. Presence or absence of LGE was evaluated qualitatively and quantitatively according to the standardized nomenclature for imaging of the heart (17 segment model).

2.2.6 Cardiac computed tomography

Cardiac computed tomography (cCT) with coronary CT angiography (Somatom 64 Multislice, Siemens, Erlangen, Germany) was performed in patients with elevated plasma cTnT, except in patients younger than 40 years with low Framingham risk and except patients with contraindications to contrast medium application (such as eGFR < 45 ml/min/1.73m², hyperthyroidism, previous allergic reaction to contrast medium). One hour prior to cCT examination patients with a heart rate > 60bpm received Bisoprolol (5 mg, 10 mg or 10 mg in combination with Ivabradine 7,5 mg depending on the heart rate). If the heart rate just before examination was still > 60 bpm, Metoprolol (2 mg) was

administered i.v.. The examination was done during breath-hold. Native images were acquired in low dose, followed by a test bolus of contrast medium (Iomeron, Bracco Austria), to determine the optimal start point. The protocol for coronary angiography used 0.6mm collimation, pitch factor of 0.2, 120 kV tube voltage and an effective tube current time product of 900 mAs. Image reconstructions included multiplanar reconstructions, maximum intensity projections and curved planar reformations in different phases of the cardiac cycle.

2.3 Statistics

Patients with previous myocardial infarction, significant coronary artery disease or other known causes of cardiac impairment other than skeletal muscle disease were excluded from further analyses. We grouped patients into six categories: myotonic dystrophies, dystrophic myopathies, non-dystrophic myotonias, inflammatory muscle diseases, primarily neurogenic disease and other myopathies. Patients were further stratified by cardiac involvement which was defined as any of the following: presence of LGE, reduced ejection fraction (EF) <50%[40], increased left ventricular mass index, increased end-diastolic volume index[41], atrial fibrillation or relevant conduction disorder (left bundle branch block or AV block ≥IIb). Values are presented as mean±SD, median [IQR] or relative and absolute frequencies. Skewed laboratory variables were log-transformed to achieve normal distribution if necessary. Pearson correlation coefficient was used to measure correlation between cTnT, cTnI, and markers of skeletal muscle damage. T-test, Mann-Whitney-U test or Fisher's exact test were used for group comparisons as appropriate. Left ventricular (LV) mass and end-diastolic volume were indexed to body surface area. A p-value <0.05 was considered statistically significant.

2.4 *In vitro* experiments

Western blot experiments of patients' skeletal muscle homogenates were performed with cTnT and cTnI specific antibodies. As reference tissue healthy human skeletal muscle, human liver and human myocardium derived from autopsy were used. The positive bands obtained in western blot analysis were subjected to on-blot digest and liquid

chromatography coupled to tandem mass spectrometry (LC-MS/MS). The resulting spectra were used in a human protein database search for protein identification. Finally, we simulated rhabdomyolysis in vitro by adding healthy skeletal muscle homogenates to healthy serum and measured cTnT and cTnI with the commercial assays in these samples.

2.4.1 Tissue specimens

Overall 9 skeletal muscle samples from patients with skeletal muscle disease were available. Four patients agreed to undergo muscle biopsy after giving informed consent. The procedure was done in local anaesthesia on an outpatient basis. Obtained muscle specimens were cryoconserved at a temperature of -80°C until further biochemical analysis. Additionally, existing skeletal muscle specimens from another 5 previously biopsied patients, that had been included in the study, were provided (4 from the Department of Pathology, Medical University of Graz and one from the Medical University of Innsbruck).

Control tissue was derived from autopsy and included human skeletal muscle, myocardium and liver tissue. All tissue samples available are listed in **Table 2**.

Table 2: Tissue samples with corresponding plasma cTnT (cut off: 14 ng/L) and cTnI levels (cut off: 26 ng/L). Available cTn measurements closest to the date of biopsy are shown. Nine patient samples were available (ID 1-9).
Samples 10 to 18 are control tissue from autopsy. Donors had no history or laboratory signs of skeletal muscle disease. Three skeletal muscle samples were available. Patient #2 had died at the age of 75 from stroke. cTnT had incidentally been determined 69 hours before death and was 16 ng/L. Patient #3 had died at the age of 79 from glioblastoma. In this patient cTnT 5 weeks prior to death was 37ng/L. Patient #4 had died from metastatic small cell lung cancer at age 59, last cTnT determination had been 5 months before death (7 ng/L). Patient #5 had died from bronchopneumonia and metastatic esophageal carcinoma at the age of 74, last cTnT had been determined 4.7 years before death.
XMPMA: X-linked myopathy with postural muscle atrophy; LGMD: Limb girdle muscular dystrophy; IBM: Inclusion body myopathy.

Sample ID	Tissue	Muscle disease	cTnT (ng/L)	cTnI (ng/L)
1	vastus lat. muscle	no confirmed myopathy	6	5
2	tibialis ant. muscle	SHARP syndrome	26	2
3	deltoid muscle	Dermatomyositis	2367	3
4	vastus lat. muscle	Polymyositis	9	6
5	tibialis ant. muscle	XMPMA	302	3
6	vastus lat. muscle	spinal muscular atrophy	58	2
7	vastus lat. muscle	LGMD	44	1
8	vastus lat. muscle	sporadic IBM	1100	22
9	vastus lat. muscle	Myositis	356	4
10	psoas muscle #2	-	16	-
11	myocardium #2	-		
12	liver #2	-		
13	psoas muscle #3	-	37	-
14	liver #3	-		
15	psoas muscle #4	-	7	-
16	myocardium #4	-		
17	myocardium #5	-	6	-
18	liver #5	-		

2.4.2 Western blots

A summary of preliminary experiments for the development of the western blot protocol can be found in the Appendix.

The following primary antibodies (kindly provided by Roche Diagnostics) against the same epitopes as the capture and detection antibodies used in the respective commercial assay were applied: cTnT monoclonal mouse antibodies M7 and M11.7 against cTnT-residues 125-131 and 136-147 (referring to isoform 6) and cTnI monoclonal mouse antibodies M3C7 and M19C7 against cTnI residues 24-40 and 41-49. Purified cTnT (Sigma #T0175) and recombinant cTnI (provided by Roche Diagnostics) were used as a reference.

For sample preparation 70-90mg of tissue were ground in a precooled mortar with liquid nitrogen and added to a tenfold amount of SDS buffer solution (aqueous solution of

10mM dithiothreitol, 100mM triethylammonium bicarbonate and 1% sodium dodecyl sulfate), sonicated, centrifuged, and cryopreserved.

30µg of the respective sample was added to sample buffer and reducing agent and heated to 70°C. The solutions were loaded on NuPAGE Novex Midi Bis-Tris Gel (4-12%, 20 slots, 1mm) together with a pre-stained standard (Novex Sharp pre-stained protein standard). For electrophoresis MOPS buffer was used and a voltage of 200 V was applied for 45 minutes. After equilibration in transfer buffer the gels were transferred to nitrocellulose membranes for 1.5 h at 180mA which were then blocked with skim milk blocking buffer (Tris-buffered saline with Tween 20 (TBS-T) and 5% skim milk powder). Protein transfer was controlled with Ponceau S staining.

After blocking and antibody incubations, TBS-T was used as washing buffer. Incubation with primary antibodies (1:10000) was performed overnight at 4°C. Horseradish-peroxidase (HRP) labelled anti-mouse secondary antibodies (1:3000) were used. For detection Amersham ECL Western Blotting Detection Reagent was used. An auto-exposition tool was used for development.

2.4.3 LC-MS/MS

Bands of interest in the western blots were subjected to LC-MS/MS. For that purpose, an identical blot was repeated with longer runtime and protein-free blocking using Pierce™ Protein-Free Blocking Buffer (Thermo Fisher Scientific, #37572). The bands in question were cut out and subjected to on-membrane digest with trypsin after reduction and alkylation. The resulting peptide extracts were dissolved in 0.1% formic acid, 5% acetonitrile and separated by nano-HPLC (Dionex Ultimate 3000) equipped with a C18, 5 µm, 100 Å, 5 x 0.3 mm enrichment column and an Acclaim PepMap RSLC nanocolumn (C18, 2 µm, 100 Å, 500 x 0.075 mm, all Thermo Fisher Scientific, Vienna, Austria). Samples were concentrated on the enrichment column for 2 min at a flow rate of 20 µl/min with 0.1% formic acid as isocratic solvent. Separation was carried out on the nanocolumn at a flow rate of 250 nl/min at 60°C using the following gradient, where solvent A was 0.1% formic acid in water and solvent B was 80% acetonitrile in water containing 0.1% formic acid: 0-5min: 5% B; 5-120 min: 5-30% B; 120-120.1 min: 30-95% B, 120.1-135 min: 95% B; 135-135.1 min: 95-5% B; 135.1-150 min: 5% B. The sample was ionized in the nanospray

source equipped with stainless steel emitters (ES528, Thermo Fisher Scientific, Vienna, Austria) and analyzed in a Orbitrap velos pro mass spectrometer (Thermo Fisher Scientific, Waltham, MA, USA) operated in positive ion mode, applying alternating full scan MS (m/z 400 to 2000) in the ion cyclotron and MS/MS by CID of the 20 most intense peaks with dynamic exclusion enabled. The LC-MS/MS data were analyzed by searching the public Swissprot database with taxonomy homo sapiens (downloaded on 11.06.2015, 42150 sequences) with Mascot 2.3 (MatrixScience, London, UK). The following search criteria were applied: Enzyme: Trypsin; maximum missed cleavage sites: 2; Cys modification: carbamidomethylation; possible multiple oxidized methionine; precursor mass tolerance 10 ppm, product mass tolerance +/- 0.8 Da. Data was filtered according to stringent peptide acceptance criteria, including 1% false discovery rate, mass deviations of maximum ±10 ppm, minimum 2 peptides per protein, Mascot Ion Score of at least 20 and a position rank 1 in Mascot search.

2.4.4 Simulation of rhabdomyolysis

In order directly study the effects of the presence of skeletal or heart muscle proteins on the commercial cTn assays an additional experiment was conducted. Serum of a healthy subject was spiked with increasing concentrations of healthy skeletal muscle homogenates to simulate rhabdomyolysis. Myocardium and liver homogenates served as controls.

Tissue homogenates (psoas muscle, myocardium and liver from autopsy) were prepared in SDS buffer solution (10 mM tris(2-carboxyethyl)phosphine (TCEP), 10% glycerol, 3 mM ethylenediaminetetraacetic acid (EDTA), 3.25% sodium dodecyl sulfate in 1x phosphate-buffered saline), homogenized with ultrasound, centrifuged and the supernatants spiked into plasma of a healthy subject at increasing concentrations with highest final SDS concentrations below 0.1%. In these samples cTnT and cTnI were measured with high sensitive immunoassays (Troponin T hs, Roche Diagnostics and STAT high sensitive Troponin I, Abbott Laboratories). For reference, Myoglobin was measured with a chemiluminescent microparticle immunoassay on an Architect i2100 analyzer (Abbott Laboratories). The protein concentrations added were chosen based on myocardial and skeletal muscle troponin concentrations in Fredericks et al.[42]. A protein concentration of

e.g. 0.1 g/L that we used in our spiking experiments is equivalent to the destruction of approximately 1.6 g of skeletal muscle (0.1 g/L in 2.5 L of total serum = 0.25 g protein. Assuming a protein content of 15% in wet weight skeletal muscle[43], this corresponds to 1.6 g of wet weight skeletal muscle released into the systemic circulation).

In a similar additional experiment recombinant human slow skeletal TnT (Cloud-clone, Huston, USA, product number RPD231Hu01) was spiked into healthy plasma, and cTnT was measured.

2.5 Complementary *in silico* explorations

The putative epitopes of the cTnT antibodies M7 (DRIERRR) and M11.7 (EQQRIRNEREKE) were subjected to a Basic Local Alignment Search Tool (BLAST) search in order to find similarities in the human proteome. The search criteria were as follows: Database = UniProtKB Human; expectation value threshold = 10; Matrix = Auto; Filtering = None; Gapped = None; Hits = 250. Additionally, alignments of the amino acid sequences of cardiac and skeletal TnT isoforms were generated using the Align tool at uniprot.org.

3 RESULTS

The main results have been previously published.[44,45]

3.1 Study cohort

Ninety-two patients were screened and underwent baseline examinations. CMR imaging was completed in 83 patients and 38 patients underwent cCT imaging. We excluded 9 patients because an initially suspected myopathy could not be verified. Another 9 patients had other potential causes of cardiac impairment and were also excluded, leaving 74 patients for analyses.

The neuromuscular diagnosis and cTn concentrations of individual patients are listed in **Table 3**. A majority of patients suffered from myotonic dystrophies (DM) type 1 and 2. Other diagnoses were less frequent and included Duchenne and Becker muscular dystrophy (DMD, BMD), facioscapulohumeral muscular dystrophy (FSHD), limb girdle muscular dystrophies (LGMD), X-linked myopathy with postural muscular atrophy (XMPMA), non-dystrophic myotonias, inflammatory myopathies, and primarily neuronal muscle diseases. Demographics and results of cardiac examinations of the cohort are shown in **Table 4**.

Table 3: List of patients in the cohort and their individual cTn and CK serum concentrations.

Diagnosis	Sex	age	cTnT	cTnI	CK
Dystrophic myopathies:					
XMPMA	m	44	296	6	1040
XMPMA	m	44	289	3	1548
XMPMA	m	57	145	12	677
XMPMA	m	60	216	8	1040
XMPMA	m	53	233	22	1011
BMD	m	60	18	11	244
BMD	m	51	13	2	466
BMD or LGMD	m	57	18	20	1266
DMD	m	21	49	43	890
DMD mutation carrier	f	28	9	58	117
FSHD	m	28	22	2	235
FSHD	f	41	31	2	234
FSHD	m	48	111	3	565
FSHD	f	31	3	2	75
Suspected FSHD	m	42	6	5	141
LGMD (not specified)**	m	47	44	3	679
LGMD 2A	m	18	68	2	1870
LGMD 2A	f	26	44	2	993
LGMD 2A*	m	67	6	2	105
Progressive muscular dystrophy (not specified)	m	56	54	5	177
Progressive muscular dystrophy (not specified)	f	54	18	2	160
Progressive muscular dystrophy (not specified)	f	55	71	5	4117
Progressive muscular dystrophy (not specified)	f	71	187	8	510
Progressive muscular dystrophy (not specified)	m	62	20	9	881
Progressive muscular dystrophy (not specified)	f	20	54	1	3730
Inflammatory myopathies:					
MCTD	f	26	26	2	363
Myositis (HMG-CoA-Reductase Ab)	f	62	247	4	6486
Dermatomyositis	f	60	18	3	186
Polymyositis	m	54	10	6	136
Polymyositis	m	36	60	2	939
Polymyositis	m	58	19	6	1105
Polymyositis/ myasthenia gravis overlap	m	63	5	4	67
Sporadic IBM	f	67	305	4	405
Sporadic IBM	m	66	1022	22	2931

Diagnosis	Sex	age	cTnT	cTnI	CK
Myotonic dystrophies:					
DM1	f	47	62	5	372
DM1	m	34	36	5	525
DM1*	f	64	14	9	285
DM1	m	51	20	5	141
DM1	f	19	11	4	208
DM1*	m	50	30	12	216
DM1	f	39	32	4	152
DM1	f	35	24	3	414
DM1	m	31	54	3	317
DM1	m	34	30	13	284
DM1	f	39	11	9	432
DM1	m	47	30	7	309
DM1	f	29	24	1	361
DM2*	f	62	25	4	223
DM2	m	53	25	7	287
DM2	m	55	18	4	743
DM2	f	52	7	2	302
DM2	f	26	18	4	371
DM2	f	74	38	9	461
DM2	f	53	7	5	294
DM2	f	34	3	2	115
DM2	f	38	97	92	561
DM2	f	74	41	16	316
DM2***	m	44	43	15	1315
DM2	m	47	48	9	1112
DM2*	m	51	10	6	602
DM2	m	56	44	7	151
DM2	f	59	24	3	58
DM2	m	65	16	10	244
DM2	f	68	17	1	139
DM2	f	58	21	4	165
DM2	f	59	10	3	238
DM2	f	41	8	3	131
DM2	f	64	20	5	362
DM2 and SBMA	m	38	49	5	1734
DM (not specified)	m	47	8	3	1109

Diagnosis	Sex	age	cTnT	cTnI	CK
Primarily neurgenic myopathies:					
ALS	m	35	67	2	1190
SBMA**	m	55	65	2	975
SBMA	m	31	19	2	232
SMA	m	21	65	2	3730
Non dystrophic myotonia:					
Becker myotonia	m	47	13	2	341
Becker myotonia	f	46	6	4	298
Thomsen myotonia	f	59	3	7	68
Thomsen myotonia	f	34	3	1	60
Thomsen myotonia	f	63	4	2	59
Thomsen myotonia	f	40	3	2	29
Thomsen myotonia	m	37	3	3	40
Others:					
Hereditary IBM	m	51	26	3	541
Mitochondrial myopathy	f	51	12	2	3083
Excluded:					
Muscular atrophy after poliomyelitis	m	56	12	3	693
no confirmed myopathy	m	43	9	11	246
no confirmed myopathy	m	49	24	5	2411
no confirmed myopathy	m	46	4	2	172
no confirmed myopathy	m	52	6	5	62
no confirmed myopathy	m	47	5	4	232
no confirmed myopathy	m	54	3	2	2053
no confirmed myopathy	m	33	7	3	611
no confirmed myopathy	m	59	85	17	460

Excluded patients:
* previous myocardial infarction
** significant coronary artery disease
*** status post myocarditis

Abbreviations:
Myotonic dystrophy Type 1 (DM1); Myotonic dystrophy Type 2 (DM2); X-linked myopathy with postural muscle atrophy (XMPMA), Becker muscular dystrophy (BMD), Duchenne muscular dystrophy (DMD); Limb girdle muscular dystrophy (LGMD); Facioscapulohumeral muscular dystrophy (FSHD); Mixed connective tissue disease (MCTD); Amyotrophic lateral sclerosis (ALS); Spinobulbar muscular atrophy (SBMA); Spinal muscular atrophy (SMA); Inclusion body myopathy (IBM); male (m); female (f).

Table 4: Characteristics of the study cohort. Continuous variables are presented as mean±SD or median [IQR], categorical variables as percentage %(n). BMI: body mass index; CK: Creatine kinase; GLS: global longitudinal strain; LAVi: left atrial volume index; EF: ejection fraction from cMR; LVMi: left ventricular mass index; EDVi: left ventricular enddiastolic volume index; LGE: late gadolinium enhancement; APB and VPB: atrial/ventricular premature beats in 24h-ECG. (Reproduced from [45] with permission of publisher)

Age (years)	46.0±14.0
Female sex	49.3% (36)
BMI (kg/m²)	26.1±5.8
Hypertension (ABPM)	52.1% (38)
Framingham risk (%)	5.1 [1.0-20.6]
cTnT (ng/L)	24.0 [11.0-247.0]
cTnI (ng/L)	3.6 [2.4-22.1]
Myoglobin (µg/L)	91.2 [47.9-377.2]
CK (U/L)	341.0 [177.0-3730.0]
CK >170 (males) >145 (females) U/L	78.1% (57)
NT-proBNP (ng/L)	59.0 [29.0-455.0]
NT-proBNP > 125 ng/L	26.0% (19)
NT-proBNP > 400 ng/L	5.5% (4)
eGFR (ml/min/1.73 m²)	111.0±27.5
Sinus rhythm	97.3% (71)
PQ time (ms)	153.0±23.0
PQ > 200 ms	2.8% (2)
QRS time (ms)	96.0±18.0
QTc interval (ms)	435.8±32.1
QTc >450 (males) >470 (females) ms	21.9% (16)
LBBB or Pacemaker	5.5% (4)
Lown 0	15.1% (11)
1	39.7% (29)
2	1.4% (1)
3	28.8% (21)
4a	8.2% (6)
4b	4.1% (3)
VPB ≤30/h	93.0% (66)
>30/h	7.0% (5)
APB ≤30/h	94.4% (67)
>30/h	5.6% (4)
EF (%)	59.9±6.8
EF < 50%	7.4% (5)
EF < 55%	22.1% (15)
EDVi (mL/m²)	73.0±11.4
EDVi normal	100.0% (67)
LVMi (g/m²)	53.5±11.4
LVMi > 85(males) >81 (females) g/m²	1.5% (1)
LGE	14.9% (10)
E/e' >15	5.5% (4)
LAVi >34 mL/m²	47.8% (33)
GLS (%)	-18.4±2.9

3.1.1 Cardiac abnormalities in patients with skeletal myopathies

Nine patients with known pre-existing cardiac disease unrelated to myopathy were excluded. Of those, 6 patients with previous myocardial infarction showed ischemic pattern LGE, segmental hypokinesia, and a trend towards lower EF and higher LA-volume. Two (hereditary IBM and LGMD) were found to have significant CAD in cCT. In the remaining patients with increased CAD risk, significant coronary artery disease (CAD) was ruled out by cCT or coronary angiography. One patient with DM2 was excluded because he suffered from dilative cardiomyopathy due to previous myocarditis.

Overall cardiac involvement was most frequent in patients suffering from dystrophic myopathies, especially in XMPMA. The prevalence of cardiac abnormalities in ECG, imaging and laboratory examinations is presented in **Figure 4** according to myopathy.

In the whole cohort, LV systolic function was impaired in 22.1% (15/68) of patients when applying an EF cut-off of 55%, and in 7.4% (5/68) using a 50% threshold. Patients with XMPMA (n=5) and dystrophinopathies (n=4) tended to have lower EFs (56.2±11.9% and 54.1±8.4%). XMPMA patients also exhibited the most impaired GLS in strain analysis (-14±4.2%).

Non-ischemic LGE was present in 14.9% (10/67). LGE was most pronounced in a patient with BMD, who had LGE in all myocardial segments (**Figure 3**). Also four out of 5 XMPMA patients, 2 out of 20 DM2 patients and single cases of FSHD, hereditary IBM, and a DMD mutation carrier showed LGE of a non-ischemic pattern.

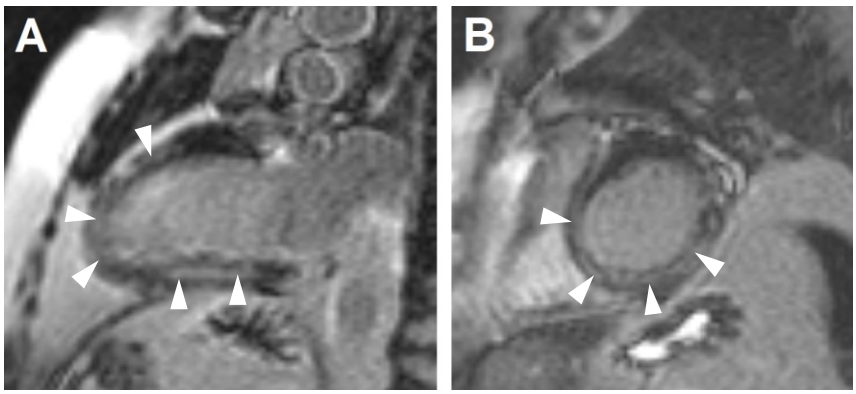

Figure 3: cMR LGE (magnitude inversion recovery) images of a two chamber (A) and basal short axis view (B) of a patient with Becker muscular dystrophy. Extensive midwall to transmural LGE (Δ) is found in all segments with relative sparing of the basal anterior wall. Blurring artifacts due to arrythmia. Significant coronary artery stenosis was excluded in coronary angiography.

No patient had LV dilation as assessed by LV-EDVi and only one patient with DM2, who also suffered from arterial hypertension, showed mild myocardial hypertrophy. Using established cut-offs (>34ml/m^2)[46] a relatively large proportion of 47.8% (33/69) had increased left atrial volumes (LAVi). Septal E/e', a marker for diastolic left ventricular function which correlates with LV filling pressures, was increased (>15)[36] in 4 patients.
Right ventricular dilation was absent in our cohort and RV systolic dysfunction (TAPSE <17 mm) rarely present (n=3). Estimated systolic pulmonary artery pressure was elevated in 4 patients.

ECG analysis revealed atrial fibrillation in one patient (XMPMA). Bundle branch block morphology was present in 8 patients (3 LBBB (2 DM1, 1 BMD), 5 RBBB). First degree AV block was present in 2 patients and higher degree AV block necessitating pacemaker implant in one patient (unspecified muscular dystrophy). QTc was prolonged in 18.9% (14/74) of patients, especially in DM2 (6/20) and other dystrophic myopathies.
Patients' 24-hour ECGs were classified according to Lown: 0 (15.5%, 11/71), I (40.8%, 29/71), II (1.4%, 1/71), IIIa (29.6%, 21/71), IVa (8.5%, 6/71), IVb (4.2%, 3/71), none was Lown V. Patients in category IV were mostly patients suffering from dystrophic myopathies. Five patients had more than a maximum of 30 ventricular premature beats (VPB) per hour (2 XMPMA, 1 BMD, 1 DM1, 1 FSHD).

NT-proBNP was elevated above 125ng/L[47] in 26 patients (19%), but only 4 patients had NT-proBNP values above 400ng/L[48] (3 XMPMA, 1 unspecified progressive muscular dystrophy).[45]

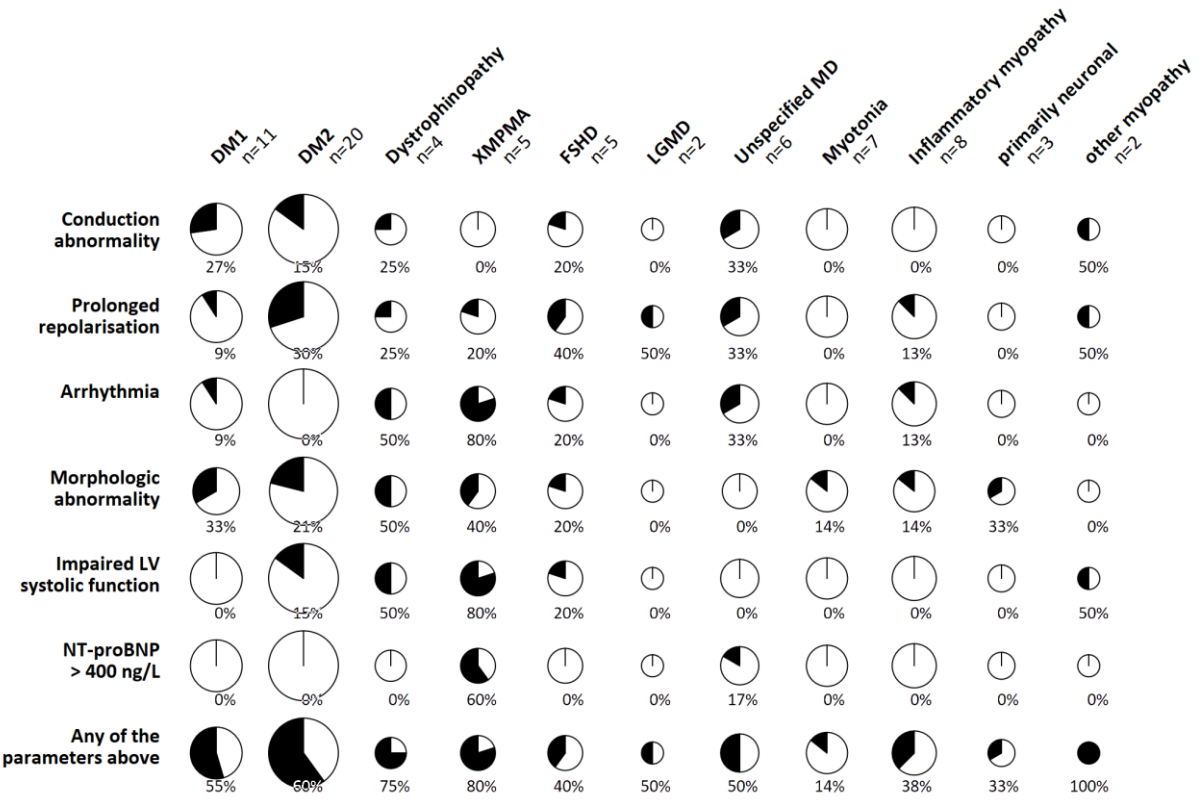

Figure 4: Cardiac involvement in myopathies**.** Area of pie reflects patient number. Conduction abnormality (AV block, LBBB or RBBB), prolonged repolarisation (increased QTc), ventricular arrhythmia (repetitive VPBs Lown 4a and 4b, or frequent VPBs > 30/h), abnormal cardiac morphology (LGE, increased EDVi or increased LVMi), impaired LV systolic function (EF<55%). (Reproduced from [45] with permission of publisher)

3.1.1.1 Cardiac abnormalities in myotonic dystrophies

The majority of our patients suffered from myotonic dystrophies type 1 and 2, which allowed more in-depth analysis and an additional comparison with an age and sex matched cohort of healthy volunteers (**Table 5**). Only patients with proven myotonic dystrophies (n=29, 11 DM1 and 18 DM2) were included, one patient with additional spinobulbar muscular atrophy and one without genetic proof were excluded from this analysis.

Patients had significantly higher LA diameter indices (27.28±3.9 vs. 25.0±3.2 mm/m²; p=0.021), QRS times (99.4±15.6 vs. 91.5±10.3 ms; p=0.027), and QTc intervals (441.1±28.1 vs. 413.0±23.3 ms; p<0.001) than controls. LGE was present in 2 DM2 patients. While one patient with DM1 had reduced EF (EF=46%), overall DM patients did not significantly differ in systolic function as assessed by EF and GLS when compared to controls.

In subgroup analyses, DM1 patients (n=11) had significantly lower EF (54.0±4.7 vs. 61.5±3.3 %; p=0.002), longer PQ intervals (168.2±26.2 vs. 145.2±19.0 ms; p=0.030), QRS

times (107.3±16.7 vs. 91.3±8.0 ms; p=0.012), and QTc intervals (434.8±28.8 vs. 408.7±28.7 ms; p=0.039) than their matched controls.

DM2 patients (n=18) had significantly higher LV mass (55.2±11.4 vs. 45.2±9.3 g/m²; p=0.013) and LA diameter indices (28.3±4.3 vs. 25.4±3.0 mm/m²; p=0.025) than controls. These changes were accompanied by higher NT-proBNP levels (110 [50-170] vs. 43 [36-93] ng/L, p=0.008), slightly reduced GLS (-19.3±1.9 vs. -21.0±2.3 %; p=0.021), and a non-significant trend towards increased E/e' ratios on tissue Doppler imaging in DM2 patients. QTc intervals were increased to 444.9±29.0 vs. 415.6±19.7 ms; p=0.001.[45]

Table 5: Comparison between patients with myotonic dystrophies (DM) and healthy controls. P-values from Student's t test, Mann-Whitney-U-test or Fisher's exact test as appropriate. For abbreviations see **Table 4**. (Reproduced from [45] with permission of publisher)

	DM1 (n=11)	**DM1-controls (n=11)**	**p**	**DM2 (n=18)**	**DM2-controls (n=18)**	**p**	**All DM (n=29)**	**All controls (n=29)**	**p**
Age	36.8±9.2	38.3±11.8	0.751	53.2±12.4	47.2±10.1	0.124	47.0±13.7	43.8±11.5	0.349
Female sex	6 (54.5%)	6 (54.5%)	-	12 (66.7%)	12 (66.7%)	-	18 (62%)	18 (62%)	-
Body mass index (kg/m²)	24.8±3.8	25.5±3.1	0.616	26.5±7.3	25.2±4.4	0.540	25.8±6.1	25.3±3.9	0.721
NT-proBNP (ng/L)	59 [19-98]	53 [42-82]	0.847	110 [50-170]	43 [36-93]	**0.008**	74 [44-155]	49 [36-88]	0.068
LVMi (g/m²)	47.1±12.3	49.4±8.9	0.656	55.2±11.4	45.2±9.3	**0.013**	52.9±12.1	46.8±9.2	0.79
EDVi (ml/m²)	72.0±12.1	77.0±10.2	0.359	75.5±16.6	74.3±10.2	0.823	74.3±15.0	75.4±10.1	0.764
EF (%)	55.7±6.6	61.5±3.3	**0.031**	59.3±5.3	59.0±4.2	0.864	58.1±5.9	60.0±4.0	0.193
EF < 50%	1 (11.1%)	0 (0%)	1.000	0 (0%)	0 (0%)	-	1 (3.8%)	0 (0%)	1.000
EF < 55%	4 (44.4%)	0 (0%)	0.082	4 (23.5%)	2 (14.3%)	0.664	8 (30.8%)	2 (8.7%)	0.080
GLS (%)	-19.1±2.3	-19.2±2.8	0.988	-19.3±1.9	-21.0±2.3	**0.021**	-19.23±2.00	-20.24±2.63	0.116
E/e'	9.9±1.5	9.3±3.6	0.625	10.7±3.3	9.0±3.0	0.118	10.41±2.77	9.14±3.17	0.109
LA diameter (mm)	47.1±6.7	45.5±5.5	0.564	51.0±6.7	46.7±5.5	**0.042**	49.5±6.9	46.2±5.4	0.050
LA diameter index (mm/m²)	25.5±2.4	24.4±3.5	0.396	28.3±4.3	25.4±3.0	**0.025**	27.28 ±3.9	25.0±3.2	**0.021**
PQ time (ms)	168.2±26.2	145.2±19.0	**0.029**	158.4±23.9	154.2±19.0	0.562	162.1 ±24.8	150.8±19.2	0.056
QRS time (ms)	107.3±16.7	91.3±8.0	**0.010**	94.6±13.1	91.6±11.7	0.473	99.4±15.6	91.5±10.3	**0.027**
QTc interval (ms)	434.8±26.8	408.7±28.7	**0.039**	444.9±29.0	415.6±19.7	**0.001**	441.1±28.1	413.0±23.3	**<0.001**
QTc prolonged	1 (9.1%)	0 (0%)	1.000	5 (27.8%)	0 (0%)	**0.045**	6 (20.7%)	0 (0%)	**0.023**
VPB (24 hours)	4 [0.5-10.0]	7 [0-24.5]	0.606	3 [1-7]	1.5 [0-10.5]	0.245	3.5 [1-8.0]	4 [0-13.5]	0.586
APB (24 hours)	2 [1-3.5]	5 [2-12.5]	0.056	13 [4-31]	8 [4-18.5]	0.423	4 [1-22.5]	7 [2.5-15.5]	0.521

3.1.2 Cardiac troponin plasma levels in skeletal myopathies

While 69% (51/74) of patients had cTnT plasma concentrations above the established assay cut-off (14ng/L), only 4% (3/74) had raised cTnI (above 26ng/L). A scatterplot showing cTnT versus cTnI measurements is presented in **Figure 5**. There was a weak but significant association between cTnT and cTnI in Pearson correlation analysis (r=0.316, p=0.006).

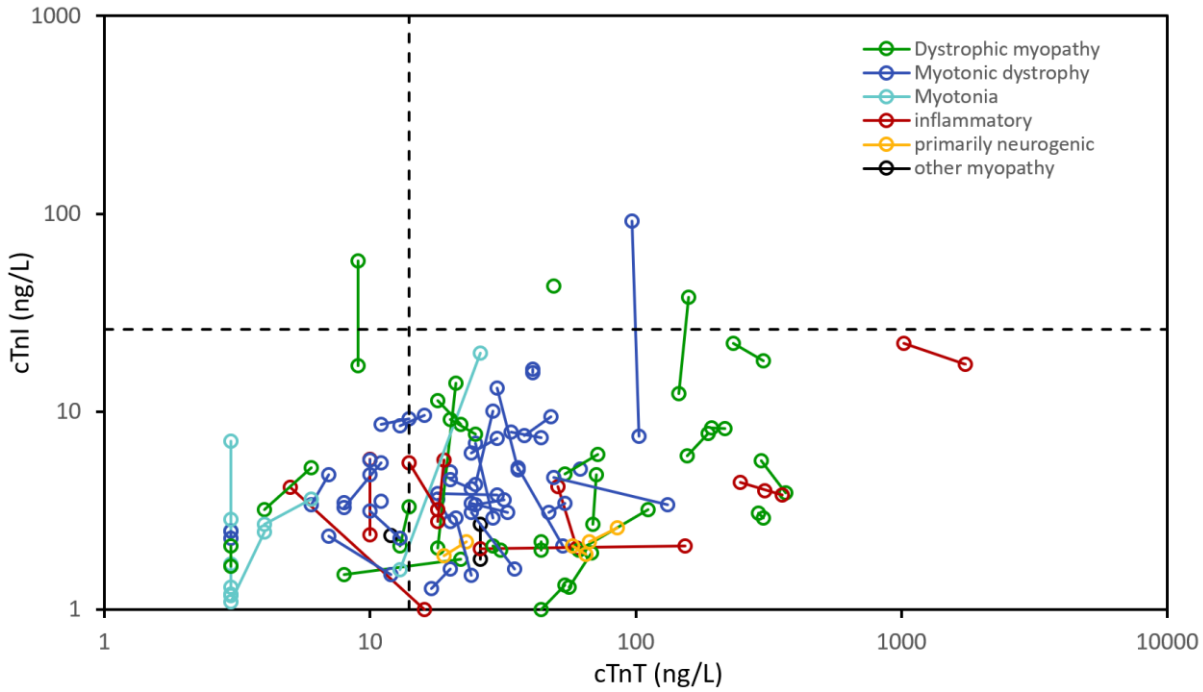

Figure 5: Scatterplot (logarithmic scale) of cTnT and cTnI at first visit and after one year. The two cTn measurements in individual patients are connected by solid lines. Assay cut-offs are shown as dashed lines (26 ng/L for cTnI and 14 ng/L for cTnT). At the first visit, 68.9% had raised cTnT, 4.1% had raised cTnI. (Reproduced from [44] with permission of publisher)

Table 6: Contingency table of raised cTnT vs. cTnI. (Reproduced from [44] with permission of publisher)

	cTnT ≤14 ng/L	cTnT >14 ng/L	sum
cTnI ≤26 ng/L	22 (30%)	49 (66%)	71 (96%)
cTnI >26 ng/L	1 (1%)	2 (3%)	3 (4%)
sum	23 (32%)	51 (69%)	74 (100%)

Most patients had either cTn levels below the respective cut-off with both assays or raised cTnT and normal cTnI (**Table 6**). The cohort was categorised into 6 groups to facilitate comparison, laboratory values including cTn levels according to myopathy category are presented in **Table 7**.

Table 7: Patient characteristics and laboratory markers of the cohort. The cohort was grouped into six categories for the purpose of presentation: Myotonic dystrophies (DM1, DM2), other dystrophic myopathies (XMPMA, DMD, BMD, FSHD, LGMD and others), non-dystrophic myotonia (Becker and Thomsen myotonia), inflammatory myopathies (Poly- and dermatomyositis, myositis, IBM), primarily neuronal diseases (SMA, SBMA, ALS) and others (hereditary IBM, mitochondrial myopathy).
For abbreviations see **Table 3**. (Reproduced from [44] with permission of publisher)

	Myotonic dystrophy (n=31)	Other dystrophic myopathies (n=22)	Non-dystrophic myotonias (n=7)	Inflammatory myopathies (n=9)	Primarily neuronal diseases (n=3)	Other myopathies (n=2)
Females	58.1% (18)	36.4% (8)	71.4% (5)	44.4% (4)	0% (0)	50% (1)
Age	46.7±13.4	44.1±15.5	46.6±10.9	54.7±14.2	29.0±7.2	51.0±0.0
BMI	26.8±7.1	23.7±4.1	27.7±5.3	28.4±4.0	23.3±2.7	29.7±0.4
cTnT (ng/L)	24 [11-36]	52 [18-145]	3 [3-6]	26 [18-247]	65 [19-67]	19 [12-26]
cTnT > 14ng/L	71.0% (22)	81.8% (18)	0% (0)	77.8% (7)	100% (3)	50% (1)
cTnI (ng/L)	5 [3-7]	5 [2-9]	3 [2-4]	4 [3-6]	2 [2-2]	3 [2-3]
cTnI > 26ng/L	3.2% (1)	9.1% (2)	0% (0)	0% (0)	0% (0)	0% (0)
NT-proBnP (ng/L)	61 [28-155]	70 [37-201]	66 [41-215]	57 [37-83]	9 [7-24]	74 [23-124]
CK (U/L)	309 [208-432]	621 [234-1040]	60 [40-298]	405 [186-1105]	1190 [232-3730]	1812 [541-3083]
CK-MB (U/L)	15 [13-19]	37 [20-60]	12 [10-15]	23 [20-44]	45 [19-75]	48 [26-70]
Myoglobin (µg/L)	81.4 [55.7-120.7]	156.5 [64.4-227.5]	24.1 [21.0-60.8]	149.0 [49.9-252.2]	196.6 [40.8-483.3]	187.4 [83.6-291.2]
eGFR (ml/min/1.73m²)	105.6±15.7	125.8±39.6	91.2±15.7	100.6±17.1	126.8±13.5	116.4±7.2

cTnT elevations were most pronounced in patients with XMPMA. Two patients had both raised cTnT and cTnI (Duchenne muscular dystrophy, myotonic dystrophy type 2) and one patient had raised cTnI but normal cTnT levels (female Duchenne mutation carrier). Interestingly, in the latter patient constantly raised cTnI levels had been detected in the past over several years (using an earlier generation cTnI assay by Abbott). In 2008 this was interpreted as myocarditis due to a subtle myocardial scar in cMR. However, when she presented again in 2010, no cardiac cause for the still elevated cTnI could be found. Intermittent cTnT assessments (4th generation assay) were also available which were all below the limit of detection. Longitudinal cTn levels of this patient are presented in **Figure 6**; cTnI levels were elevated in 42 out of 44 measurements, while cTnT concentrations were normal in all available 9 measurements.

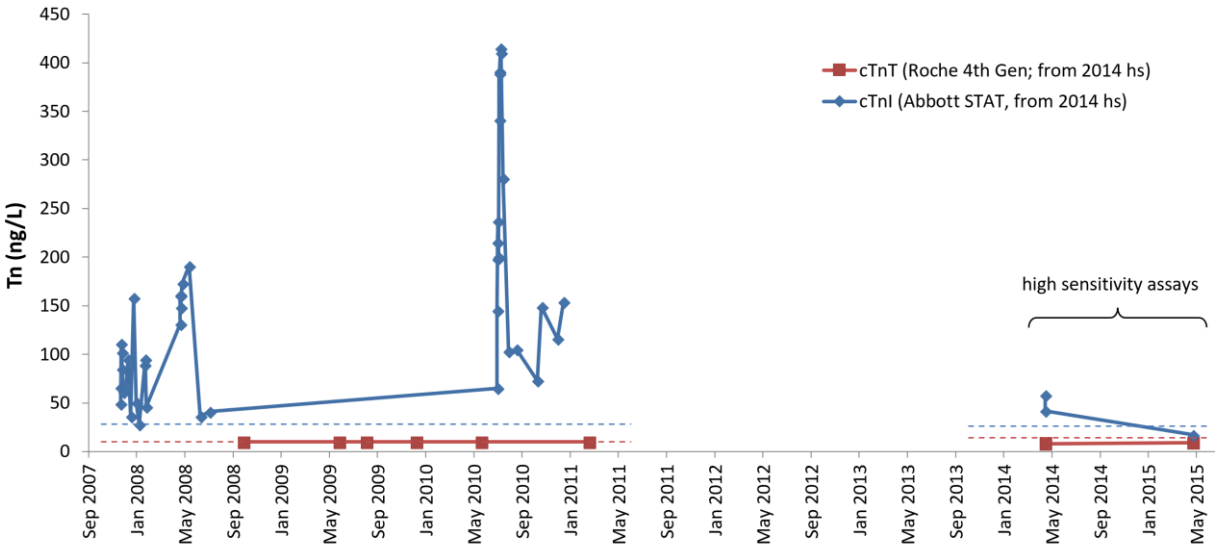

Figure 6: Available cTnT and cTnI measurements of a female Duchenne mutation carrier, who was the only patient in our cohort with elevated cTnI but normal cTnT. From 2014 on, measurements were done with high sensitivity (hs) cTnT and cTnI assays (Roche Diagnostics and Abbott Laboratories), before 2014 with earlier generation assays of the same manufacturers. The respective cut-offs are indicated as dashed lines.

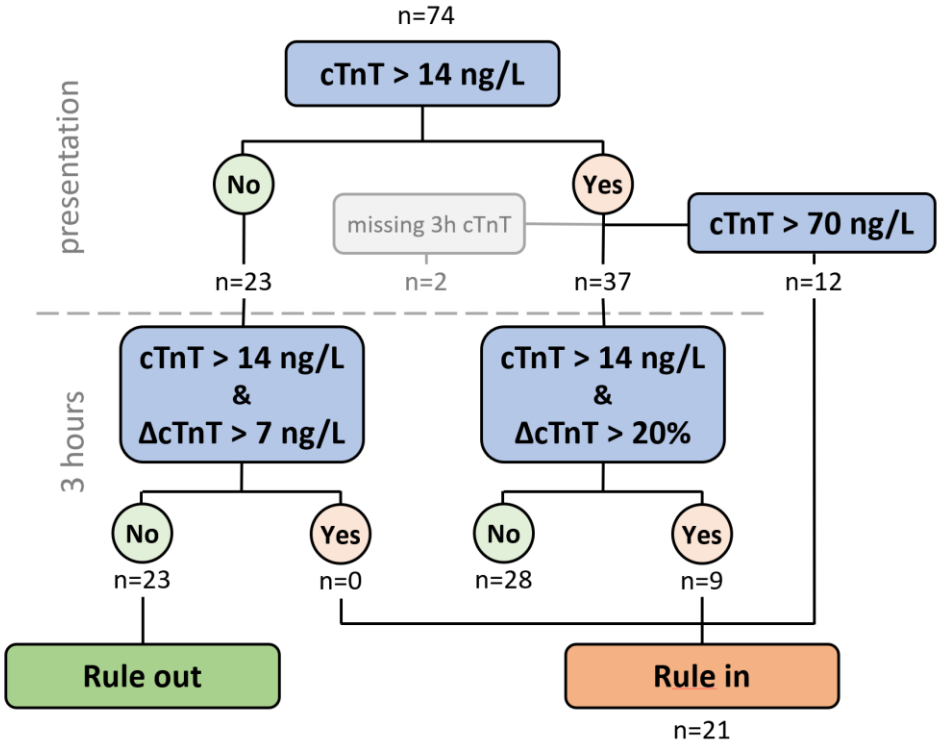

Figure 7: Flowchart of the 3-hour ESC algorithm applied on the data of the study cohort, assuming an appropriate clinical presentation. 29.2% (21/72) would have been ruled in for myocardial infarction with recommendation for further invasive management.

Longitudinal measurements of cTnT after three hours and after one year showed that cTnT levels were chronically elevated, however with considerable fluctuation. In the entire cohort delta cTnT was 0.1±9.4 ng/L after three hours and -6.7±27.6 ng/L at one year. However, 15.3% (11/72) had a three-hour delta >10ng/L and 27.8% (20/72) or 29.2% (21/72) would have fulfilled rule-in criteria for myocardial infarction when applying a proposed two-hour algorithm[49] or the three-hour ESC algorithm[50] on our data (**Figure 7**).

3.1.2.1 Cardiac Troponins and markers of skeletal muscle damage

CK and myoglobin levels in the blood reflect myocyte damage and are clinically used as an indicator of disease activity in myopathies. CK was raised in the majority of patients (78%, 58/74). CK and myoglobin levels strongly and significantly correlated with cTnT (r=0.679, p<0.001; r=0.786, p<0.001) but not with cTnI (r=0.124, p=0.293; r=0.182, p=0.121), which is also reflected in the scatterplots in **Figure 8**.

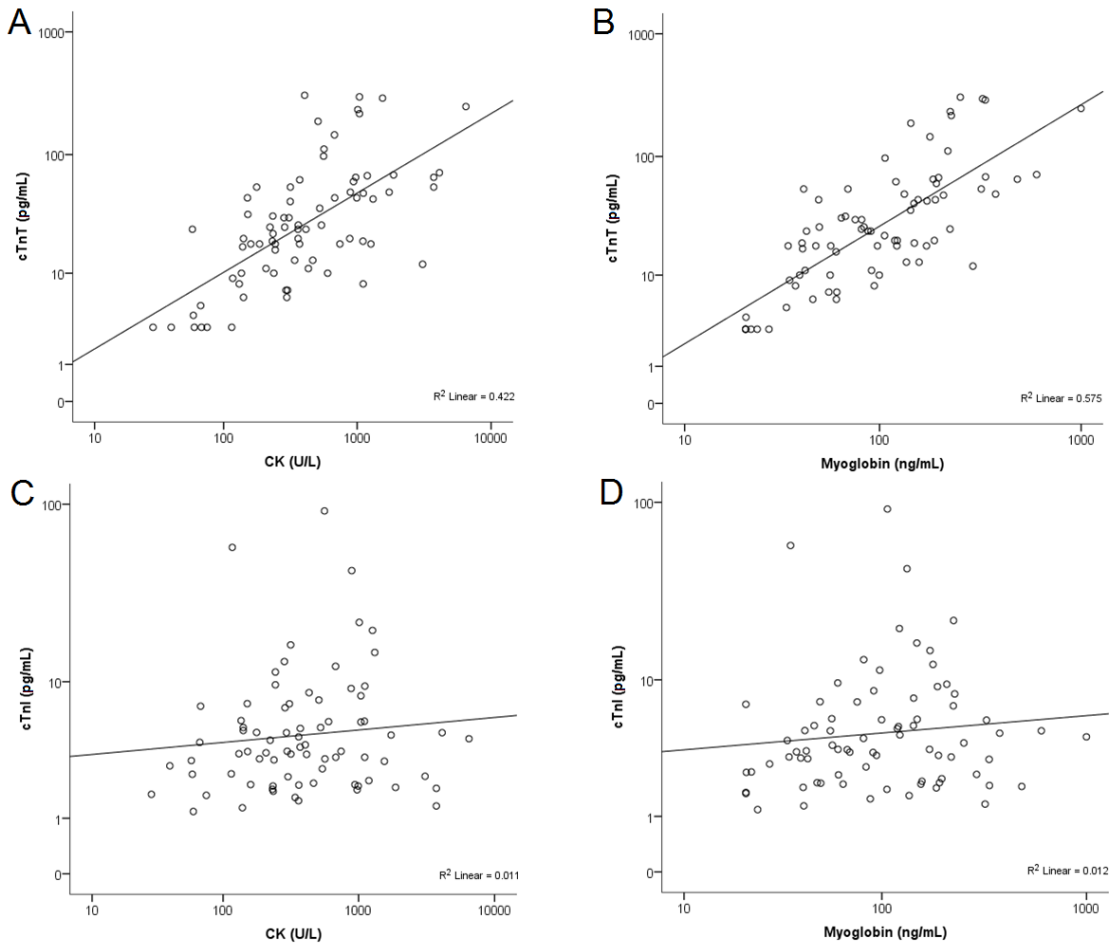

Figure 8: Scatterplots of cTnT and cTnI against CK and myoglobin. Logarithmic scale. (Reproduced from [44] with permission of publisher)

While CK-MM is the predominating CK-isoform in skeletal muscle, CK-MB is the prevailing isoform in the heart. Though CK-MB was an important marker for diagnosing myocardial infarction before the advent of cTn tests, it is also expressed in skeletal muscle and therefore not entirely cardiac specific. In our patients CK-MB was moderately elevated (median CK-MB 19 [14-38] U/L; CK-MB > 25 U/L in 30.1%) as expected in patients with myopathy,[51] with a low CK-MB/CK ratio (4.7±2.0% in patients with elevated CK-MB), indicative of a non-cardiac origin.

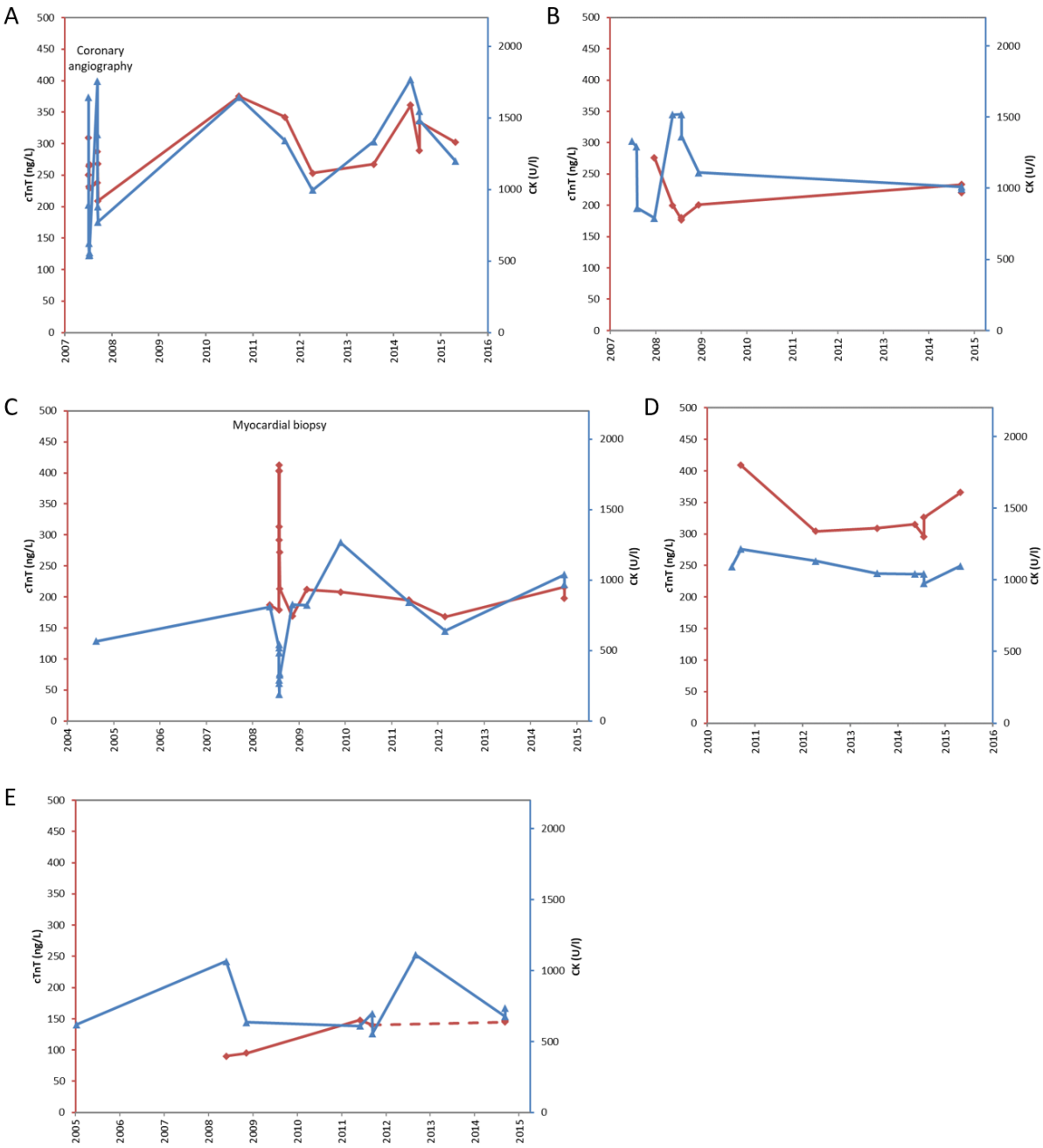

Figure 9: Longitudinal concurrent determinations of cTnT (red) and CK (blue) in five patients with XMPMA. Dashed line indicates missing data. (Reproduced from [44] with permission of publisher)

As the study group's interest in cTnT was initially induced by observations in patients with XMPMA, the longitudinal behaviour of CK and cTnT was assessed retrospectively in five patients by means of line charts (**Figure 9**), where CK and cTnT showed largely parallel curve characteristics.

3.1.2.2 Cardiac Troponins and cardiac abnormalities

For the purpose of correlating cTn levels with cardiac abnormalities, cardiac involvement was defined as any of the following: Presence of late gadolinium enhancement (LGE), EF <50%, increased LV mass index or end-diastolic volume index, atrial fibrillation or relevant conduction disorder (left bundle branch block or AV block ≥ IIb). These criteria are stricter than those used above (**Figure 4**) in order to increase discriminatory power.

According to these criteria, signs of cardiac disease were present in 23% (16/70) of the cohort (**Table 8**).

cTnI, NT-proBNP, and — to a lesser extent — cTnT were significantly higher in patients with cardiac involvement (**Table 8**, p<0.001, p=0.003, p=0.025, respectively), while CK and myoglobin were not (p=0.169, p=0.205). Importantly, in patients without signs of cardiac disease cTnT remained elevated in the majority of patients (67%, 36/54) and the proportion of patients above the diagnostic cut-off did not differ between groups.

Table 8: Cardiac involvement in the cohort, defined as any of the following: presence of late gadolinium enhancement (LGE), EF <50%, increased LV mass index (LVMi), increased end-diastolic volume index (EDVi), atrial fibrillation (Afib) or relevant conduction disorder (LBBB or AV block ≥IIb). Cardiac and skeletal muscle markers are presented according to cardiac involvement. P-values from Student's t-test, Mann-Whitney-U test or Fisher's exact test. (Reproduced from [44] with permission of publisher)

	All patients		
LGE	16.2% (11/68)		
EF <50%	7.2% (5/69)		
Increased LVMi	1.5% (1/68)		
Increased EDVi	0% (0/68)		
Afib, LBBB or AV block ≥IIb	6.8% (5/74)		
Cardiac involvement (any of the variables above)	**yes** 22.9% (16/70)	**no** 77.1% (54/70)	**p**
cTnT (ng/L)	37 [15-181]	23 [10-49]	0.025
cTnT >14 ng/L	75.0% (12)	66.7% (36)	0.760
cTnI (ng/L)	9 [6-22]	3 [2-5]	<0.001
cTnI >26 ng/L	18.8% (3)	0% (0)	0.010
NT-proBNP (ng/L)	128 [49-328]	56 [24-108]	0.003
CK (U/L)	619 [277-1026]	309 [160-602]	0.169
CK-MB (U/L)	25 [16-50]	18 [13-38]	0.160
Myoglobin (µg/L)	102.1 [79.6-206.1]	81.3 [41.6-157.4]	0.205
eGFR (ml/min/1.73m^2)	117.4±40.0	109.0±23.6	0.769
Framingham risk (%)	10.0 [4.1-14.9]	4.6 [0.9-9.2]	0.043

3.2 *In vitro* experiments

In order to investigate the mechanisms causing elevated measured cTnT in our cohort we tested cTnT and cTnI antibodies in western blots of patients' skeletal muscle samples and healthy control tissue (skeletal muscle, myocardium and liver). Furthermore, we simulated rhabdomyolysis by spiking healthy skeletal muscle homogenate into healthy plasma and measured cTn in order to test if this would cause positive test results.

3.2.1 Western blots

Our final western blots comprised skeletal muscle biopsy samples of 9 patients and healthy tissue samples from autopsy (two skeletal muscle, one myocardium, one liver sample). The antibodies applied were directed against the same epitopes as the capture and detection antibodies used in the respective commercial cTn immunoassay.

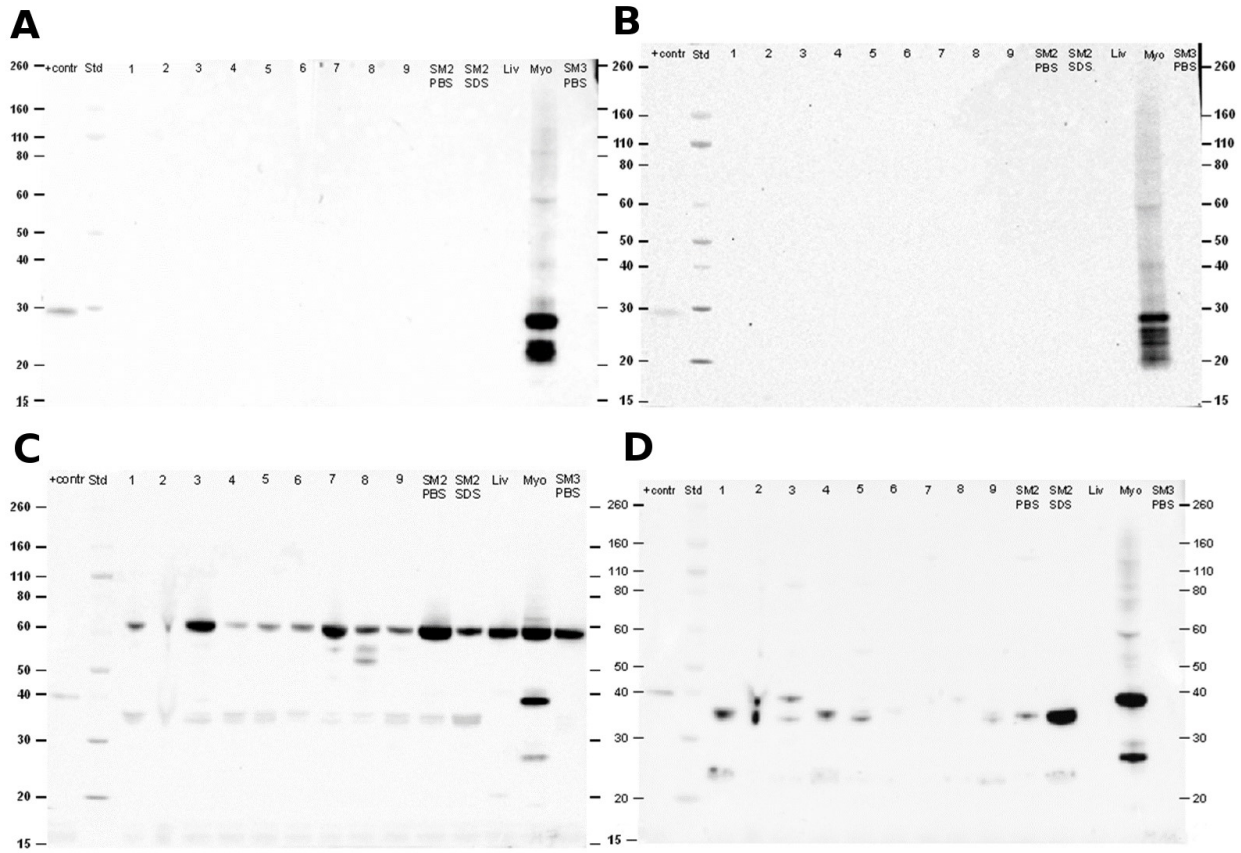

Figure 10: Western blots of myopathic skeletal muscle and reference tissue probed with cTn antibodies.
A: Anti cTnI (M3C7); **B**: Anti cTnI (M19C7); **C**: Anti cTnT (M7); **D**: Anti cTnT (M11.7).
Purified cTnT and recombinant cTnI positive controls (+contr); protein size standard (Std); skeletal muscle samples of patients with different myopathies (lanes 1-9, ID according to **Table 2**); Healthy skeletal muscle (SM2, SM3), liver (Liv), and myocardium (Myo) from autopsy. (Reproduced from [44] with permission of publisher)

Using the cTnI antibodies only myocardium showed positive bands (**Figure 10**, A and B).
In blots probed with the cTnT antibodies (**Figure 10**, C and D), we detected one to three bands per lane in skeletal muscle samples with either cTnT antibody at molecular weights approximately 5 kDa below cTnT. These bands had much lower signal than the cTnT band in the myocardium lane. Interestingly, these bands were present not only in diseased skeletal muscle (**Figure 11**) but also in healthy skeletal muscle reference tissues (**Figure 12**) and can also be seen in our preliminary western blots (see **Appendix**).

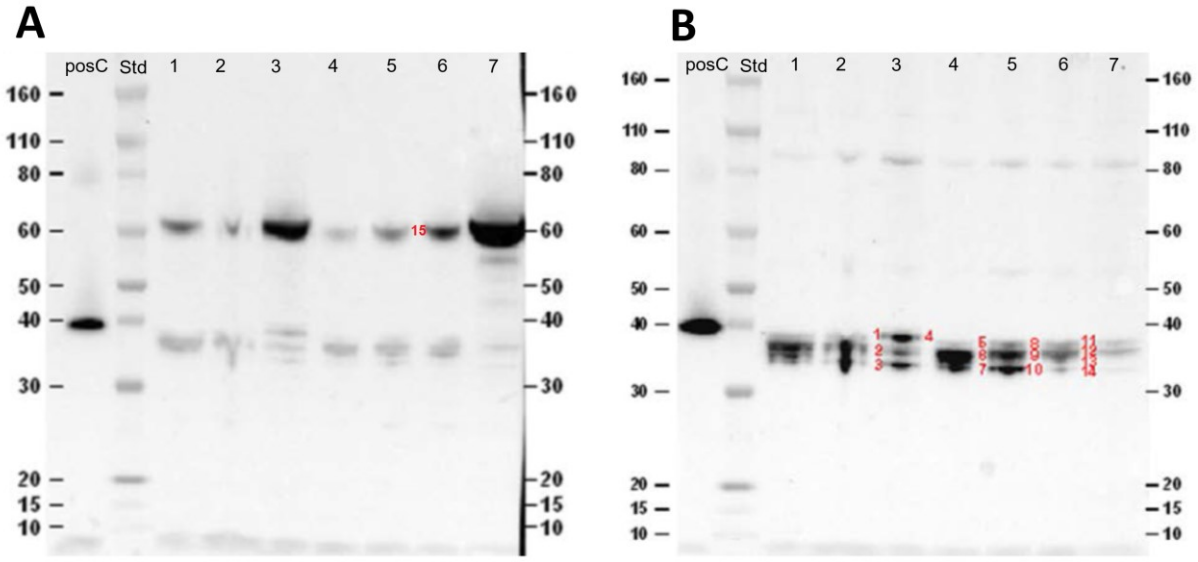

Figure 11: Western blots of patient samples with cTnT antibodies M7 (**A**) and M11.7 (**B**).
Purified human cTnT (posC); molecular weight standard (Std); sample IDs 1-7 according to **Table 2**.
Primary anti-cTnT antibodies M7 and M11.7 (dilution 1:10000). Secondary antibody: Anti-mouse HRP-linked antibody (dilution 1:3000). Bands marked with red numbers were subjected to LC-MS/MS. (Reproduced from [44] with permission of publisher)

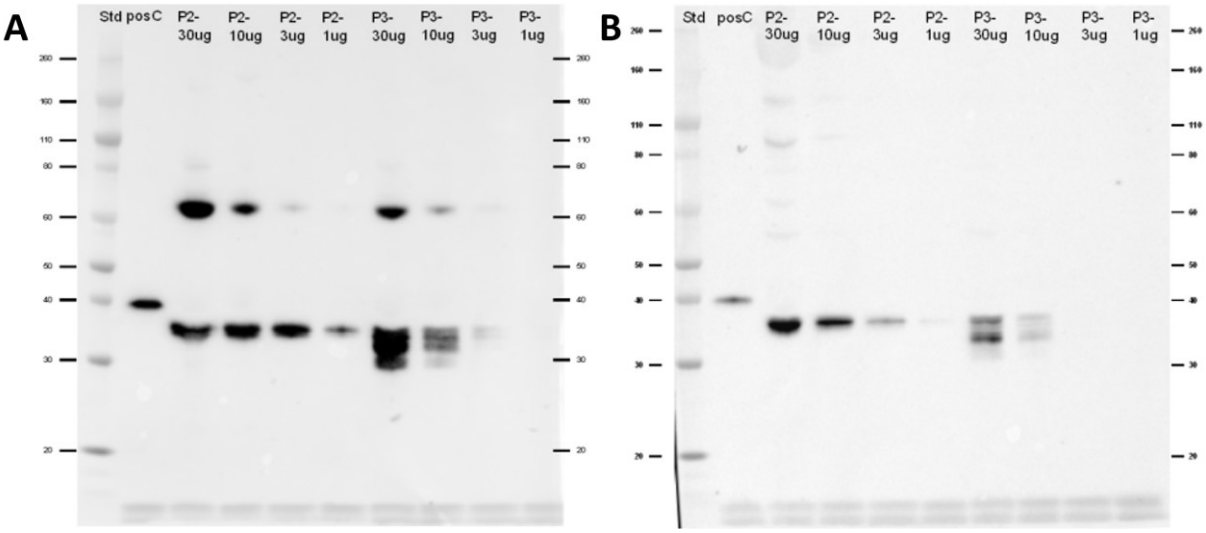

Figure 12: Western blots of two healthy skeletal muscle samples (psoas muscle #2 and #3) at increasing protein concentrations tested with anti-cTnT antibodies M7 (**A**) and M11.7 (**B**). Molecular weight standard (Std); purified human cTnT (posC). (Reproduced from [44] with permission of publisher)

The M7 cTnT antibody additionally detected a strong positive band in all samples including liver tissue at approx. 60 kDa. This band was not detected with the M11.7 antibody and is therefore not recognized in the clinically used assay, which requires

positivity with both antibodies. As expected, myocardium showed a typical band with both antibodies at the molecular weight of cTnT while liver tissue did not show positive bands at a molecular weight consistent with Tn (for molecular masses of troponin isoforms see **Table 9**).

Table 9: Human Troponin subunits and isoforms and their molecular masses (from uniprot.org [52]).

Troponin	UniProt ID	Molecular weight (kDa)
cTnT, cardiac muscle	P45379	36
sTnT, slow skeletal muscle	P13805	33
fTnT, fast skeletal muscle	P45378	32
cTnI , cardiac muscle	P19429	24
sTnI, slow skeletal muscle	P19237	22
fTnI, fast skeletal muscle	P48788	21
TnC	P63316 & P02585	18

3.2.2 LC-MS/MS

Bands of interest that were detected with both cTnT antibodies in western blots (labelled with red numbers in **Figure 11**) were subjected to LC-MS/MS. Detailed results from the database search of LC-MS/MS spectra can be found in the **Appendix**. Among other proteins, skeletal sTnT was identified in all samples and skeletal fTnT in all but one sample (sample 8). There was no evidence of the cardiac isoform in any of the bands, whereas purified cTnT which served as positive control was clearly identified with this method. No troponin isoform was found in the 60 kDa band of the M7 antibody.

3.2.3 Simulation of rhabdomyolysis

In order to investigate if skeletal muscle proteins would cause positive test results not only in the western blot setting but also in the commercial immunoassay we spiked healthy human plasma with healthy skeletal muscle homogenates and then measured cTnT, cTnI, and myoglobin concentrations (**Figure 13**). Myocardium and liver tissue homogenates served as positive and negative controls.

Measured cTnT and cTnI linearly increased with rising concentrations of myocardial muscle protein spiked in plasma samples. With skeletal muscle spikes, for cTnT we found a comparable linear increase at higher protein input concentrations resulting in a rightward shift of the cTnT concentration curve when compared to myocardium. Measured concentrations were higher than in non-muscle control tissue (liver). In contrast, cTnI measurements yielded much lower values in the same approach and remained below the established assay cut-off and below liver tissue.

cTnT was additionally measured in healthy plasma samples spiked with recombinant human slow TnT (**Figure 14**), showing concentration dependent cTnT measurements at high concentrations of sTnT. Mean cross-reaction was 0.024%.

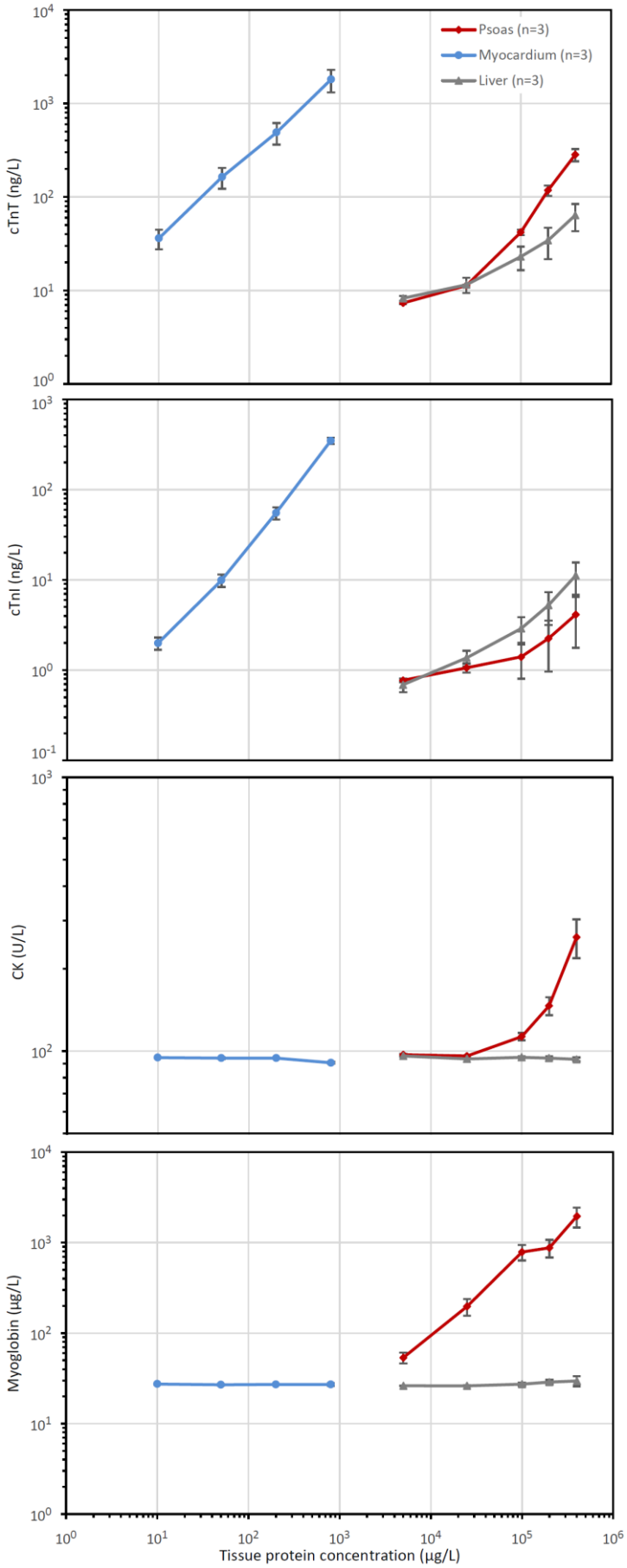

Figure 13: Measured cTnT, cTnI, CK and Myoglobin concentrations in plasma samples spiked with increasing concentrations of skeletal muscle (red), myocardium (blue), or liver homogenates (grey) (mean ± SEM). Logarithmic scale. (Reproduced from [44] with permission of publisher)

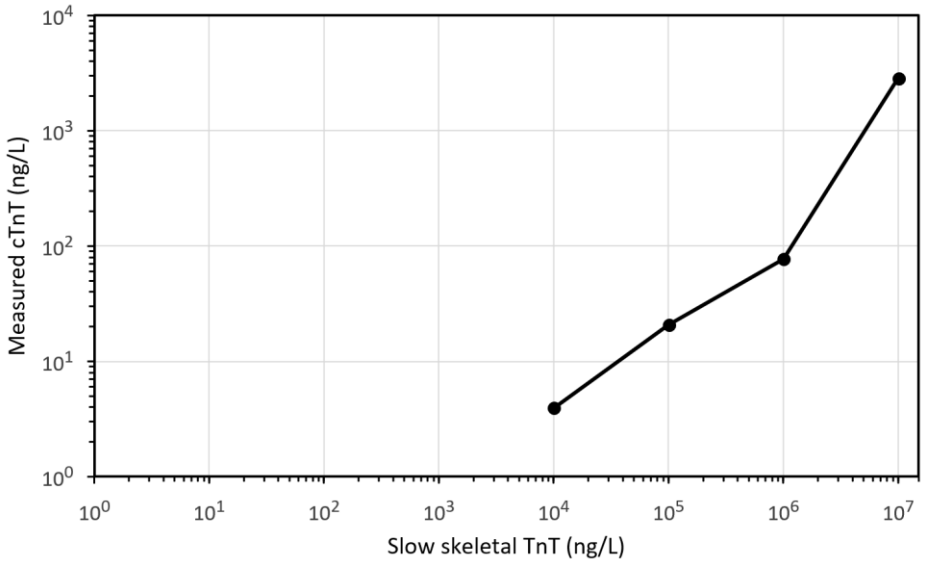

Figure 14: Measured cTnT in plasma samples spiked with increasing concentrations of recombinant human slow TnT. Logarithmic scale.

3.3 Complementary *in silico* explorations

The putative epitopes of the cTnT antibodies M7 (DRIERRR) and M11.7 (EQQRIRNEREKE) were subjected to a peptide similarity search in the human proteome. Similarity search for the M7 epitope identified cTnT isoforms and slow skeletal TnT isoforms (**Table 10**). The query for the M11.7 epitope found cTnT isoforms, fast and slow skeletal TnT isoforms and several other proteins such as ELKS/Rab6-interacting/CAST family member 1, Ensconsin, A-kinase anchor protein 9, Cilia- and flagella-associated protein 45, Scaffold attachment factor B1 and B2 (**Table 11**). In contrast to the TnT isoforms none of these other proteins were identified in the database search of LC-MS/MS data from immunoreactive skeletal muscle bands (**Appendix**).

Table 10: BLAST search results of the putative M7 epitope (DRIERRR) in the UniProtKB database (human). TnT isoforms are highlighted: cTnT, sTnT. (Accessed 06.07.2019; continued on the next page)

Identifier	Name	Identity	Score	E-value
P45379	TNNT2_HUMAN - Troponin T, cardiac muscle	100%	56	0.80
P45379-11	TNNT2_HUMAN - Isoform 11 of Troponin T, cardiac m...	100%	56	0.80
P45379-10	TNNT2_HUMAN - Isoform 10 of Troponin T, cardiac m...	100%	56	0.80
P45379-8	TNNT2_HUMAN - Isoform 8 of Troponin T, cardiac mu...	100%	56	0.80
P45379-7	TNNT2_HUMAN - Isoform 7 of Troponin T, cardiac mu...	100%	56	0.80
P45379-6	TNNT2_HUMAN - Isoform 6 of Troponin T, cardiac mu...	100%	56	0.80
P45379-5	TNNT2_HUMAN - Isoform 5 of Troponin T, cardiac mu...	100%	56	0.80
P45379-4	TNNT2_HUMAN - Isoform 4 of Troponin T, cardiac mu...	100%	56	0.80
P45379-3	TNNT2_HUMAN - Isoform 3 of Troponin T, cardiac mu...	100%	56	0.80
P45379-2	TNNT2_HUMAN - Isoform 2 of Troponin T, cardiac mu...	100%	56	0.80
Q15607	Q15607_HUMAN - Cardiac troponin T	100%	56	0.80

Identifier	Name	Identity	Score	E-value
A0A0A0MRJ4	A0A0A0MRJ4_HUMAN - Troponin T, cardiac muscle	100%	56	0.80
E7EPN8	E7EPN8_HUMAN - Troponin T, cardiac muscle	100%	56	0.80
A0A0A0MRJ5	A0A0A0MRJ5_HUMAN - Troponin T, cardiac muscle	100%	56	0.80
Q15608	Q15608_HUMAN - Troponin T	100%	56	0.80
E7EPW4	E7EPW4_HUMAN - Troponin T, cardiac muscle	100%	56	0.80
A0A499FJM7	A0A499FJM7_HUMAN - Troponin T, cardiac muscle	100%	56	0.80
Q7Z554	Q7Z554_HUMAN - Troponin T cardiac isoform	100%	56	0.80
A0A024R953	A0A024R953_HUMAN - Troponin T type 2 (Cardiac), isofor...	100%	56	0.80
P13805	TNNT1_HUMAN - Troponin T, slow skeletal muscle	85.7%	50	5.70
P13805-3	TNNT1_HUMAN - Isoform 3 of Troponin T, slow skele...	85.7%	50	5.70
P13805-2	TNNT1_HUMAN - Isoform 2 of Troponin T, slow skele...	85.7%	50	5.70
M0QX01	M0QX01_HUMAN - Troponin T, slow skeletal muscle	85.7%	50	5.70
Q56R93	Q56R93_HUMAN - Nemaline myopathy mutant slow skele...	85.7%	50	5.70
Q05DL6	Q05DL6_HUMAN - TNNT1 protein	85.7%	50	5.70
Q56R94	Q56R94_HUMAN - Nemaline myopathy mutant slow skele...	85.7%	50	5.70
K7EQL4	K7EQL4_HUMAN - Troponin T, slow skeletal muscle	85.7%	50	5.70
M0QZU8	M0QZU8_HUMAN - Troponin T, slow skeletal muscle	85.7%	50	5.70
A8K5N7	A8K5N7_HUMAN - cDNA FLJ75373, highly similar to Ho...	85.7%	50	5.70
M0QZY5	M0QZY5_HUMAN - Troponin T, slow skeletal muscle	85.7%	50	5.70
Q3B759	Q3B759_HUMAN - TNNT1 protein	85.7%	50	5.70
A0A024R4S3	A0A024R4S3_HUMAN - Troponin T type 1 (Skeletal, slow),...	85.7%	50	5.70

Table 11: BLAST search results of the putative M11.7 epitope (EQQRIRNEREKE) in the UniProtKB database (human). TnT isoforms are highlighted: cTnT, fTnT, sTnT. (Accessed 06.07.2019; continued on the next page)

Identifier	Name	Identity	Score	E-value
P45379	TNNT2_HUMAN - Troponin T, cardiac muscle	100%	95	0.0000031
P45379-12	TNNT2_HUMAN - Isoform 12 of Troponin T, cardiac m...	100%	95	0.0000031
P45379-11	TNNT2_HUMAN - Isoform 11 of Troponin T, cardiac m...	100%	95	0.0000031
P45379-10	TNNT2_HUMAN - Isoform 10 of Troponin T, cardiac m...	100%	95	0.0000031
P45379-9	TNNT2_HUMAN - Isoform 9 of Troponin T, cardiac mu...	100%	95	0.0000031
P45379-8	TNNT2_HUMAN - Isoform 8 of Troponin T, cardiac mu...	100%	95	0.0000031
P45379-7	TNNT2_HUMAN - Isoform 7 of Troponin T, cardiac mu...	100%	95	0.0000031
P45379-6	TNNT2_HUMAN - Isoform 6 of Troponin T, cardiac mu...	100%	95	0.0000031
P45379-5	TNNT2_HUMAN - Isoform 5 of Troponin T, cardiac mu...	100%	95	0.0000031
P45379-4	TNNT2_HUMAN - Isoform 4 of Troponin T, cardiac mu...	100%	95	0.0000031
P45379-3	TNNT2_HUMAN - Isoform 3 of Troponin T, cardiac mu...	100%	95	0.0000031
P45379-2	TNNT2_HUMAN - Isoform 2 of Troponin T, cardiac mu...	100%	95	0.0000031
Q15607	Q15607_HUMAN - Cardiac troponin T	100%	95	0.0000031
A0A0A0MRJ4	A0A0A0MRJ4_HUMAN - Troponin T, cardiac muscle	100%	95	0.0000031
E7EPN8	E7EPN8_HUMAN - Troponin T, cardiac muscle	100%	95	0.0000031
A0A0A0MRJ5	A0A0A0MRJ5_HUMAN - Troponin T, cardiac muscle	100%	95	0.0000031
A9QLG2	A9QLG2_HUMAN - Troponin T type 2 cardiac	100%	95	0.0000031
Q15608	Q15608_HUMAN - Troponin T	100%	95	0.0000031
E7EPW4	E7EPW4_HUMAN - Troponin T, cardiac muscle	100%	95	0.0000031
A0A499FJM7	A0A499FJM7_HUMAN - Troponin T, cardiac muscle	100%	95	0.0000031
Q7Z554	Q7Z554_HUMAN - Troponin T cardiac isoform	100%	95	0.0000031
A0A024R953	A0A024R953_HUMAN - Troponin T type 2 (Cardiac), isofor...	100%	95	0.0000031
P45378	TNNT3_HUMAN - Troponin T, fast skeletal muscle	75%	68	0.020
P45378-7	TNNT3_HUMAN - Isoform 7 of Troponin T, fast skele...	75%	68	0.020
P45378-6	TNNT3_HUMAN - Isoform 6 of Troponin T, fast skele...	75%	68	0.020
P45378-5	TNNT3_HUMAN - Isoform 5 of Troponin T, fast skele...	75%	68	0.020
P45378-4	TNNT3_HUMAN - Isoform 4 of Troponin T, fast skele...	75%	68	0.020
P45378-3	TNNT3_HUMAN - Isoform 3 of Troponin T, fast skele...	75%	68	0.020
P45378-2	TNNT3_HUMAN - Isoform 2 of Troponin T, fast skele...	75%	68	0.020
C9JZN9	C9JZN9_HUMAN - Troponin T, fast skeletal muscle	75%	68	0.020
H9KVA2	H9KVA2_HUMAN - Troponin T, fast skeletal muscle	75%	68	0.020
A0A286YFB1	A0A286YFB1_HUMAN - Troponin T, fast skeletal muscle	75%	68	0.020
C9JCA5	C9JCA5_HUMAN - Troponin T, fast skeletal muscle	75%	68	0.020
F8WA37	F8WA37_HUMAN - Troponin T, fast skeletal muscle	75%	68	0.020
Q9UL16	CFA45_HUMAN - Cilia- and flagella-associated prot...	75%	66	0.038
Q9UL16-2	CFA45_HUMAN - Isoform 2 of Cilia- and flagella-as...	75%	66	0.038
A8K884	A8K884_HUMAN - cDNA FLJ77178	75%	66	0.038
A0A087X182	A0A087X182_HUMAN - Cilia- and flagella-associated prot...	75%	66	0.038
P13805	TNNT1_HUMAN - Troponin T, slow skeletal muscle	66.7%	60	0.26
P13805-3	TNNT1_HUMAN - Isoform 3 of Troponin T, slow skele...	66.7%	60	0.26
P13805-2	TNNT1_HUMAN - Isoform 2 of Troponin T, slow skele...	66.7%	60	0.26
M0QX01	M0QX01_HUMAN - Troponin T, slow skeletal muscle	66.7%	60	0.26
Q56R93	Q56R93_HUMAN - Nemaline myopathy mutant slow skele...	66.7%	60	0.26

Identifier	Name	Identity	Score	E-value
Q05DL6	Q05DL6_HUMAN - TNNT1 protein	66.7%	60	0.26
Q56R94	Q56R94_HUMAN - Nemaline myopathy mutant slow skele...	66.7%	60	0.26
K7EQL4	K7EQL4_HUMAN - Troponin T, slow skeletal muscle	66.7%	60	0.26
M0QZU8	M0QZU8_HUMAN - Troponin T, slow skeletal muscle	66.7%	60	0.26
A8K5N7	A8K5N7_HUMAN - cDNA FLJ75373, highly similar to Ho...	66.7%	60	0.26
M0QZY5	M0QZY5_HUMAN - Troponin T, slow skeletal muscle	66.7%	60	0.26
Q3B759	Q3B759_HUMAN - TNNT1 protein	66.7%	60	0.26
A0A024R4S3	A0A024R4S3_HUMAN - Troponin T type 1 (Skeletal, slow),...	66.7%	60	0.26
Q2NKX8	ERC6L_HUMAN - DNA excision repair protein ERCC-6-...	87.5%	54	1.8
B5MDQ0	B5MDQ0_HUMAN - DNA excision repair protein ERCC-6-...	87.5%	54	1.8
Q8IUD2	RB6I2_HUMAN - ELKS/Rab6-interacting/CAST family m...	63.6%	52	3.5
Q8IUD2-5	RB6I2_HUMAN - Isoform 5 of ELKS/Rab6-interacting/...	63.6%	52	3.5
Q8IUD2-4	RB6I2_HUMAN - Isoform 4 of ELKS/Rab6-interacting/...	63.6%	52	3.5
Q8IUD2-3	RB6I2_HUMAN - Isoform 3 of ELKS/Rab6-interacting/...	63.6%	52	3.5
Q8IUD2-2	RB6I2_HUMAN - Isoform 2 of ELKS/Rab6-interacting/...	63.6%	52	3.5
B4DG07	B4DG07_HUMAN - cDNA FLJ58159, highly similar to RA...	63.6%	52	3.5
X6RLX0	X6RLX0_HUMAN - ELKS/Rab6-interacting/CAST family m...	63.6%	52	3.5
G8JLD3	G8JLD3_HUMAN - ELKS/Rab6-interacting/CAST family m...	63.6%	52	3.5
X6RM00	X6RM00_HUMAN - ELKS/Rab6-interacting/CAST family m...	63.6%	52	3.5
O94844	RHBT1_HUMAN - Rho-related BTB domain-containing p...	70.0%	51	4.9
Q14244	MAP7_HUMAN - Ensconsin	63.6%	51	4.9
Q96JM4	LRIQ1_HUMAN - Leucine-rich repeat and IQ domain-c...	58.3%	51	4.9
Q14244-7	MAP7_HUMAN - Isoform 7 of Ensconsin	63.6%	51	4.9
Q14244-6	MAP7_HUMAN - Isoform 6 of Ensconsin	63.6%	51	4.9
Q14244-5	MAP7_HUMAN - Isoform 5 of Ensconsin	63.6%	51	4.9
Q14244-4	MAP7_HUMAN - Isoform 4 of Ensconsin	63.6%	51	4.9
Q14244-3	MAP7_HUMAN - Isoform 3 of Ensconsin	63.6%	51	4.9
Q14244-2	MAP7_HUMAN - Isoform 2 of Ensconsin	63.6%	51	4.9
Q96JM4-2	LRIQ1_HUMAN - Isoform 2 of Leucine-rich repeat an...	58.3%	51	4.9
A0A087WZ40	A0A087WZ40_HUMAN - Ensconsin	63.6%	51	4.9
B7Z3Y3	B7Z3Y3_HUMAN - cDNA FLJ50557, highly similar to Ho...	63.6%	51	4.9
B7ZB64	B7ZB64_HUMAN - cDNA, FLJ79428, highly similar to H...	63.6%	51	4.9
A0A140VJN5	A0A140VJN5_HUMAN - Testicular tissue protein Li 111	58.3%	51	4.9
B7Z3E1	B7Z3E1_HUMAN - cDNA FLJ50537, highly similar to Ho...	63.6%	51	4.9
B2R704	B2R704_HUMAN - cDNA, FLJ93207, highly similar to H...	63.6%	51	4.9
A0A024QZL4	A0A024QZL4_HUMAN - Rho-related BTB domain containing 1...	70.0%	51	4.9
Q9C0F0	ASXL3_HUMAN - Putative Polycomb group protein ASX...	72.7%	50	6.7
Q99996	AKAP9_HUMAN - A-kinase anchor protein 9	70.0%	50	6.7
Q99996-6	AKAP9_HUMAN - Isoform 6 of A-kinase anchor protei...	70.0%	50	6.7
Q99996-5	AKAP9_HUMAN - Isoform 5 of A-kinase anchor protei...	70.0%	50	6.7
Q99996-3	AKAP9_HUMAN - Isoform 3 of A-kinase anchor protei...	70.0%	50	6.7
Q99996-1	AKAP9_HUMAN - Isoform 1 of A-kinase anchor protei...	70.0%	50	6.7
A0A2R8Y461	A0A2R8Y461_HUMAN - Putative Polycomb group protein ASX...	72.7%	50	6.7
Q5GIA7	Q5GIA7_HUMAN - Antigen MU-RMS-40.16A	70.0%	50	6.7
A0A0A0MRF6	A0A0A0MRF6_HUMAN - A-kinase anchor protein 9	70.0%	50	6.7
A0A2R8Y590	A0A2R8Y590_HUMAN - A-kinase anchor protein 9	70.0%	50	6.7
Q96KG3	Q96KG3_HUMAN - AKAP350C	70.0%	50	6.7
Q9UFL2	Q9UFL2_HUMAN - Uncharacterized protein DKFZp564G22...	70.0%	50	6.7
A0A0A0MRE9	A0A0A0MRE9_HUMAN - A-kinase anchor protein 9	70.0%	50	6.7
Q14151	SAFB2_HUMAN - Scaffold attachment factor B2	70.0%	49	9.3
Q15424	SAFB1_HUMAN - Scaffold attachment factor B1	70.0%	49	9.3
Q8IXJ9	ASXL1_HUMAN - Putative Polycomb group protein ASX...	72.7%	49	9.3
Q15424-4	SAFB1_HUMAN - Isoform 4 of Scaffold attachment fa...	70.0%	49	9.3
Q15424-3	SAFB1_HUMAN - Isoform 3 of Scaffold attachment fa...	70.0%	49	9.3
Q15424-2	SAFB1_HUMAN - Isoform 2 of Scaffold attachment fa...	70.0%	49	9.3
Q8IXJ9-2	ASXL1_HUMAN - Isoform 2 of Putative Polycomb grou...	72.7%	49	9.3
B7ZLP5	B7ZLP5_HUMAN - SAFB protein	70.0%	49	9.3
B7Z2F6	B7Z2F6_HUMAN - cDNA FLJ54744, highly similar to Sc...	70.0%	49	9.3
A0A2R8Y5U1	A0A2R8Y5U1_HUMAN - Putative Polycomb group protein ASX...	72.7%	49	9.3
B7Z959	B7Z959_HUMAN - cDNA FLJ54736, highly similar to Sc...	70.0%	49	9.3
B7Z2Z1	B7Z2Z1_HUMAN - cDNA FLJ59523, highly similar to Sc...	70.0%	49	9.3
B3KVI8	B3KVI8_HUMAN - cDNA FLJ16604 fis, clone TESTI40080...	72.7%	49	9.3
B7Z1C7	B7Z1C7_HUMAN - cDNA FLJ59451, highly similar to Sc...	70.0%	49	9.3
A8K329	A8K329_HUMAN - cDNA FLJ76656, highly similar to Ho...	70.0%	49	9.3
K7EII0	K7EII0_HUMAN - Scaffold attachment factor B1	70.0%	49	9.3
B7Z5X3	B7Z5X3_HUMAN - cDNA FLJ59404, highly similar to Sc...	70.0%	49	9.3
A0A494C1R1	A0A494C1R1_HUMAN - Putative Polycomb group protein ASX...	72.7%	49	9.3
Q76L82	Q76L82_HUMAN - Additional sex combs like 1 (Drosop...	72.7%	49	9.3

Figure 15: Alignment of the cardiac and fast skeletal TnT isoforms cTnT (uniprot ID P45379) and fTnT (uniprot ID P45378). Similarities are highlighted in grey. Dark grey: Single, fully conserved residue. Medium grey: Strongly similar properties (scoring > 0.5 in the Gonnet PAM 250 matrix). Light grey: Weakly similar properties (scoring =< 0.5 in the Gonnet PAM 250 matrix). Adapted from uniprot.org (accessed 06.07.2019). The putative epitopes of the M7 and M11.7 antibodies are indicated.

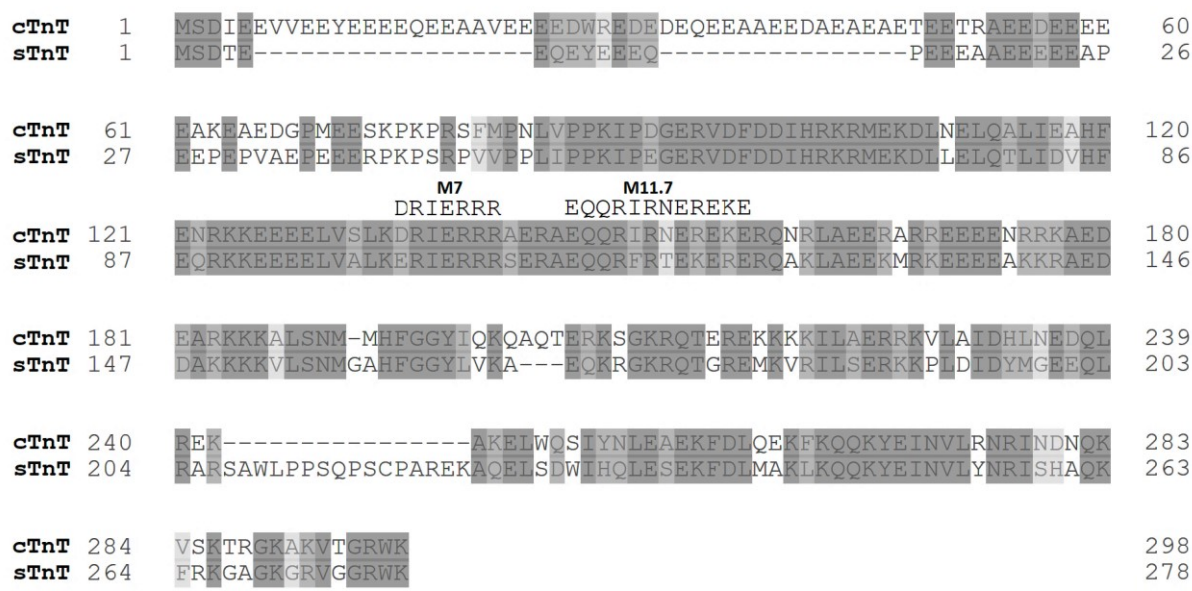

Figure 16: Alignment of the cardiac and slow skeletal TnT isoforms cTnT (uniprot ID P45379) and sTnT (uniprot ID P13805).
Similarities are highlighted in grey. Dark grey: Single, fully conserved residue. Medium grey: Strongly similar properties (scoring > 0.5 in the Gonnet PAM 250 matrix). Light grey: Weakly similar properties (scoring =< 0.5 in the Gonnet PAM 250 matrix). Adapted from uniprot.org (accessed 06.07.2019). The putative epitopes of the M7 and M11.7 antibodies are indicated.

To illustrate homology between cardiac and skeletal TnT isoforms an amino acid sequence alignment of cTnT, sTnT and fTnT was performed (**Figure 15** and **Figure 16**). A strong homology with cTnT was observed at the epitope of the M7 antibody especially for sTnT but also fTnT. At the M11.7 epitope three amino acid residues were different in fTnT (of which two have strongly similar properties) and four were different in sTnT (three with strongly similar and one with weakly similar properties).

4 DISCUSSION

Three main aspects of this study shall be discussed in the following paragraphs. First, one major finding is elevated cTnT plasma levels in a large proportion of patients with skeletal myopathies while cTnI is rarely elevated. Secondly, our results suggest that what causes cTnT elevation in most of these patients is likely a cross-reaction with skeletal muscle TnT. Thirdly, the cardiac phenotype of a cohort of rare skeletal muscle diseases was thoroughly characterised in this study, and this will be put in a larger context.

4.1 Cardiac Troponin T is elevated in patients with skeletal muscle disease

In our cohort the majority of patients (69%) had slightly to moderately elevated cTnT plasma levels (using the 99th percentile of a healthy reference population as a cut-off as recommended by cardiologic societies[6,31]), while at the same time only few patients had elevated cTnI (4%).

4.1.1 cTn elevation in skeletal muscle disease in other studies

This observation confirms previous reports by Rittoo et al.[18], who studied a total of 52 patients with different neuromuscular diseases that similarly showed a large proportion (82%) of abnormal plasma cTnT (Roche 4th generation or in part high-sensitive cTnT) while cTnI was largely normal (8% elevated cTnI with Siemens cTnI-Ultra). Recently Lilleker et al.[53] reported on a multicentre cohort of 123 patients with different inflammatory myopathies, of which 59% had elevated cTnT (Roche high-sensitive cTnT) and only 11% elevated cTnI (Siemens cTnI Ultra or Abbott ARCHITECT STAT cTnI). Wens et al. studied a cohort of 122 patients with Pompe disease and found elevated cTnT (high sensitive) in 82% and normal cTnI in all patients, however with a conventional cTnI assay (Beckmann Coulter, Access AccuTnI).[26] Though a certain difference between cTnT and cTnI in these studies may be explained by the different sensitivities of the assays used, the discrepancy between cTnT and cTnI was considerable and disproportional. The two cTn assays used in our study had well comparable sensitivities, both fulfilling criteria for so-called high sensitivity assays (defined as a total imprecision (CV) <10% at the 99th percentile value

and measurable concentrations above the assay's limit of detection for at least 50% of healthy individuals).[54]

Preceding studies with earlier generation and less sensitive assays had also reported on elevated cTnT in skeletal muscle disease. Elevated cTnT was found in 41% of 39 patients with polymyositis or dermatomyositis (3% elevated cTnI).[55] In DMD cohorts cTnT was elevated in 50% of 14 patients (all normal cTnI),[56] and in 58% of 50 patients.[57] Conversely, one study found a large proportion (71%) of elevated cTnI (Dade Behring Opus assay) in 129 DMD and BMD patients, yet without measuring cTnT, which raises the question if certain cTnI assays may suffer from similar problems as the cTnT test, as this finding could not be reproduced by others using different cTnI assays.[58] In contrast to affected male patients with X-linked dystrophinopathies, a study on 129 DMD or BMD female mutation carriers found only 2% elevated cTnT and no cTnI elevation.[59] In two cohorts of inclusion body myositis cTnT was elevated in 78% of 51 patients (2% elevated cTnI)[22] and in 62% of 42 patients[20].

The prevalence of elevated cTnT depends on the myopathy studied, since certain myopathies showed largely normal cTnT (e.g. non-dystrophic myotonias) in our cohort, while others had pronounced elevation, especially patients with different dystrophic myopathies, with particularly high levels in XMPMA and dystrophinopathies.

4.1.2 Chronic vs. acute cTnT elevation

In contrast to acute cardiomyocyte damage where cTn shows a peak with a rapid rise and fall pattern during the first days after the event,[7] cTnT elevation in skeletal muscle disease is a chronic condition with persistently high levels over time observed in our cohort and other studies.[18,20] Still a wide variation of measured cTnT concentrations over time has been reported[18] and indeed our study showed that there can be considerable short term fluctuations of cTnT levels that can pose a diagnostic challenge. The standard deviation of the three-hour-delta of cTnT was 9.4 ng/L, which means there is a relatively large variability considering an URL of 14 ng/L.

There are different approaches to assess the rise and fall pattern of cTn utilizing either absolute or relative changes in cTn levels. One universal perfect method and cut-off to

assess delta change from two measurements likely does not exist, as the change in cTn levels strongly depends on the point in time of sampling. This is because different points on the cTn concentration curve after an acute event (e.g. during upslope, peak or downslope) will result in grossly different deltas. Especially when the sampling-period includes the peak it is possible to have no delta at all from two measurements. Studies investigating the optimal delta-approach are difficult to perform and often suffer from various biases.[60] One study suggests the use of an absolute change is superior to a relative change.[61] Interestingly, they suggest a delta cTnT after two hours of 7 ng/L as a cut-off from ROC analysis which is well within our cohorts three-hour-delta's standard deviation. In a later publication, this study group proposed a two-hour algorithm to rule in myocardial infarction with a two-hour delta cut-off for cTnT of 10 ng/L or cTnT levels above 53 ng/L, which (though we used a three-hour interval) was the case in almost one third of the patients in our cohort. An ESC consensus approach uses three-hour sampling and relies on an absolute change (50% of the URL) in case of an initial cTn measurement below the URL and on a 20% relative change for initially elevated cTn (given the second measurement is above the URL).[62] Also with this algorithm almost one third of our patients would have been ruled in for myocardial infarction (**Figure 7**). The ESC algorithm has been validated recently and showed moderate performance with a sensitivity for cTnT of only 54%[63], largely owed to the dichotomous approach of the algorithm. Other algorithms mostly stratify patients into three groups (rule-out, observation and rule-in) and lately tend to use shorter intervals of two hours or even one hour.[49,64,65]

The variation of cTnT that was observed in our cohort without acute myocardial damage has two components, analytical variation and intra-individual biological variation. Analytical variation and imprecision is especially high at the lower end of the measurement range, as was the case in a cohort of healthy individuals with a very low median cTnT of 1.5 ng/L, where analytical CV was 53% and intra-individual CV was 48%.[66] At these low cTnT levels this imprecision necessitates a very high relative change (larger than 84% within four hours) to differentiate a rising pattern from analytical and biological variation,[66] which highlights the importance of using absolute change instead of relative change, especially in the lower measurement range. The claim for a low intra-assay CV of high sensitivity cTn assays (<10% at the URL)[54] therefore not only aims to ensure a correct

classification with regard to elevated and normal cTn levels, but also to reduce uncertainty in the assessment of dynamic cTn changes. As the analytical variation of the cTnT assay is low as demanded for a high sensitivity assay, most of the variation observed in our cohort can be explained by biological intra-individual variation, which was also the case in healthy individuals with low level cTnT, where hourly intra-individual CV was twice as high as analytical CV.[67] However, if assay cross-reaction with skeletal TnT is the main reason for cTnT elevation in our patients (see **section 4.2.3** below), the much lower affinity of the assay's antibodies to skeletal TnT will likely increase analytical imprecision and thus variability.

4.1.3 cTnT cut-off in skeletal muscle disease

Irrespective of the reason why cTnT is elevated in myopathic patients, using the same cTnT cut-off to diagnose myocardial infarction as in the general population does not seem appropriate. The cTnT cut-off (URL) is defined as the 99th percentile of a healthy reference population and has been determined in various cohorts for the high sensitive cTnT assay. The URL initially reported and usually used in clinical practice is 13.5 ng/L[17] and consecutive studies arrived at similar numbers, e.g. 15 ng/L,[68,69] 16.9 ng/L,[70] or 13.9 ng/L (males) and 11.3 ng/L (females), respectively.[71] Age and gender specific cut-offs have been proposed, and likewise higher cut-offs in myopathic patients would mitigate diagnostic uncertainties. Unfortunately, different myopathies also have different mean cTnT levels, necessitating large cohorts of every single skeletal muscle disease to establish normal values. Due to rarity and diversity of the countless skeletal muscle diseases this is an unrealistic claim, but could possibly be achieved in the more common myopathies such as myotonic dystrophies and dystrophinopathies. As cTnT levels are closely related to the extent of skeletal muscle involvement and CK and myoglobin levels, normalisation of cTnT levels for skeletal muscle markers would seem a simpler solution, if not limited by the fact that in acute myocardial infarction also the standard unspecific skeletal muscle markers show massive deflection (**Figure 17**). One reasonable approach may be to determine a "baseline" cTnT in patients with skeletal muscle disease as part of a routine cardiac evaluation, which can later be used as a reference in case the patient presents with an acute coronary syndrome.

Yet, the most obvious and simplest solution is the use of cTnI instead of cTnT, which is however subject to availability. Though generally cTnT and cTnI are very similar in their diagnostic accuracy,[7] in the specific case of coexisting skeletal muscle disease our study shows that cTnI may be the better choice for diagnosing acute myocardial injury.

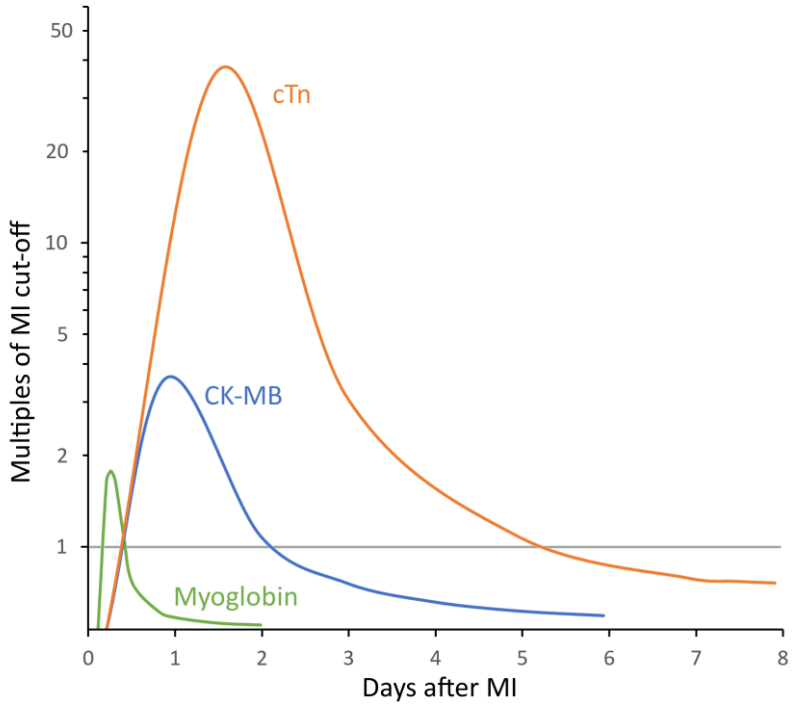

Figure 17: Schematic release kinetics of different cardiac markers after acute myocardial infarction (MI). (Image created based on Fig. 1 in Wu et al. [72])

In this context, there are reports that the cut-offs of the cTnT and cTnI assay are not biologically equivalent, at least in the acute setting. In one study, 18% of patients were inconsistently classified as myocardial infarction with either cTnT or cTnI (same assays as in our study), mainly because the cTnI cut-off had lower sensitivity compared to the cTnT cut-off. In that cohort a cTnI cut-off biologically equivalent to the 14 ng/L cTnT cut-off was calculated to be 8.7 ng/L instead of the 26.2 ng/L specified by the manufacturer.[73] Also in direct comparison of the two assays in a healthy population, the cTnI 99th percentile was lower at 13 ng/L,[69] however other studies arrived at a higher 99th percentile at 36 (males) and 15 ng/L (females)[68] or 39.0 (males) and 23.5 ng/L (females)[71]. Either way, a lower cTnI cut-off would not substantially change our results. Instead of 3 patients (4%) above the 26 ng/L cut-off only few more (7 patients, 9%) were above a lower 13 ng/L cTnI cut-off, compared to 51 patients (69%) with elevated cTnT.

4.1.4 Other conditions causing cTn elevation in the absence of myocardial infarction

There are other conditions that can cause chronic elevation of both cTnT and cTnI, such as chronic heart failure, arterial hypertension, significant valvular heart disease, chronic pulmonary hypertension, chronic kidney disease, anemia, diabetes mellitus, infiltrative cardiac diseases and drug cardiotoxicity. Also in the acute setting diseases other than myocardial infarction can cause cTn elevation, including myopericarditis, acute pulmonary embolism, acute heart failure, atrial tachyarrythmias, cardiac trauma, after stroke, in systemic hypotension, hypovolemia and sepsis.[74,75] Elevated cTn has also been observed after strenuous endurance exercise such as marathon runs.[76,77] Mechanisms are believed to be multifactorial and depending on the condition. They include myocardial ischemia due to decreased oxygen supply or increased oxygen demand, direct cardiomyocyte injury or excessive myocardial wall stress.[78] In renal disease an additional factor may be decreased cTn clearance from the circulation.[75] There are also analytical issues that may confound cTn measurements, including hemolysis, the presence of heterophilic antibodies, human antimouse antibodies or fibrin clots.[75]

cTn elevation not associated with acute coronary syndrome is frequent and can account for two thirds of observed cTn elevations in patients presenting at an emergency department[75] and more than half of cTn elevations in hospitalized patients.[79] Though not related to acute myocardial infarction these cTn elevations are of clinical significance as they can predict outcome and prognosis. cTnT was associated with increased all-cause mortality in patients with end stage renal disease,[80] it predicted cardiovascular death and heart failure in patients with stable coronary artery disease[81] and both cTnT and cTnI were associated with adverse outcomes in patients with acute and chronic heart failure.[82] Also in the general population the mostly normal but often detectable cTnT levels carry prognostic information.[83] If cTnT has predictive value also in skeletal myopathies still needs to be established.

4.2 Cardiac or skeletal muscle origin of measured plasma cardiac Troponin T in skeletal mucle disease

Several hypotheses could explain cTnT elevation and the discrepant finding of largely normal cTnI in skeletal myopathies. One explanation that leaves the presumed cardiac specificity of cTnT untouched is that cardiac involvement variably found in skeletal muscle diseases manifests in cTn release from the myocardium, while at the same time cTnT is more sensitive for these subtle cardiac changes than cTnI. Alternatively, cTnT may be re-expressed in diseased skeletal muscle and subsequently detected in the blood, which still leaves the claim of the assay's analytical specificity for cTnT unaffacted. Finally, myopathic skeletal muscle may release proteins different from cTnT into the circulation that are then spuriously detected by the assay due to cross-reaction. While our results favour the latter hypothesis, a combination of these mechanisms is possible.

4.2.1 Arguments for a cardiac origin

Certain skeletal muscle diseases are known to variably exhibit cardiac abnormalities, e.g. dystrophinopathies that develop a dilated cardiomyopathy[84] or XMPMA with an asymmetric mid-septal and apical hypertrophic cardiomyopathy.[29] In fact, these were the patient groups with most pronounced cTnT elevation in our study.

cTn can be elevated in patients with cardiomyopathies. In patients with hypertrophic cardiomyopathies elevated cTnT was found in 26-54% and elevated cTnI in 22%, both with high sensitivity assays.[85] cTn levels correlate with severity of myocardial hypertrophy, myocardial fibrosis and adverse events.[85–87] In a cohort of patients with Fabry disease 40% had elevated cTnT, which was also associated with fibrosis.[88] The mechanisms leading to cTn elevation in cardiomyopathies are not clear, but microvascular ischemia, increased myocyte death and replacement fibrosis have been proposed.[85]

Though in cardiomyopathies reports on grossly divergent results between cTnT and cTnI are not known, it must be noted that cTnT and cTnI are two different proteins with different biological behaviour. There is a bound myofilament fraction and a free cytoplasmatic fraction of cTn subunits in the cardiomyocyte. cTn release from cardiomyocytes not only happens in myocardial necrosis, but also via other more regulated mechanisms, such as the formation of membrane blebs where only the

cytosolic cTn fraction is released into the circulation.[89,90] Released cTnT is degraded within hours[91] and partially cleared by the kidneys.[89] In acute myocardial infarction cTnT and cTnI have markedly different release kinetics, with cTnT exhibiting a second peak at around day three after the acute event that is absent in cTnI, which is likely due to different compartimentation of the two proteins.[92,93] Though the author is not aware of extensive comparisons of cTnT and cTnI chronic release and degradation, it is quite conceivable that cTnT and cTnI behave differently in this respect, possibly rendering one more sensitive for subtle chronic myocardial damage. Additionally, the ability of a cTn assay to detect not only the intact protein but also degradation products is of major importance, as fragmented forms are prevailing both in acute and especially in chronic plasma cTn elevation.[89] Different cTnT and cTnI assays likely have different sensitivities for degradation products as they employ different antibodies. If the antibody epitopes or the sequence between the two epitopes of the capture and detection antibody include a cleavage site, the resulting degradation products will not be detected by the assay.

Thus, the divergent results between cTnT and cTnI could theoretically be explained by different release and degradation kinetics as well as different assay sensitivities.

4.2.2 Arguments for a skeletal muscle origin

Although different mechanisms may lead to divergent cTnT and cTnI levels, the discrepancy found in skeletal muscle disease is substantial and is consistently found not only in our study, but also in other cohorts and with various assays,[15,18,26,53] while other causes of chronic cTn elevation (e.g. chronic heart failure, chronic kidney disease, sepsis) seemingly affect both cTnT and cTnI.[94] Both markers are also frequently elevated in cardiomyopathies[85] and though concomitant cardiomyopathy would be the putative cause for a myocardium derived plasma cTn in skeletal muscle disease, here only cTnT is affected, indicating an origin other than the heart.

Patients with different dystrophic myopathies had most pronounced cTnT elevation when compared to non-dystrophic diseases (e.g. myotonia). While admittedly these myopathies more often exhibit cardiac abnormalities, they at the same time have more severe skeletal muscle involvement including muscle fibre degeneration and necrosis. This strong confounding factor makes it hard to differentiate a cardiac from a skeletal muscle origin

of plasma cTnT from clinical data alone. Still there are skeletal muscle diseases where a cardiac involvement is highly unlikely, namely primarily neuronal diseases with secondary muscle wasting such as ALS or SBMA. Though we had very few patients in this category in our cohort, they exhibited elevated cTnT which is in line with data from larger cohorts.[25]

We also tried to systematically analyse the association between cardiac abnormalities and cTn levels in our cohort and found that even though there was a small difference in absolute cTnT between patients with and without cardiac abnormalities, the proportion of elevated cTnT was not different. cTnI levels on the other hand, while mostly below the cut-off, were well associated with cardiac involvement.

Although we tried the best to apply valid criteria for defining cardiac involvement, our definition is still somewhat arbitrary. A more robust approach is the correlation analysis of serum markers of skeletal muscle injury and cTn, where we found a strong correlation between cTnT and skeletal muscle markers CK and myoglobin that are used clinically to assess the severity of skeletal muscle damage. This correlation has already been described for earlier generation assays,[21,55] and is absent in cTnI. Although CK and myoglobin are unspecific and are similarly expressed in myocardium, the high levels constantly present in skeletal muscle disease are highly unlikely to originate from the heart, and it can be assumed that these markers reflect the extent of skeletal muscle damage. CK has been shown to correlate well with the more specific skeletal TnI in skeletal muscle disease.[95] The unspecific cardiac CK isoform CK-MB is also expressed in skeletal muscle and therefore often found elevated in skeletal muscle disease.[51] Still the low proportion of CK-MB in total CK also indicates a skeletal origin of CK in our patients. Conversely, in a cohort of patients with acute rhabdomyolysis a recent study did not find an association of measured cTnT with CK while both cTnT and cTnI were elevated.[96] However, this is likely explained by the underlying diseases in this particular cohort which were “acutely medical” (not defined in detail) in the vast majority, where cTnT from a cardiac origin may be the main contributor to measured cTnT.

In summary, the discrepant results of cTnT and cTnI indicate a non-cardiac source of cTnT. The strong correlation of cTnT (and not cTnI) with markers of skeletal muscle damage implies a skeletal muscle origin, while at the same time the small association of cTnT with signs of cardiac involvement is to be interpreted as a confounding effect of more severe skeletal muscle involvement in myopathies with cardiac abnormalities.

4.2.3 Evidence of a cross-reaction with skeletal TnT

In order to support the suspicion of a skeletal muscle origin of measured plasma cTnT, we conducted several *in-vitro* experiments applying the antibodies used in the commercial cTnT and cTnI assays. In short, we did not find evidence of cTnT re-expression in diseased skeletal muscle, but cross-reactivity of the antibodies with a protein that likely resembles skeletal TnT.

Our central western blot experiment is depicted in **Figure 10**. Here we tested skeletal muscle biopsy specimen from patients with different myopathies and healthy control tissue (myocardium, liver, skeletal muscle) and applied both the capture and detection antibodies that are used in the cTnT and cTnI assay. The cTnI antibodies were only reactive with the positive control and proteins in the myocardial band, resembling cTnI at just below 30 kDa and smaller proteins that likely represent cTnI fragments. No band was observed in any of the skeletal muscle lanes. This result is what can be expected from cTnI specific antibodies.

In contrast, in the western blots probed with the cTnT antibodies (**Figure 10**, **C** and **D**) several unexpected bands were detected. One band appeared at approx. 60 kDa with the cTnT-M7 antibody that was present in all tissue samples including skeletal muscle and liver. This band may be caused by unspecific binding to albumin or a different protein other than Tn, because first, it is present in liver tissue and secondly, no Tn isoform was detected in this band with LC-MS/MS. Whatever protein causes this band, it is not relevant for a potential false-positive result of the commercial immunoassay as it is not detected with the capture antibody M11.7.

However, there were other bands that were detected with both antibodies and that can thus cause a cross-reaction of the assay. These one to three suspicious bands were present only in skeletal muscle lanes, irrespective of disease status, at a molecular weight lower than the cTnT bands. They potentially correspond to skeletal TnT, which is supported by LC-MS/MS results, where the skeletal isoforms sTnT or fTnT were present in all of these bands. Importantly, no cTnT could be detected with LC-MS/MS in these bands. Additionally, at the appropriate molecular weight of cTnT no bands were identified. Others have hypothesised that regeneration processes occurring in myopathic muscle

may cause abnormal protein expression of e.g. cardiac or fetal TnT isoforms.[15] Conversely, the suspicious bands were similarly present in diseased (**Figure 11**) and healthy (**Figure 12**) skeletal muscle specimens, which implies that this is not caused by an abnormal TnT expression pattern in diseased skeletal muscle, but rather that cross-reaction also occurs in healthy individuals.

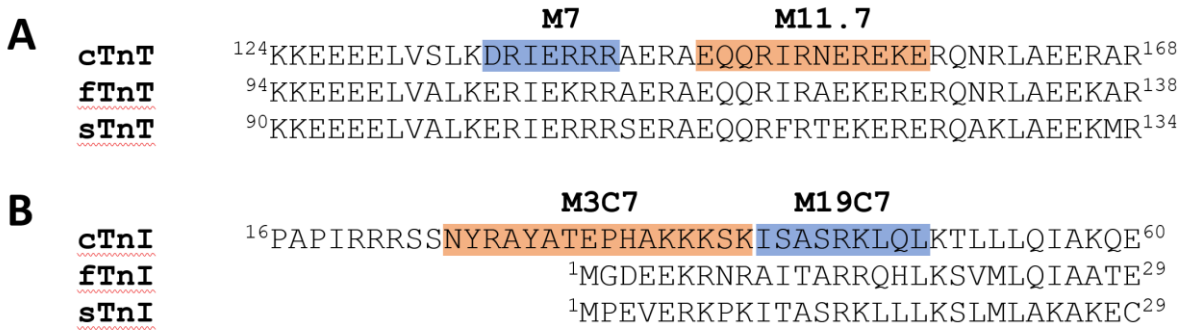

Figure 18: Alignment of sections of the TnT (**A**) and TnI (**B**) cardiac, fast skeletal and slow skeletal isoforms. The putative antibody epitopes are highlighted on the cardiac isoform: Capture antibody (*orange*), detection antibody (*blue*). Alignment from uniprot.org (accessed 30.11.2018). (Reproduced from [44] with permission of publisher)

A cross-reaction with skeletal TnT isoforms does not seem far-fetched when looking at the antibody epitopes on cTnT and the corresponding sequences of the skeletal isoforms (**Figure 18**). A marked homology between the isoforms in the region of the cTnT epitopes can be observed, with only one aspartate replaced by glutamate when comparing cTnT and sTnT at the M7 epitope, both amino acids having similar biochemical properties with both negatively charged side chains. Differences are slightly larger, but homology is still considerable at the M11.7 epitope, where in sTnT one isoleucine is replaced by phenylalanine (both hydrophobic side chains), one asparagine by threonine (both uncharged side chains), one arginine by lysine and one lysine by arginine (both positively charged side chains). Again, all of these amino acid substitutes share similar biochemical properties.

In contrast, the epitopes of the cTnI antibodies are even reaching over the end of the amino acid chain of the skeletal TnI isoforms for the capture antibody and only little homology is found for the detection antibody.

In this context, it should be noted that there are slightly differing reports of the cTnT epitopes in the literature. The manufacturer states, the M7 epitope comprises amino acid residues 125-131 (Roche Diagnostics package insert 2013-07, V 6.0 German), thereby

apparently referring to cTnT isoform 6 (the predominant isoform in adult heart) which is equivalent to 135-141 (DRIERRR) in the canonical isoform 1 (see **Figure 18**). Utilising mass spectrometric epitope mapping one study identified the M7 epitope as VSLKDRIEKR in bovine cTnT,[97] corresponding to residues 131-140 in human cTnT. The M11.7 antibody epitope is declared as comprising residues 146-157 (EQQRIRNEREKE), whereas the epitope was identified to be QQRIRAEREKER in bovine cTnT using an affinity based mass spectrometric approach,[98] which corresponds to residues 147-158 in human cTnT.

The findings in our western blots raise a high suspicion of a cross-reaction of the antibodies with skeletal muscle proteins, most likely skeletal TnT isoforms. To investigate if this cross-reaction also translates into false positive results in the commercial immunoassay we did an additional experiment where in a simulation of rhabdomyolysis we spiked healthy human plasma with healthy skeletal muscle homogenates and then measured cTnT, cTnI, CK and myoglobin concentrations (**Figure 13**). We found that cTnT measurements were dependent on the amount of skeletal muscle protein added. When compared to myocardium, much higher concentrations of skeletal muscle protein were necessary for cTnT measurements to become elevated, which shows that the cross reaction with skeletal muscle proteins, though present, is very small. On the contrary, in the same skeletal muscle spiked samples cTnI measurements, though also showing a slight increase at higher concentrations, stayed below the reference limit even at the highest input concentrations and were not markedly different and even slightly lower than in the samples spiked with liver tissue. To support that the cross-reacting protein is in fact skeletal TnT we similarly measured cTnT in healthy plasma samples after adding increasing concentrations of recombinant slow skeletal TnT and found a cross-reaction of 0.02%. Unfortunately, pure fast skeletal TnT was not available, so cross-reaction with the fast TnT isoform could not be assessed and may be different.

Recently, in reply to our data, Vroemen et al. reported a similar experiment with purified human skeletal TnT.[99] They also found increased measured cTnT dependent on skeletal TnT concentration. From their figure cross-reaction seems to be around 0.02%, similar to our result with recombinant slow skeletal TnT. The manufacturer states slightly deviating numbers and specifies cross-reaction with skeletal TnT as 0.003% (Roche Diagnostics package insert 2013-07, V 6.0 German).

Though the cross reaction of the cTnT assay is apparently very small, it can become relevant in patients with extensive skeletal muscle damage, especially when considering that in the human body skeletal muscle mass is approx. 100 times higher than myocardial mass. In our *in vitro* simulation of rhabdomyolysis, CK and myoglobin can serve as a rough estimate of the extent of skeletal muscle destruction in skeletal muscle disease. Yet, it must be noted that our model experiment does not account for the physiologically very different kinetics of these markers, with a more rapid release and clearance of myoglobin after skeletal muscle damage compared to CK.[100,101] Still at the highest skeletal muscle input concentration that resulted in markedly elevated cTnT measurements, CK was approx. 300 U/L and myoglobin approx. 2000 µg/L, concentrations also found in skeletal muscle disorders. In a larger cohort of DMD patients mean CK was 7443 U/L[102] and in a cohort of patients with rhabdomyolysis median peak CK was 8626 U/L and median peak myoglobin 3335 µg/L.[103] Though generally not as high as in acute rhabdomyolysis, skeletal muscle markers in our cohort showed a large variation, in the group of dystrophic myopathies median CK and myoglobin was 621 [234-1040] U/L and 156.5 [64.4-227.5] µg/L, respectively.

Research on skeletal Tn release in myopathy remains limited, but studies showed that CK and skeletal TnI are closely correlated[95] and skeletal TnI is elevated by several orders of magnitude in different forms of muscular dystrophies.[102] The author is not aware of studies focussing on skeletal TnT release in myopathy.

In contrast to cTnT where there is only one manufacturer of tests, there is a large number of different cTnI tests available, utilizing a diversity of antibodies and test principles and featuring different diagnostic accuracies. It is therefore important to note that the observed superiority of cTnI in our study with regard to false positive test results cannot be generalised to other cTnI assays. It is possible that other cTnI tests suffer from similar problems as the cTnT test.

4.2.4 cTnT re-expression or cross-reaction with skeletal TnT in the literature

The cTnT antibodies used in the commercial immunoassay are claimed to be highly specific for cTnT. In the original publication that evaluated the two cTnT antibodies, western blots with these antibodies did not show bands in skeletal muscle lanes.[12] This finding is different from our results and can potentially be explained with different sample preparation techniques, additional TnT purification and different exposure during western blot development. Nevertheless, there are hints of a certain cross-reactivity also in this validation study where at high concentrations of skeletal muscle protein the assay started to become positive.

One study compared cTnT concentrations (using the same antibodies) in different tissues. Measured cTnT concentrations were 1717 times higher in human myocardium than in skeletal muscle.[42] Such detection of cTnT in skeletal muscle is usually interpreted as cTnT expression in skeletal muscle,[24,42] but can similarly be explained by a small cross-reaction of the cTnT antibodies.

Using the same antibodies M7 and M11.7, Ricchiuti at al. reported positive bands in skeletal muscle specimens of patients with chronic kidney disease.[104] They argued that in all cases the cTnT epitopes detected with the capture antibody were on different proteins than the ones detected with the detection antibody and therefore an immunoassay using these two antibodies would not detect such isoforms. Similarly, Jaffe et al. used the same cTnT antibodies in western blots of skeletal muscle specimens of patients with skeletal myopathies.[15] They found positive bands of similar molecular weight with both antibodies and concluded that their results show that the claim for a unique specificity of the cTnT assay can not be sustained. It must be noted that the western blots presented in their publication do not necessarily allow to draw these conclusions. However, in contrast to our results, both studies did not report any positive bands in healthy skeletal muscle.[15,104]

The cTnT M7 antibody was used by Hammerer-Lercher et al. on western blots with skeletal muscle samples of DMD patients, however no positive bands were reported.[56] Valaperta et al. studied a cohort of patients with myotonic dystrophies and included western blots of skeletal muscle biopsies, they likewise did not report positive bands with the cTnT antibodies M7 and 5D8 (identical epitope of M11.7).[24] Only small snippets of the western blot gels are presented in these publications and apparent underexposure of gels may hide the faint bands that we detected in our experiments.

Messner et al. found mRNA expression of both cTnT and cTnI in skeletal muscle biopsies of patients with Duchenne muscular dystrophy, however the presence of cTnT or I on the protein level was not assessed.[105] Wens et al. reported their results of a large cohort of patients with Pompe disease.[26] They were not only able to identify mRNA of cTnT in skeletal muscle of their patients but also a tryptic peptide specific for cTnT by mass spectrometry. Their conclusion of cTnT expression in skeletal muscle in Pompe disease is based on the identification of fragments of one short cTnT peptide and may be of limited specificity. While Wens et al. did not detect cTnT in healthy skeletal muscle with their method, Vroemen et al.[99] detected western blot bands that are compatible with cTnT in a single sample of purified skeletal TnT. It may be argued that this finding may have been caused by contamination with cardiac protein in a purchased sample specified as having 95% purity.

In synopsis, our results are highly indicative of a cross-reaction of the cTnT assay with skeletal TnT isoforms, but there is some controversial evidence from other studies that favours re-expression of cTnT in skeletal muscle. Nonwithstanding our results, there may be certain myopathies with expression of cTnT in diseased skeletal muscle that we did not include in our study.

It also cannot be excluded that some additional myocardium derived cTnT adds to overall measured cTnT in certain conditions. Considering the low avidity of the cTnT antibodies to skeletal TnT, in the simultaneous presence of cTnT the effect of skeletal TnT on total measured cTnT levels will likely decrease due to competitive binding.

Yet, the largest contribution to elevated cTnT in skeletal muscle diseases is likely the discussed small cross-reaction in conjunction with grossly elevated skeletal Tn.

4.2.5 Limitations and outlook

Our suspicion of a cross reaction of the cTnT assay with skeletal TnT isoforms should be confirmed by similar experiments in larger samples of healthy and diseased tissue samples. The extent of cross-reaction could only be estimated for slow TnT and should also be tested for fast TnT.

Plasma levels of skeletal TnT isoforms have not been evaluated extensively in skeletal myopathies. The order of magnitude of skeletal TnT elevation is of interest, as high levels of skeletal TnT (expectedly similar to skeletal TnI[102]) would further support the hypothesis of a relevant cross-reaction. Also, the nature of plasma skeletal TnT with regard to what fragments and degradation products prevail can be helpful for further assay improvement and development.

The clinical significance of elevated cTnT in myopathies with respect to the incidence of diagnostic uncertainties and resulting unnecessary diagnostic workup still needs to be established.

4.3 Cardiac involvement in skeletal myopathies

Different myopathies exhibit different cardiac abnormalities with varying frequencies, ranging from a normal cardiac phenotype, subtle functional impairment or rhythm disorders, to increased incidence of sudden cardiac death or pronounced cardiomyopathy and heart failure.[106] Even within one specific skeletal myopathy, the cardiac phenotype can be highly variable. To predict cardiac involvement and associated cardiac risk in the individual patient is a difficult challenge. Studies that try to characterise cardiac involvement in these patients often suffer from a small sample size due to the rarity of skeletal muscle diseases. A lack of accounting for underlying coronary or other cardiovascular disease that has a high prevalence in the general population can potentially bias results towards a higher prevalence of cardiac involvement. In our study, patients with underlying cardiovascular disease could be identified and excluded, which allowed to assess the prevalence of genuine cardiac involvement. Our cohort reflects the patient collective presenting in a tertiary neuromuscular center and is a cross-section through the great variety of skeletal muscle disorders. The primary aim of the study was not to characterize myocardial involvement in a specific myopathy. Thus, the cohort is very heterogenious, and the report on infrequent myopathies can only be anecdotal. Still the more frequent diseases in our cohort could be analysed in more detail, especially myotonic dystrophies (DM) were prevalent enough to allow statistical analysis.

As DM are multisystem disorders, they involve not only skeletal muscle but also endocrine, central nervous, ophthalmologic, and other systems. Also cardiac involvement has been described, presence of cardiac abnormalities is variable, they often include conduction defects and arrhythmias[107], where the biggest concern is an increased risk of sudden cardiac death[108,109], which has been linked to severe ECG abnormalities.[110] In our study, although in most of the patients ECG findings were unremarkable using established cut-offs, in direct comparison to healthy controls, depolarisation (QRS time and BBB) and repolarisation (QTc interval) were significantly longer. Importantly, prolonged QTc has been shown to be associated with poorer prognosis in the general population.[111,112] Drugs that further prolong QTc intervals such as certain antibiotics or antidepressants should therefore be used with caution in these patients. In our study the PQ inverval prolongation reported in previous studies[24] was not as pronounced, still DM1 patients had longer PQ intervals than controls and one DM2 patient had 1st degree AV-block.

Left atrial volumes were larger in DM patients than in controls, especially in DM2 patients, that also exhibited higher LV mass. Concurrently, NT-proBNP, a biomarker reflecting diastolic wall stress and filling pressures, was also higher in these patients supporting the imaging findings. Of all DM patients, only one (4%) had a reduced EF below 50%. Using the same cut-off, previous studies found a slightly higher prevalence of impaired systolic left ventricular function between 9 and 19%.[113,114] However, 31% were below an EF cut-off of 55%, which is a larger proportion than the previously reported 12 to 18 % in studies applying this cut-off.[115,116] These deviating numbers between studies are likely a result of differences in methodology (echocardiography vs. MRI) and patient selection. Nevertheless, in direct comparison to a matched healthy cohort only DM1 patients had significantly reduced LV function as assessed by EF. While EF is a volumetric surrogate of LV function, GLS is a parameter of myocardial deformation thus more directly reflecting myocardial contraction. GLS was reported to be associated with cardiovascular events in DM1[117] and was slightly decreased in our DM1 patients.

LGE is a cMR marker of myocardial fibrosis. In our DM cohort only two patients (6.5%) had non-ischemic LGE, which is lower than in previous studies that reported a prevalence of myocardial fibrosis in DM between 14 and 40%.[116,118]

cTnT was often elevated in patients with myotonic dystrophies, in contrast to patients with non-dystrophic myotonias. This marker could thus support a clinical suspicion in patients with typical findings of myotonia before genetic workup.

The seven patients with non-dystrophic myotonias, apart from one patient with borderline EF, all had normal cardiac examinations.

Cardiac involvement was most pronounced in patients with certain dystrophic myopathies, especially XMPMA and dystrophinopathies.

XMPMA is known to be associated with spongiform cardiomyopathy that is charactarised by apical, myocardial fibrosis, and decreased systolic function.[29] Five patients with XMPMA were included in our study, of these three had LGE in cMR, EF was reduced in two, GLS was reduced in four, and one had atrial fibrillation. Two patients were in Lown category IV.

Patients with dystrophinopathies develop a well-studied dilated cardiomyopathy in the course of their disease.[84] Of the patients with proven DMD or BMD in our cohort, one patient with BMD had the most pronounced cardiac involvement. He had LGE in all myocardial segments, reduced EF, LBBB and a maximum of 42 VPB/h and several couplets and triplets in 24-hour ECG recordings.

Cardiac involvement in other dystrophic myopathies is less studied due to the rarity of diseases. In our four patients with FSHD one had RBBB, a common finding in FSHD[119], and prolonged QTc interval; two had suspected sinuatrial-block II.

Two young patients with LGMD 2A did not show any cardiac abnormalities.

Several patients suffered from a progressive muscular dystrophy, where a specific diagnosis had not been possible. Also, some of these patients had cardiac abnormalities, such as AV-block IIa and III, RBBB, repetitive VPBs, or raised NT-proBNP.

Our cohort also comprised 9 patients with inflammatory muscle diseases. In this group, one 67-year-old patient with sporadic IBM had one episode of supraventricular tachycardia in her 24-hour ECG, one patient had prolonged QTc, and another mildly reduced EF; otherwise no cardiac abnormalities were found.

Three patients had a primarily neuronal disease with consecutive muscle wasting. As expected, they showed no evidence of cardiac disease.

In summary, the prevalence of genuine cardiac involvement varies substantially between different myopathies and its severity is highly variable within disease entities. Cardiac abnormalities were prevalent especially in patients with dystrophic myopathies, whereas in non-dystrophic myotonia or inflammatory muscle disease cardiac involvement was rare in our cohort. These findings emphasise the necessity of cardiologic screening examinations especially in patients with dystrophic myopathies.[45]

With respect to cTnT, although presence of cardiac abnormalities was weakly associated with cTnT levels, there was no difference in the proportion of patients with elevated cTnT (**Table 8**). Thus, cTnT is not a useful parameter to determine cardiac involvement in skeletal myopathy.

4.4 Conclusion

This study confirmed previous reports on elevated cTnT in patients with skeletal myopathies and showed a pronounced disagreement with parallel cTnI measurements. According to our results, the predominant cause for cTnT elevation in these patients is a small cross-reaction with skeletal TnT isoforms, while a cardiac cTnT origin or re-expression of cTnT in diseased skeletal muscle could not be substantiated.

The prevalence of skeletal muscle disease is low in the general population, therefore in the vast majority of patients presenting with acute coronary syndrome, both cTnT and cTnI are excellent markers for diagnosing myocardial infarction, in line with current guidelines.[7] However, cTnI may be preferred in skeletal myopathies.

5 REFERENCES

1. Farah CS, Reinach FC. The troponin complex and regulation of muscle contraction. FASEB J. 1995;9:755–67.

2. Gomes AV, Potter JD, Szczesna-Cordary D. The Role of Troponins in Muscle Contraction. IUBMB Life. 2002;54:323–33.

3. Streng AS, de Boer D, van der Velden J, van Dieijen-Visser MP, Wodzig WKWH. Posttranslational modifications of cardiac troponin T: An overview. J Mol Cell Cardiol. 2013;63:47–56.

4. TNNT2 - Troponin T, cardiac muscle - Homo sapiens (Human) - TNNT2 gene & protein [Internet]. [cited 2018 Apr 26]. Available from: http://www.uniprot.org/uniprot/P45379

5. TNNI3 - Troponin I, cardiac muscle - Homo sapiens (Human) - TNNI3 gene & protein [Internet]. [cited 2018 Apr 26]. Available from: http://www.uniprot.org/uniprot/P19429

6. Alpert JS, Thygesen K, Antman E, Bassand JP. Myocardial infarction redefined—A consensus document of The Joint European Society of Cardiology/American College of Cardiology Committee for the Redefinition of Myocardial Infarction. Eur Heart J. 2000;21:1502–13.

7. Thygesen K, Alpert JS, Jaffe AS, Chaitman BR, Bax JJ, Morrow DA, et al. Fourth universal definition of myocardial infarction (2018). Eur Heart J. 2019;40:237–69.

8. Li D, Keffer J, Corry K, Vazquez M, Jialal I. Nonspecific elevation of troponin T levels in patients with chronic renal failure. Clin Biochem. 1995;28:474–7.

9. Katus HA, Haller C, Müller-Bardorff M, Scheffold T, Remppis A. Cardiac troponin T in end-stage renal disease patients undergoing chronic maintenance hemodialysis. Clin Chem. 1995;41:1201–3.

10. Kobayashi S, Tanaka M, Tamura N, Hashimoto H, Hirose S. Serum cardiac troponin T in polymyositis/dermatomyositis. Lancet. 1992;340:726.

11. Bodor GS, Survant L, Voss EM, Smith S, Porterfield D, Apple FS. Cardiac troponin T composition in normal and regenerating human skeletal muscle. Clin Chem. 1997;43:476–84.

12. Müller-Bardorff M, Hallermayer K, Schröder A, Ebert C, Borgya A, Gerhardt W, et al. Improved troponin T ELISA specific for cardiac troponin T isoform: assay development and analytical and clinical validation. Clin Chem. 1997;43:458–66.

13. Apple FS, Ricchiuti V, Voss EM, Anderson PA, Ney A, Odland M. Expression of cardiac troponin T isoforms in skeletal muscle of renal disease patients will not cause false-

positive serum results by the second generation cardiac troponin T assay. Eur Heart J. 1998;19 Suppl N:N30-33.

14. Haller C, Zehelein J, Remppis A, Müller-Bardorff M, Katus HA. Cardiac troponin T in patients with end-stage renal disease: absence of expression in truncal skeletal muscle. Clin Chem. 1998;44:930–8.

15. Jaffe AS, Vasile VC, Milone M, Saenger AK, Olson KN, Apple FS. Diseased Skeletal Muscle: a noncardiac source of increased circulating concentrations of cardiac troponin T. J Am Coll Cardiol. 2011;58:1819–24.

16. Thygesen K, Alpert JS, White HD, Joint ESC/ACCF/AHA/WHF Task Force for the Redefinition of Myocardial Infarction. Universal definition of myocardial infarction. Eur Heart J. 2007;28:2525–38.

17. Giannitsis E, Kurz K, Hallermayer K, Jarausch J, Jaffe AS, Katus HA. Analytical Validation of a High-Sensitivity Cardiac Troponin T Assay. Clin Chem. 2010;56:254–61.

18. Rittoo D, Jones A, Lecky B, Neithercut D. Elevation of cardiac troponin T, but not cardiac troponin I, in patients with neuromuscular diseases: implications for the diagnosis of myocardial infarction. J Am Coll Cardiol. 2014;63:2411–20.

19. Schwarzmeier JD, Hamwi A, Preisel M, Resl C, Preusser M, Sluga E, et al. Positive troponin T without cardiac involvement in inclusion body myositis. Hum Pathol. 2005;36:917–21.

20. Lindberg C, Klintberg L, Oldfors A. Raised troponin T in inclusion body myositis is common and serum levels are persistent over time. Neuromuscul Disord NMD. 2006;16:495–7.

21. Aggarwal R, Lebiedz-Odrobina D, Sinha A, Manadan A, Case JP. Serum cardiac troponin T, but not troponin I, is elevated in idiopathic inflammatory myopathies. J Rheumatol. 2009;36:2711–4.

22. Cox FM, Delgado V, Verschuuren JJ, Ballieux BE, Bax JJ, Wintzen AR, et al. The heart in sporadic inclusion body myositis: a study in 51 patients. J Neurol. 2010;257:447–51.

23. Egholm G, Pareek M. Drug-Induced Rhabdomyolysis with Elevated Cardiac Troponin T. Case Rep Med. 2015;2015:270204.

24. Valaperta R, Gaeta M, Cardani R, Lombardi F, Rampoldi B, De Siena C, et al. High-sensitive cardiac troponin T (hs-cTnT) assay as serum biomarker to predict cardiac risk in myotonic dystrophy: A case-control study. Clin Chim Acta Int J Clin Chem. 2016;463:122–8.

25. Mach L, Konecny T, Helanova K, Jaffe AS, Sorenson EJ, Somers VK, et al. Elevation of cardiac troponin T in patients with amyotrophic lateral sclerosis. Acta Neurol Belg. 2016;116:557–64.

26. Wens SCA, Schaaf GJ, Michels M, Kruijshaar ME, van Gestel TJM, In 't Groen S, et al. Elevated Plasma Cardiac Troponin T Levels Caused by Skeletal Muscle Damage in Pompe Disease. Circ Cardiovasc Genet. 2016;9:6–13.

27. Mannoji H, Hayashi F, Kubota T, Ikeda Y, Ishibashi-Ueda H, Kato S, et al. Differential Expression of Cardiac Troponin T and I in a Patient with Isolated Skeletal Muscular Sarcoidosis. Intern Med Tokyo Jpn. 2016;55:3215–7.

28. Sribhen K, Phankingthongkum R, Wannasilp N. Skeletal Muscle Disease as Noncardiac Cause of Cardiac Troponin T Elevation. J Am Coll Cardiol. 2012;59:1334–5.

29. Binder JS, Weidemann F, Schoser B, Niemann M, Machann W, Beer M, et al. Spongious Hypertrophic Cardiomyopathy in Patients With Mutations in the Four-and-a-Half LIM Domain 1 Gene. Circ Cardiovasc Genet. 2012;5:490–502.

30. World Medical Association. World Medical Association Declaration of Helsinki: ethical principles for medical research involving human subjects. JAMA. 2013;310:2191–4.

31. Thygesen K, Alpert JS, Jaffe AS, Simoons ML, Chaitman BR, White HD, et al. Third Universal Definition of Myocardial Infarction. J Am Coll Cardiol. 2012;60:1581–98.

32. Saenger AK, Beyrau R, Braun S, Cooray R, Dolci A, Freidank H, et al. Multicenter analytical evaluation of a high-sensitivity troponin T assay. Clin Chim Acta Int J Clin Chem. 2011;412:748–54.

33. Krintus M, Kozinski M, Boudry P, Capell NE, Köller U, Lackner K, et al. European multicenter analytical evaluation of the Abbott ARCHITECT STAT high sensitive troponin I immunoassay. Clin Chem Lab Med. 2014;52:1657–65.

34. Zhou X, Zhu D, Liao Y, Liu W, Liu H, Ma Z, et al. Synthesis, labeling and bioanalytical applications of a tris(2,2'-bipyridyl)ruthenium(II)-based electrochemiluminescence probe. Nat Protoc. 2014;9:1146–59.

35. Lown B, Wolf M. Approaches to sudden death from coronary heart disease. Circulation. 1971;44:130–42.

36. Nagueh SF, Smiseth OA, Appleton CP, Byrd BF, Dokainish H, Edvardsen T, et al. Recommendations for the Evaluation of Left Ventricular Diastolic Function by Echocardiography: An Update from the American Society of Echocardiography and the European Association of Cardiovascular Imaging. Eur Heart J Cardiovasc Imaging. 2016;17:1321–60.

37. Ingul CB, Torp H, Aase SA, Berg S, Stoylen A, Slordahl SA. Automated analysis of strain rate and strain: feasibility and clinical implications. J Am Soc Echocardiogr. 2005;18:411–8.

38. Schmid J, Kaufmann R, Grübler MR, Verheyen N, Weidemann F, Binder JS. Strain Analysis by Tissue Doppler Imaging: Comparison of Conventional Manual Measurement with a Semiautomated Approach. Echocardiogr Mt Kisco N. 2016;33:372–8.

39. Kramer CM, Barkhausen J, Flamm SD, Kim RJ, Nagel E, Society for Cardiovascular Magnetic Resonance, et al. Standardized cardiovascular magnetic resonance (CMR) protocols 2013 update. J Cardiovasc Magn Reson. 2013;15:91.

40. Yancy CW, Jessup M, Bozkurt B, Butler J, Casey DE, Drazner MH, et al. 2013 ACCF/AHA guideline for the management of heart failure: a report of the American College of Cardiology Foundation/American Heart Association Task Force on Practice Guidelines. J Am Coll Cardiol. 2013;62:e147-239.

41. Kawel-Boehm N, Maceira A, Valsangiacomo-Buechel ER, Vogel-Claussen J, Turkbey EB, Williams R, et al. Normal values for cardiovascular magnetic resonance in adults and children. J Cardiovasc Magn Reson Off J Soc Cardiovasc Magn Reson. 2015;17:29.

42. Fredericks S, Merton GK, Lerena MJ, Heining P, Carter ND, Holt DW. Cardiac troponins and creatine kinase content of striated muscle in common laboratory animals. Clin Chim Acta Int J Clin Chem. 2001;304:65–74.

43. Haus JM, Carrithers JA, Carroll CC, Tesch PA, Trappe TA. Contractile and connective tissue protein content of human skeletal muscle: effects of 35 and 90 days of simulated microgravity and exercise countermeasures. Am J Physiol - Regul Integr Comp Physiol. 2007;293:R1722–7.

44. Schmid J, Liesinger L, Birner-Gruenberger R, Stojakovic T, Scharnagl H, Dieplinger B, et al. Elevated Cardiac Troponin T in Patients With Skeletal Myopathies. J Am Coll Cardiol. 2018;71:1540–9.

45. Schmid J, Beer M, Berghold A, Stojakovic T, Scharnagl H, Dieplinger B, et al. Cardiac involvement in a cross-sectional cohort of myotonic dystrophies and other skeletal myopathies. ESC Heart Fail. 2020;(accepted manuscript).

46. Lang RM, Badano LP, Mor-Avi V, Afilalo J, Armstrong A, Ernande L, et al. Recommendations for cardiac chamber quantification by echocardiography in adults: an update from the American Society of Echocardiography and the European Association of Cardiovascular Imaging. Eur Heart J Cardiovasc Imaging. 2015;16:233–70.

47. Ponikowski P, Voors AA, Anker SD, Bueno H, Cleland JGF, Coats AJS, et al. 2016 ESC Guidelines for the diagnosis and treatment of acute and chronic heart failure: The Task Force for the diagnosis and treatment of acute and chronic heart failure of the

European Society of Cardiology (ESC). Developed with the special contribution of the Heart Failure Association (HFA) of the ESC. Eur J Heart Fail. 2016;18:891–975.

48. Dickstein K, Cohen-Solal A, Filippatos G, McMurray JJV, Ponikowski P, Poole-Wilson PA, et al. ESC Guidelines for the diagnosis and treatment of acute and chronic heart failure 2008: the Task Force for the Diagnosis and Treatment of Acute and Chronic Heart Failure 2008 of the European Society of Cardiology. Developed in collaboration with the Heart Failure Association of the ESC (HFA) and endorsed by the European Society of Intensive Care Medicine (ESICM). Eur Heart J. 2008;29:2388–442.

49. Reichlin T, Cullen L, Parsonage WA, Greenslade J, Twerenbold R, Moehring B, et al. Two-hour Algorithm for Triage Toward Rule-out and Rule-in of Acute Myocardial Infarction Using High-sensitivity Cardiac Troponin T. Am J Med. 2015;128:369–79.

50. Roffi M, Patrono C, Collet J-P, Mueller C, Valgimigli M, Andreotti F, et al. 2015 ESC Guidelines for the management of acute coronary syndromes in patients presenting without persistent ST-segment elevation: Task Force for the Management of Acute Coronary Syndromes in Patients Presenting without Persistent ST-Segment Elevation of the European Society of Cardiology (ESC). Eur Heart J. 2016;37:267–315.

51. Lott JA, Landesman PW. The enzymology of skeletal muscle disorders. Crit Rev Clin Lab Sci. 1984;20:153–90.

52. UniProt [Internet]. [cited 2015 Jun 28]. Available from: http://www.uniprot.org/

53. Lilleker JB, Diederichsen ACP, Jacobsen S, Guy M, Roberts ME, Sergeant JC, et al. Using serum troponins to screen for cardiac involvement and assess disease activity in the idiopathic inflammatory myopathies. Rheumatol Oxf Engl. 2018;57:1041–6.

54. Apple FS, Collinson PO, IFCC Task Force on Clinical Applications of Cardiac Biomarkers. Analytical characteristics of high-sensitivity cardiac troponin assays. Clin Chem. 2012;58:54–61.

55. Erlacher P, Lercher A, Falkensammer J, Nassonov EL, Samsonov MI, Shtutman VZ, et al. Cardiac troponin and β-type myosin heavy chain concentrations in patients with polymyositis or dermatomyositis. Clin Chim Acta. 2001;306:27–33.

56. Hammerer-Lercher A, Erlacher P, Bittner R, Korinthenberg R, Skladal D, Sorichter S, et al. Clinical and experimental results on cardiac troponin expression in Duchenne muscular dystrophy. Clin Chem. 2001;47:451–8.

57. Ergul Y, Ekici B, Nisli K, Tatli B, Binboga F, Acar G, et al. Evaluation of the North Star Ambulatory Assessment scale and cardiac abnormalities in ambulant boys with Duchenne muscular dystrophy. J Paediatr Child Health. 2012;48:610–6.

58. Castro-Gago M, Gómez-Lado C, Eirís-Puñal J. Cardiac troponin I for accurate evaluation of cardiac status in myopathic patients. Brain Dev. 2009;31:184.

59. Hoogerwaard EM, Schouten Y, van der Kooi AJ, Gorgels JP, de Visser M, Sanders GT. Troponin T and troponin I in carriers of Duchenne and Becker muscular dystrophy with cardiac involvement. Clin Chem. 2001;47:962–3.

60. Jaffe AS, Moeckel M, Giannitsis E, Huber K, Mair J, Mueller C, et al. In search for the Holy Grail: Suggestions for studies to define delta changes to diagnose or exclude acute myocardial infarction: a position paper from the study group on biomarkers of the Acute Cardiovascular Care Association. Eur Heart J Acute Cardiovasc Care. 2014;3:313–6.

61. Reichlin T, Irfan A, Twerenbold R, Reiter M, Hochholzer W, Burkhalter H, et al. Utility of absolute and relative changes in cardiac troponin concentrations in the early diagnosis of acute myocardial infarction. Circulation. 2011;124:136–45.

62. Thygesen K, Mair J, Giannitsis E, Mueller C, Lindahl B, Blankenberg S, et al. How to use high-sensitivity cardiac troponins in acute cardiac care. Eur Heart J. 2012;33:2252–7.

63. Pickering JW, Greenslade JH, Cullen L, Flaws D, Parsonage W, George P, et al. Validation of presentation and 3 h high-sensitivity troponin to rule-in and rule-out acute myocardial infarction. Heart Br Card Soc. 2016;102:1270–8.

64. Reichlin T, Schindler C, Drexler B, Twerenbold R, Reiter M, Zellweger C, et al. One-Hour Rule-out and Rule-in of Acute Myocardial Infarction Using High-Sensitivity Cardiac Troponin T. Arch Intern Med. 2012;172:1211.

65. Than M, Cullen L, Aldous S, Parsonage WA, Reid CM, Greenslade J, et al. 2-Hour accelerated diagnostic protocol to assess patients with chest pain symptoms using contemporary troponins as the only biomarker: the ADAPT trial. J Am Coll Cardiol. 2012;59:2091–8.

66. Vasile VC, Saenger AK, Kroning JM, Jaffe AS. Biological and Analytical Variability of a Novel High-Sensitivity Cardiac Troponin T Assay. Clin Chem. 2010;56:1086–90.

67. Frankenstein L, Wu AHB, Hallermayer K, Wians FH, Giannitsis E, Katus HA. Biological variation and reference change value of high-sensitivity troponin T in healthy individuals during short and intermediate follow-up periods. Clin Chem. 2011;57:1068–71.

68. Apple FS, Ler R, Murakami MM. Determination of 19 cardiac troponin I and T assay 99th percentile values from a common presumably healthy population. Clin Chem. 2012;58:1574–81.

69. Kimenai DM, Henry RM, van der Kallen CJ, Dagnelie PC, Schram MT, Stehouwer CD, et al. Direct comparison of clinical decision limits for cardiac troponin T and I. Heart. 2016;102:610–6.

70. Chenevier-Gobeaux C, Meune C, Blanc M-C, Cynober L, Jaffray P, Lefevre G. Analytical evaluation of a high-sensitivity troponin T assay and its clinical assessment in acute coronary syndrome. Ann Clin Biochem. 2011;48:452–8.

71. Mueller T, Egger M, Leitner I, Gabriel C, Haltmayer M, Dieplinger B. Reference values of galectin-3 and cardiac troponins derived from a single cohort of healthy blood donors. Clin Chim Acta Int J Clin Chem. 2016;456:19–23.

72. Wu AH, Apple FS, Gibler WB, Jesse RL, Warshaw MM, Valdes R. National Academy of Clinical Biochemistry Standards of Laboratory Practice: recommendations for the use of cardiac markers in coronary artery diseases. Clin Chem. 1999;45:1104–21.

73. Wildi K, Gimenez MR, Twerenbold R, Reichlin T, Jaeger C, Heinzelmann A, et al. Misdiagnosis of Myocardial Infarction Related to Limitations of the Current Regulatory Approach to Define Clinical Decision Values for Cardiac Troponin. Circulation. 2015;131:2032–40.

74. Park KC, Gaze DC, Collinson PO, Marber MS. Cardiac troponins: from myocardial infarction to chronic disease. Cardiovasc Res. 2017;113:1708–18.

75. Giannitsis E, Katus HA. Cardiac troponin level elevations not related to acute coronary syndromes. Nat Rev Cardiol. 2013;10:623–34.

76. Roca E, Nescolarde L, Lupón J, Barallat J, Januzzi JL, Liu P, et al. The Dynamics of Cardiovascular Biomarkers in non-Elite Marathon Runners. J Cardiovasc Transl Res. 2017;10:206–8.

77. Lippi G, Schena F, Salvagno GL, Tarperi C, Aloe R, Guidi GC. Comparison of conventional and highly-sensitive troponin I measurement in ultra-marathon runners. J Thromb Thrombolysis. 2012;33:338–42.

78. Jeremias A, Gibson CM. Narrative review: alternative causes for elevated cardiac troponin levels when acute coronary syndromes are excluded. Ann Intern Med. 2005;142:786–91.

79. McFalls EO, Larsen G, Johnson GR, Apple FS, Goldman S, Arai A, et al. Outcomes of hospitalized patients with non-acute coronary syndrome and elevated cardiac troponin level. Am J Med. 2011;124:630–5.

80. Khan NA, Hemmelgarn BR, Tonelli M, Thompson CR, Levin A. Prognostic value of troponin T and I among asymptomatic patients with end-stage renal disease: a meta-analysis. Circulation. 2005;112:3088–96.

81. Omland T, de Lemos JA, Sabatine MS, Christophi CA, Rice MM, Jablonski KA, et al. A sensitive cardiac troponin T assay in stable coronary artery disease. N Engl J Med. 2009;361:2538–47.

82. Kociol RD, Pang PS, Gheorghiade M, Fonarow GC, O'Connor CM, Felker GM. Troponin elevation in heart failure prevalence, mechanisms, and clinical implications. J Am Coll Cardiol. 2010;56:1071–8.

83. de Lemos JA, Drazner MH, Omland T, Ayers CR, Khera A, Rohatgi A, et al. Association of troponin T detected with a highly sensitive assay and cardiac structure and mortality risk in the general population. JAMA. 2010;304:2503–12.

84. Yilmaz A, Sechtem U. Cardiac involvement in muscular dystrophy: advances in diagnosis and therapy. Heart. 2012;98:420–9.

85. Kehl DW, Buttan A, Siegel RJ, Rader F. Clinical utility of natriuretic peptides and troponins in hypertrophic cardiomyopathy. Int J Cardiol. 2016;218:252–8.

86. Hasler S, Manka R, Greutmann M, Gämperli O, Schmied C, Tanner FC, et al. Elevated high-sensitivity troponin T levels are associated with adverse cardiac remodelling and myocardial fibrosis in hypertrophic cardiomyopathy. Swiss Med Wkly. 2016;146:w14285.

87. Gawor M, Śpiewak M, Kubik A, Wróbel A, Lutyńska A, Marczak M, et al. Circulating biomarkers of hypertrophy and fibrosis in patients with hypertrophic cardiomyopathy assessed by cardiac magnetic resonance. Biomark Biochem Indic Expo Response Susceptibility Chem. 2018;23:676–82.

88. Seydelmann N, Liu D, Krämer J, Drechsler C, Hu K, Nordbeck P, et al. High-Sensitivity Troponin: A Clinical Blood Biomarker for Staging Cardiomyopathy in Fabry Disease. J Am Heart Assoc. 2016;5:e002839.

89. Hammarsten O, Mair J, Möckel M, Lindahl B, Jaffe AS. Possible mechanisms behind cardiac troponin elevations. Biomark Biochem Indic Expo Response Susceptibility Chem. 2018;23:725–34.

90. Hickman PE, Potter JM, Aroney C, Koerbin G, Southcott E, Wu AHB, et al. Cardiac troponin may be released by ischemia alone, without necrosis. Clin Chim Acta. 2010;411:318–23.

91. Cardinaels EPM, Mingels AMA, Rooij T van, Collinson PO, Prinzen FW, Dieijen-Visser MP van. Time-Dependent Degradation Pattern of Cardiac Troponin T Following Myocardial Infarction. Clin Chem. 2013;59:1083–90.

92. Laugaudin G, Kuster N, Petiton A, Leclercq F, Gervasoni R, Macia J-C, et al. Kinetics of high-sensitivity cardiac troponin T and I differ in patients with ST-segment elevation myocardial infarction treated by primary coronary intervention. Eur Heart J Acute Cardiovasc Care. 2016;5:354–63.

93. Katus HA, Remppis A, Scheffold T, Diederich KW, Kuebler W. Intracellular compartmentation of cardiac troponin T and its release kinetics in patients with reperfused and nonreperfused myocardial infarction. Am J Cardiol. 1991;67:1360–7.

94. Newby LK, Jesse RL, Babb JD, Christenson RH, De Fer TM, Diamond GA, et al. ACCF 2012 expert consensus document on practical clinical considerations in the interpretation of troponin elevations: a report of the American College of Cardiology Foundation task force on Clinical Expert Consensus Documents. J Am Coll Cardiol. 2012;60:2427–63.

95. Kiely P, Bruckner F, Nisbet J, Daghir A. Serum skeletal troponin I in inflammatory muscle disease: relation to creatine kinase, CKMB and cardiac troponin I. Ann Rheum Dis. 2000;59:750–1.

96. du Fay de Lavallaz J, Zehntner T, Puelacher C, Walter J, Strebel I, Rentsch K, et al. Rhabdomyolysis: A Noncardiac Source of Increased Circulating Concentrations of Cardiac Troponin T? J Am Coll Cardiol. 2018;72:2936–7.

97. Macht M, Fiedler W, Kürzinger K, Przybylski M. Mass spectrometric mapping of protein epitope structures of myocardial infarct markers myoglobin and troponin T. Biochemistry. 1996;35:15633–9.

98. Deininger S-O, Macht M, Marquardt A, Przybylski M, Damoc E, Kohlmann M. 'Affinity-proteomics': direct protein identification from biological material using mass spectrometric epitope mapping. Anal Bioanal Chem. 2004;378:1102–11.

99. Vroemen WHM, de Boer D, Streng AS, Mingels AMA, Meex SJR. Elevated Cardiac Troponin T in Skeletal Myopathies: Skeletal TnT Cross-Reactivity and/or Cardiac TnT Expression? J Am Coll Cardiol. 2018;72:347–9.

100. Lippi G, Schena F, Salvagno GL, Montagnana M, Gelati M, Tarperi C, et al. Acute variation of biochemical markers of muscle damage following a 21-km, half-marathon run. Scand J Clin Lab Invest. 2008;68:667–72.

101. Ahmadi S, Sinclair PJ, Davis GM. Muscle oxygenation after downhill walking-induced muscle damage. Clin Physiol Funct Imaging. 2008;28:55–63.

102. Burch PM, Pogoryelova O, Goldstein R, Bennett D, Guglieri M, Straub V, et al. Muscle-Derived Proteins as Serum Biomarkers for Monitoring Disease Progression in Three Forms of Muscular Dystrophy. J Neuromuscul Dis. 2015;2:241–55.

103. Kasaoka S, Todani M, Kaneko T, Kawamura Y, Oda Y, Tsuruta R, et al. Peak value of blood myoglobin predicts acute renal failure induced by rhabdomyolysis. J Crit Care. 2010;25:601–4.

104. Ricchiuti V, Voss EM, Ney A, Odland M, Anderson PA, Apple FS. Cardiac troponin T isoforms expressed in renal diseased skeletal muscle will not cause false-positive results by the second generation cardiac troponin T assay by Boehringer Mannheim. Clin Chem. 1998;44:1919–24.

105. Messner B, Baum H, Fischer P, Quasthoff S, Neumeier D. Expression of messenger RNA of the cardiac isoforms of troponin T and I in myopathic skeletal muscle. Am J Clin Pathol. 2000;114:544–9.

106. Arbustini E, Di Toro A, Giuliani L, Favalli V, Narula N, Grasso M. Cardiac Phenotypes in Hereditary Muscle Disorders: JACC State-of-the-Art Review. J Am Coll Cardiol. 2018;72:2485–506.

107. Lau JK, Sy RW, Corbett A, Kritharides L. Myotonic dystrophy and the heart: A systematic review of evaluation and management. Int J Cardiol. 2015;184:600–8.

108. Mathieu J, Allard P, Potvin L, Prévost C, Bégin P. A 10-year study of mortality in a cohort of patients with myotonic dystrophy. Neurology. 1999;52:1658–62.

109. Schoser BGH, Ricker K, Schneider-Gold C, Hengstenberg C, Dürre J, Bültmann B, et al. Sudden cardiac death in myotonic dystrophy type 2. Neurology. 2004;63:2402–4.

110. Groh WJ, Groh MR, Saha C, Kincaid JC, Simmons Z, Ciafaloni E, et al. Electrocardiographic Abnormalities and Sudden Death in Myotonic Dystrophy Type 1. N Engl J Med. 2008;358:2688–97.

111. Elming H, Holm E, Jun L, Torp-Pedersen C, Køber L, Kircshoff M, et al. The prognostic value of the QT interval and QT interval dispersion in all-cause and cardiac mortality and morbidity in a population of Danish citizens. Eur Heart J. 1998;19:1391–400.

112. Straus SMJM, Kors JA, De Bruin ML, van der Hooft CS, Hofman A, Heeringa J, et al. Prolonged QTc Interval and Risk of Sudden Cardiac Death in a Population of Older Adults. J Am Coll Cardiol. 2006;47:362–7.

113. Tanawuttiwat T, Tomaselli G, Nazarian S. The Controversial Epidemiology of Left Ventricular Dysfunction in Patients With Myotonic Dystrophy Type 1-Reply. JAMA Cardiol. 2017;2:1044–1045.

114. Bhakta D, Groh MR, Shen C, Pascuzzi RM, Groh WJ. Increased mortality with left ventricular systolic dysfunction and heart failure in adults with myotonic dystrophy type 1. Am Heart J. 2010;160:1137–41.

115. Wahbi K, Meune C, Bécane HM, Laforêt P, Bassez G, Lazarus A, et al. Left ventricular dysfunction and cardiac arrhythmias are frequent in type 2 myotonic dystrophy: A case control study. Neuromuscul Disord. 2009;19:468–72.

116. Tanawuttiwat T, Wagner KR, Tomaselli G, Nazarian S. Left Ventricular Dysfunction and Conduction Disturbances in Patients With Myotonic Muscular Dystrophy Type I and II. JAMA Cardiol. 2017;2:225–8.

117. Garcia R, Rehman M, Goujeau C, Degand B, Le Gal F, Stordeur B, et al. Left ventricular longitudinal strain impairment predicts cardiovascular events in asymptomatic type 1 myotonic dystrophy. Int J Cardiol. 2017;243:424–30.

118. Petri H, Ahtarovski KA, Vejlstrup N, Vissing J, Witting N, Køber L, et al. Myocardial fibrosis in patients with myotonic dystrophy type 1: a cardiovascular magnetic resonance study. J Cardiovasc Magn Reson. 2014;16:59.

119. Labombarda F, Maurice M, Simon J-P, Legallois D, Guyant-Maréchal L, Bedat-Millet A-L, et al. Cardiac Abnormalities in Type 1 Facioscapulohumeral Muscular Dystrophy. J Clin Neuromuscul Dis. 2017;18:199–206.

APPENDIX

Preliminary western blots

In order to set up the planned Western Blot experiments on diseased skeletal muscle specimens, healthy myocardial and skeletal muscle tissue obtained at autopsy was used. Different sample preparation techniques were compared and the following antibodies provided by Roche Diagnostics were tested: The two monoclonal mouse anti-cTnT antibodies M7 and M11.7 and the two monoclonal mouse anti-cTnI antibodies (M3C7 and M19C7) detect the same epitopes as the antibodies used in the respective commercial cTnT and cTnI immunoassay.

Rec-hcTnI was provided by Roche Diagnostics, pure rec-hcTnT was purchased from Sigma Aldrich (T0175).

Sample preparation:

Two methods for sample preparation were compared:

Ultraturax preparation: 80-110mg tissue was weighed in with a tenfold amount of buffer solution (aqueous solution of 10mM Dithiothreitol, 100mM Triethylammonium bicarbonate and 1% sodium dodecyl sulfate) and homogenized with Ultraturax. After centrifugation the supernatant was stored at -20°C.

Mortar preparation: 70-90mg of tissue were grinded in a precooled mortar with liquid nitrogen and added to a tenfold amount of buffer solution (as above). Homogenization was done with ultrasound, the samples were then centrifuged and the supernatant was stored at -20°C.

In western blots of human psoas and cardiac muscle specimens from autopsy prepared with either mortar or Ultraturax preparation did not show a perceptible difference between the preparation techniques (**Supplementary figure 1, Supplementary figure 2**). For all subsequent experiments mortar preparation was used.

Western blot setup development:

30µg of the respective sample was added to sample buffer and reducing agent and heated to 70°C. The solutions were loaded on NuPAGE Novex Midi Bis-Tris Gel (4-12%, 20

Slot, 1mm) together with a pre-stained standard (Novex Sharp Pre-stained Protein Standard). For electrophoresis MOPS buffer was used and a voltage of 200V was applied for 45 minutes. After equilibration in transfer buffer the gels were transferred to nitrocellulose membranes for 1.5h at 180mA and blocked with protein-free blocking buffer. Protein transfer was controlled by staining with Panceau S. In the wash steps after blocking and antibody incubations Tris-Buffered Saline with Tween 20 (TBS-T) was used. Incubation with primary antibodies (1:1000 dilution) was done overnight at 4°C. Horseradish-peroxidase (HRP) labelled anti-mouse antibodies (1:1000 dilution) served as secondary antibodies. For detection Amersham ECL Western Blotting Detection Reagent was used. An exposition time of approx. 5 sec. was sufficient.

Supplementary figure 1 shows the blot after Pancau-S staining (proteins are made visible in pink).

Western blot results of immunostaining are shown in **Supplementary figure 2**. Both cTnT antibodies (A and B) showed positive bands in the skeletal muscle lanes (1 and 2) and the myocardium lanes (3 and 4) whereas the cTnI antibodies (C and D) only detected bands in the myocardium lanes.

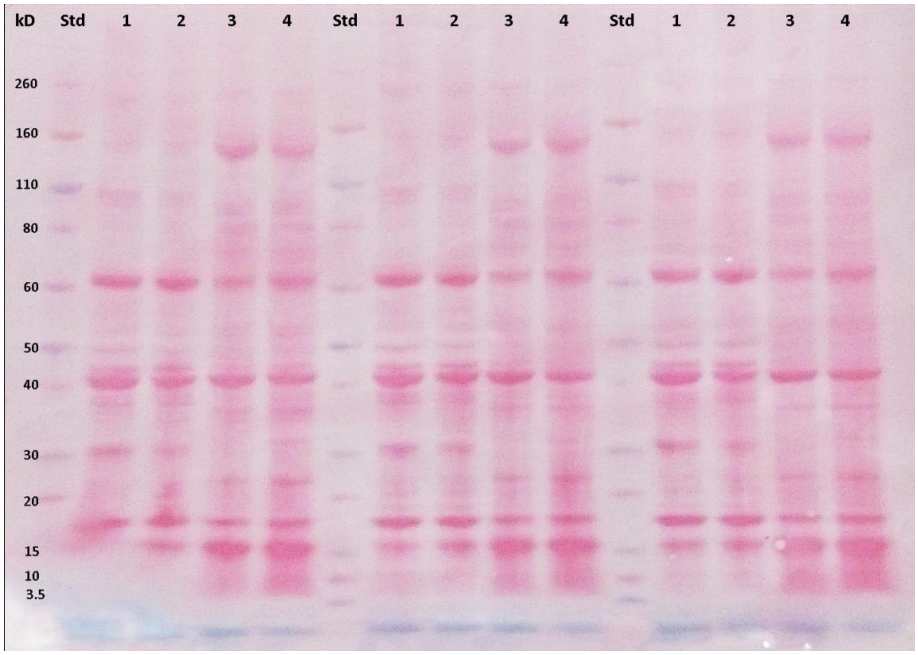

Supplementary figure 1: Western blot after transfer onto nitrocellulose membrane and Panceau-S staining. Each lane was loaded with 30 µg of protein or 2µl of standard (Std).
Lane 1: psoas (Ultraturax preparation), *2*: psoas (mortar preparation), *3*: myocardium (Ultraturax), *4*: myocardium (mortar).

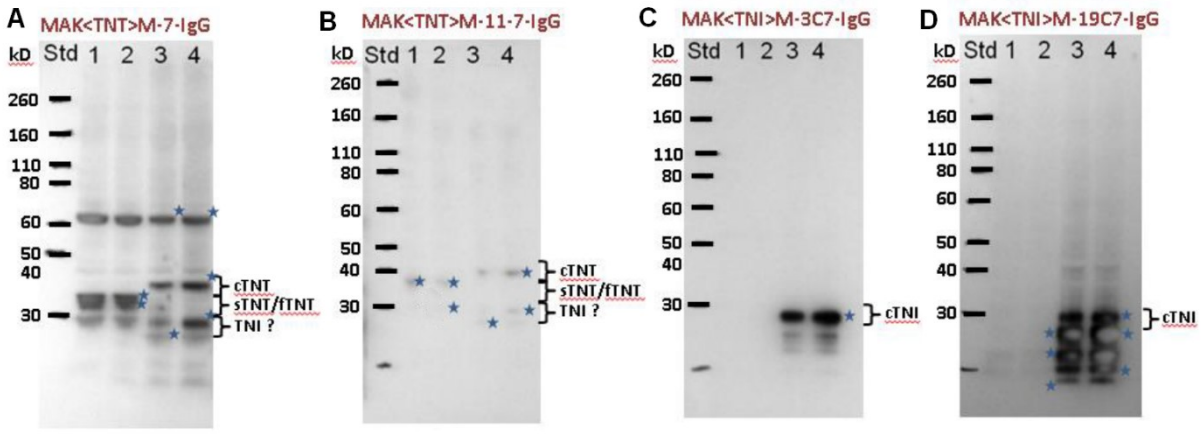

Supplementary figure 2: Western blots. *Lane 1*: psoas (Ultraturax preparation), *2*: psoas (mortar preparation), *3*: myocardium (Ultraturax), *4*: myocardium (mortar).
Primary antibodies (dilution 1:1000): Anti-cTnT: M7 (**A**) and M11.7 (**B**). Anti-cTnI: M3C7 (**C**) and M19C7 (**D**). Secondary anti-mouse HRP-linked IgG antibody in 1:1000 dilution. Bands with similar molecular weight as cTnT (cardiac), sTnT (slow skeletal), fTnT (fast skeletal) and cTnI are marked with curly brackets. Potential candidates for LC-MS/MS are marked with asterisks.

After these first experiments the protocol was adapted and different antibody concentrations were tested in order to reduce possible unspecific binding of antibodies with skeletal muscle protein. Additionally another skeletal muscle specimen was introduced (rectus femoris muscle) and samples were spiked with 25 ng and 50 ng of recombinant human (rec-h) cTnI and rec-hcTnT. Electrophoresis and blotting were done as described in the first experiments. Unlike above, nitrocellulose membranes were then blocked with skim milk blocking buffer (TBS-T and 5% skim milk powder). Antibody dilutions of 1:1000, 1:3000 and 1: 10000 were prepared using the skim milk buffer solution and stored at -20°C. Dilution of the secondary anti-mouse HRP-linked antibody was 1:3000. Exposition times were one to two minutes.

The provided rec-hcTnT was not pure as assumed, but mixed with serum proteins. Consecutively the lanes spiked with rec-hcTnT showed massive protein overloading (not shown), which was erroneously interpreted as a wrong concentration declaration. Thus in the rec-hcTnT spikes in western blots below (**Supplementary figure 3**) were further diluted and therefore not visible.

Results of immunostaining with the anti-cTnT (A) and anti-cTnI (B) antibodies are shown in **Supplementary figure 3** (spiked with the diluted unpure rec-hcTnT) and **Supplementary figure 4** (spiked with diluted rec-hcTnI). Similar to the first preliminary experiments with higher antibody concentrations, also in these western blots positive

bands were not only seen in myocardial samples with the anti-cTnT antibodies, but also in both skeletal muscle samples. The anti-cTnI antibody detected positive bands only in myocardium and rec-hcTnI spiked lanes.

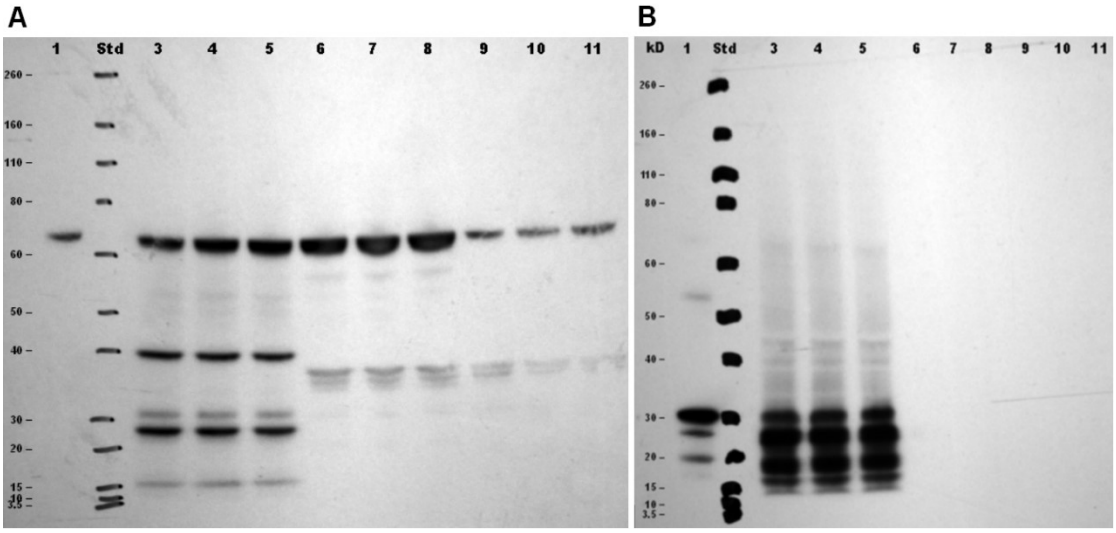

Supplementary figure 3: Western blots. *Lane 1*: 50ng unpure rec-hcTnT + 50ng rec-hcTnI; *2*: Standard; *3-5*: myocardium; *6-8*: psoas; *9-11*: rectus fem.; the muscle specimens each without and with 25ng or 50ng diluted unpure rec-hcTnT.
Incubation with anti-cTnT antibody M7 (**A**) and anti-cTnI antibody M19C7 (**B**) (dilution 1:10000). Secondary antibody: Anti-mouse HRP linked antibody (dilution 1:3000).

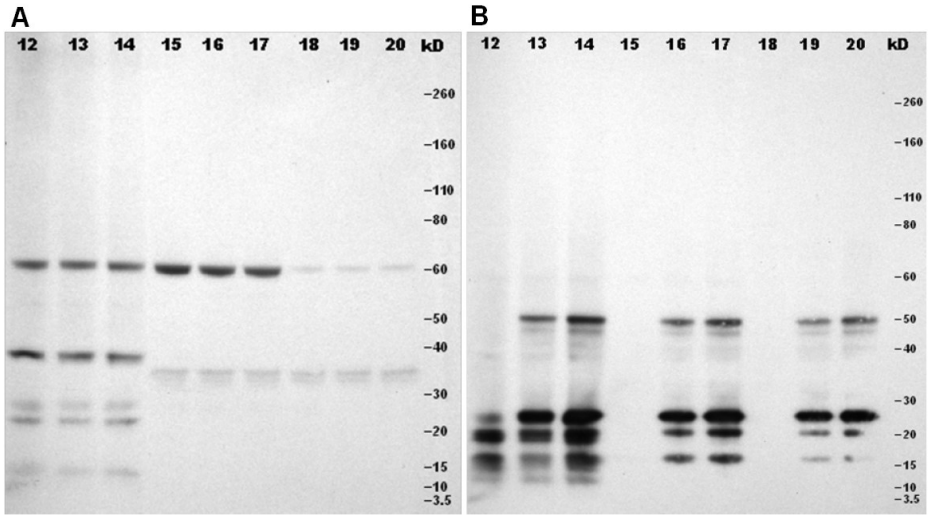

Supplementary figure 4: Western blots. *Lane 12-13*: myocardium; *15-17*: psoas; *18-20*: rectus fem.; the muscle specimens each without and with 25ng or 50ng rec-hcTnI.
Incubation with anti-cTnT antibody M7 (**A**) and anti-cTnI antibody M19C7 (**B**) (dilution 1:10000). Secondary antibody: Anti-mouse HRP-linked antibody (dilution 1:3000).

As the provided rec-hcTnT turned out not to be pure rec-hcTnT, but diluted with serum proteins, new rec-hcTnT was purchased and the experiments with rec-hcTnT spikes were

repeated with the anti cTnT antibodies (**Supplementary figure 5**) using antibody dilutions of 1:10000 and 1:1000. The rec-hcTnT now clearly enhanced the myocardial bands at the molecular weight of cTnT, however the faint positive bands in skeletal muscle were still present at approximately 5 kDa below cTnT.

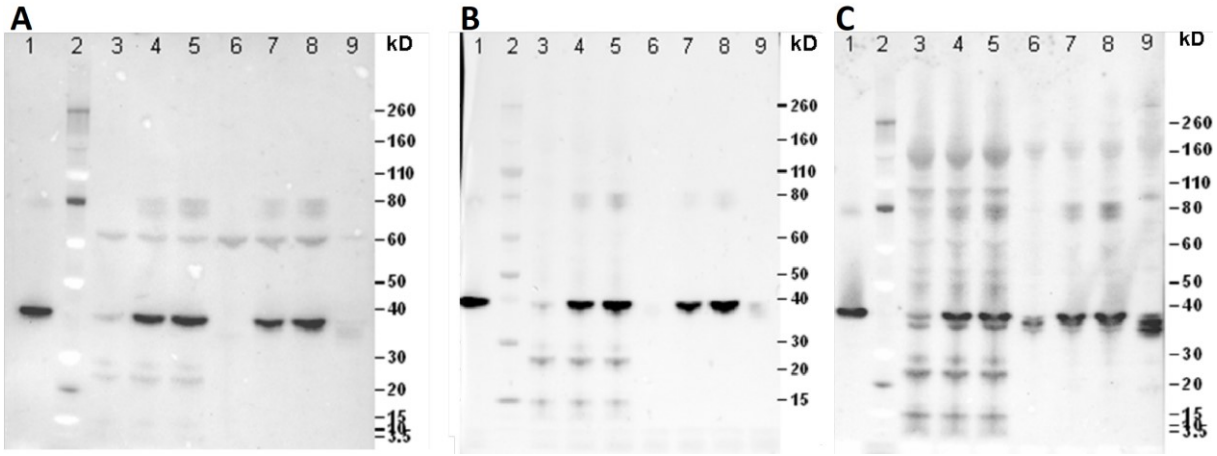

Supplementary figure 5: Western blots. *Lane 2*: standard; *3-5*: myocardium, *6-8*: M. psoas; *9*: M. rectus femoris. Rec-hcTnT spikes in lanes 4 and 7 (25ng) and lanes 1, 5 and 8 (50ng).
Incubation with anti-cTnT antibody (**A**) M7 and (**B**) M11.7 (dilution both 1:10000) and (**C**) M11.7 (dilution 1:1000). Secondary antibody: Anti-mouse HRP-linked antibody (dilution 1:3000).

A comparison with an anti-TSH antibody was done to exclude cross reactivity with the secondary HRP-linked anti-mouse antibody (**Supplementary figure 6**).

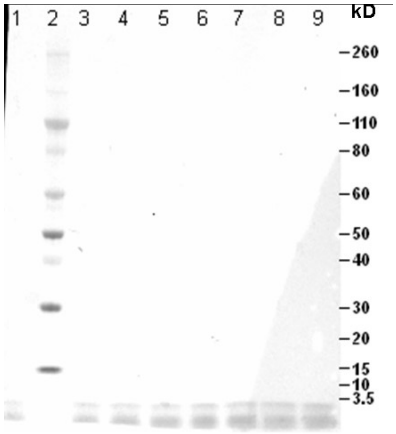

Supplementary figure 6: Lanes as in Supplementary figure 5. Incubation with anti-TSH antibody (dilution 1:10000). Secondary antibody: Anti-mouse HRP-linked antibody (dilution 1:3000).

Detailed results from database search of LC-MS/MS data

Supplementary table 1: Proteins identified in a database search of LC-MS/MS data from western blot bands 1-15 (from **Figure 11**) and purified cTnT as positive control. Troponin isoforms are highlighted. Proteins are sorted by molecular weight.
Accession (= uniprot ID); *Score* ("Mascot Protein Score" represents the LOG_{10} of a calculated probability, that the observed match between the experimental data (LC-MS/MS fragment ion masses) and the database sequence is a random event (http://www.matrixscience.com/help/interpretation_help.html#SCORING); a higher score means lower probability of a random match); *Coverage* (percent coverage = number of amino acids in all found peptides / total number of amino acids in the entire protein sequence); *MW* (molecular weight of the protein, calculated from amino acid sequence).

Purified cTnT:

Accession	Description	Score	Coverage	MW [kDa]
P81605	Dermcidin	440.9	35.5	11.3
P01834	Ig kappa chain C region	82.4	32.1	11.6
P69905	Hemoglobin subunit alpha	245.5	30.3	15.2
P68871	Hemoglobin subunit beta	1466.0	71.4	16.0
P12273	Prolactin-inducible protein	357.6	15.1	16.6
P02144	Myoglobin	273.6	29.2	17.2
P05976	Myosin light chain 1/3, skeletal muscle isoform	155.7	11.9	21.1
P07451	Carbonic anhydrase 3	703.3	21.5	29.5
P07951	Tropomyosin beta chain	289.6	8.1	32.8
P06753	Tropomyosin alpha-3 chain	165.1	12.6	32.9
P45379	Troponin T, cardiac muscle	15510.9	45.6	35.9
P04406	Glyceraldehyde-3-phosphate dehydrogenase	686.3	17.0	36.0
Q13642	Four and a half LIM domains protein 1	351.5	8.4	36.2
Q5E9B5	Actin, gamma-enteric smooth muscle	542.5	16.5	41.8
P02533	Keratin, type I cytoskeletal 14	1142.0	30.3	51.5
P13645	Keratin, type I cytoskeletal 10	4675.5	50.3	58.8
P04259	Keratin, type II cytoskeletal 6B	923.1	15.8	60.0
P35527	Keratin, type I cytoskeletal 9	4138.3	56.5	62.0
P13647	Keratin, type II cytoskeletal 5	734.9	15.3	62.3
P35908	Keratin, type II cytoskeletal 2 epidermal	4510.4	45.5	65.4
P04264	Keratin, type II cytoskeletal 1	6996.3	57.1	66.0
P02768	Serum albumin	58.4	5.3	69.3
Q02413	Desmoglein-1	160.3	3.3	113.7

Band 1:

Accession	Description	Score	Coverage	MW [kDa]
P59665	Neutrophil defensin 1	96.1	19.2	10.2
P81605	Dermcidin	155.0	22.7	11.3
P69905	Hemoglobin subunit alpha	231.6	25.4	15.2
P68871	Hemoglobin subunit beta	1031.2	68.0	16.0
P60660	Myosin light polypeptide 6	38.4	16.6	16.9
P02144	Myoglobin	26.4	19.5	17.2
P05976	Myosin light chain 1/3, skeletal muscle isoform	328.7	38.1	21.1
P08590	Myosin light chain 3	402.0	37.4	21.9
P45378	Troponin T, fast skeletal muscle	144.9	6.7	31.8
P07951	Tropomyosin beta chain	2450.4	29.9	32.8
P13805	Troponin T, slow skeletal muscle	143.2	17.6	32.9
P06753	Tropomyosin alpha-3 chain	597.7	16.5	32.9
P20774	Mimecan	100.6	11.7	33.9
P04406	Glyceraldehyde-3-phosphate dehydrogenase	967.9	23.3	36.0
P01857	Ig gamma-1 chain C region	336.3	17.3	36.1
Q15327	Ankyrin repeat domain-containing protein 1	889.7	44.5	36.2
Q13642	Four and a half LIM domains protein 1	802.2	22.9	36.2
Q15417	Calponin-3	120.7	13.7	36.4
P00338	L-lactate dehydrogenase A chain	54.0	5.7	36.7
O43684	Mitotic checkpoint protein BUB3	70.5	11.3	37.1
Q15365	Poly(rC)-binding protein 1	998.3	28.9	37.5
Q03591	Complement factor H-related protein 1	320.5	7.9	37.6
Q9UDY4	DnaJ homolog subfamily B member 4	503.7	14.5	37.8
Q14103	Heterogeneous nuclear ribonucleoprotein D0	158.5	6.8	38.4
P40121	Macrophage-capping protein	82.9	5.5	38.5
Q9UJZ1	Stomatin-like protein 2, mitochondrial	225.6	8.7	38.5
P07355	Annexin A2	374.7	26.6	38.6
P04083	Annexin A1	577.8	19.7	38.7
Q53GG5	PDZ and LIM domain protein 3	433.1	14.0	39.2
P04075	Fructose-bisphosphate aldolase A	2890.5	48.4	39.4
Q9GZV1	Ankyrin repeat domain-containing protein 2	800.4	35.6	39.8
Q8NDY3	[Protein ADP-ribosylarginine] hydrolase-like protein 1	154.6	13.0	40.1
P04899	Guanine nucleotide-binding protein G(i) subunit alpha-2	239.4	10.4	40.4
O95299	NADH dehydrogenase [ubiquinone] 1 alpha subcomplex subunit 10, mitochondrial	63.9	7.3	40.7
P01893	Putative HLA class I histocompatibility antigen, alpha chain H	130.1	10.2	40.9
O15143	Actin-related protein 2/3 complex subunit 1B	84.5	8.3	40.9
P21810	Biglycan	134.7	7.6	41.6
P60712	Actin, cytoplasmic 1	2997.2	45.3	41.7
Q5BKX8	Muscle-related coiled-coil protein	62.3	5.8	41.9
P68138	Actin, alpha skeletal muscle	6742.1	63.1	42.0
P30740	Leukocyte elastase inhibitor	469.5	14.8	42.7
P06732	Creatine kinase M-type	1180.7	31.5	43.1
Q9BXN1	Asporin	157.2	5.0	43.4
P51888	Prolargin	130.7	6.3	43.8
P00558	Phosphoglycerate kinase 1	97.0	7.0	44.6
Q9BTV4	Transmembrane protein 43	86.4	12.0	44.8
P00738	Haptoglobin	484.0	16.0	45.2
O43813	LanC-like protein 1	136.7	6.3	45.3
P60842	Eukaryotic initiation factor 4A-I	203.0	5.9	46.1
P13929	Beta-enolase	333.2	13.1	47.0
O60664	Perilipin-3	135.1	10.6	47.0
P06733	Alpha-enolase	755.3	20.5	47.1
P07437	Tubulin beta chain	253.0	8.1	49.6
Q9BQE3	Tubulin alpha-1C chain	111.8	4.2	49.9
P68104	Elongation factor 1-alpha 1	135.4	4.1	50.1
P08779	Keratin, type I cytoskeletal 16	1629.4	32.8	51.2
P55084	Trifunctional enzyme subunit beta, mitochondrial	45.9	5.1	51.3
P02679	Fibrinogen gamma chain	140.2	5.5	51.5
P02533	Keratin, type I cytoskeletal 14	2131.4	40.5	51.5
P31930	Cytochrome b-c1 complex subunit 1, mitochondrial	42.8	4.6	52.6
P17661	Desmin	1630.2	37.7	53.5
P08670	Vimentin	564.3	23.6	53.6
Q9UBF9	Myotilin	66.9	7.4	55.4
P02675	Fibrinogen beta chain	734.1	30.4	55.9
P14618	Pyruvate kinase isozymes M1/M2	878.5	23.7	57.9
P13645	Keratin, type I cytoskeletal 10	4646.4	39.9	58.8
P25705	ATP synthase subunit alpha, mitochondrial	242.2	8.9	59.7
P02538	Keratin, type II cytoskeletal 6A	1105.1	20.9	60.0
P04259	Keratin, type II cytoskeletal 6B	1141.4	19.2	60.0
P35527	Keratin, type I cytoskeletal 9	4982.1	65.3	62.0
P13647	Keratin, type II cytoskeletal 5	1184.9	25.4	62.3
P06744	Glucose-6-phosphate isomerase	280.9	6.8	63.1
Q5T749	Keratinocyte proline-rich protein	63.8	9.8	64.1
P35908	Keratin, type II cytoskeletal 2 epidermal	5254.1	51.0	65.4

P04264	Keratin, type II cytoskeletal 1	7940.1	53.7	66.0
O60662	Kelch-like protein 41	51.2	3.5	68.0
P02768	Serum albumin	3260.4	33.2	69.3
P08107	Heat shock 70 kDa protein 1A/1B	194.6	12.0	70.0
P11142	Heat shock cognate 71 kDa protein	365.3	11.9	70.9
Q9Y2J8	Protein-arginine deiminase type-2	120.8	4.7	75.5
O75112	LIM domain-binding protein 3	69.5	4.8	77.1
Q15063	Periostin	348.8	10.9	93.3
P11217	Glycogen phosphorylase, muscle form	270.0	6.7	97.0
P35609	Alpha-actinin-2	1815.5	26.4	103.8
O14983	Sarcoplasmic/endoplasmic reticulum calcium ATPase 1	170.2	5.5	110.2
Q02413	Desmoglein-1	72.2	2.4	113.7
P18206	Vinculin	81.2	2.4	123.7
Q00872	Myosin-binding protein C, slow-type	89.8	4.0	128.2
Q9UKX2	Myosin-2	3305.3	21.8	222.9
P12883	Myosin-7	4069.8	26.1	223.0
P11055	Myosin-3	1500.0	9.1	223.8
Q5D862	Filaggrin-2	85.7	1.0	247.9
Q86YZ3	Hornerin	182.6	5.3	282.2
Q14315	Filamin-C	82.9	1.0	290.8
P15924	Desmoplakin	84.7	1.0	331.6
P12111	Collagen alpha-3(VI) chain	1272.1	8.4	343.5
P20929	Nebulin	71.5	0.7	772.4
Q8WZ42	Titin	216.3	0.3	3813.7

Band 2:

Accession	Description	Score	Coverage	MW [kDa]
P81605	Dermcidin	304.1	22.7	11.3
P69905	Hemoglobin subunit alpha	569.2	25.4	15.2
P68871	Hemoglobin subunit beta	1127.6	61.9	16.0
P12273	Prolactin-inducible protein	85.8	18.5	16.6
P02144	Myoglobin	151.0	28.6	17.2
Q96A32	Myosin regulatory light chain 2, skeletal muscle isoform	155.0	13.6	19.0
P50461	Cysteine and glycine-rich protein 3	113.8	18.0	21.0
P05976	Myosin light chain 1/3, skeletal muscle isoform	283.2	18.6	21.1
P05090	Apolipoprotein D	164.2	25.9	21.3
P08590	Myosin light chain 3	247.1	27.2	21.9
P14649	Myosin light chain 6B	76.0	10.1	22.7
P51858	Hepatoma-derived growth factor	129.3	15.4	26.8
O75822	Eukaryotic translation initiation factor 3 subunit J	47.6	8.5	29.0
Q14847	LIM and SH3 domain protein 1	176.8	10.3	29.7
P21796	Voltage-dependent anion-selective channel protein 1	67.8	12.0	30.8
P29692	Elongation factor 1-delta	62.8	12.8	31.1
P45880	Voltage-dependent anion-selective channel protein 2	334.1	22.1	31.5
Q9NP98	Myozenin-1	225.3	31.8	31.7
P45378	Troponin T, fast skeletal muscle	1126.7	29.4	31.8
Q92629	Delta-sarcoglycan	594.6	14.9	32.1
P06748	Nucleophosmin	211.7	23.5	32.6
P09493	Tropomyosin alpha-1 chain	3851.7	42.3	32.7
P07951	Tropomyosin beta chain	2173.1	28.9	32.8
P08865	40S ribosomal protein SA	407.9	12.9	32.8
P52907	F-actin-capping protein subunit alpha-1	896.0	39.2	32.9
P13805	Troponin T, slow skeletal muscle	2409.4	26.3	32.9
P47755	F-actin-capping protein subunit alpha-2	1048.0	58.7	32.9
P06753	Tropomyosin alpha-3 chain	2668.5	41.1	32.9
P53004	Biliverdin reductase A	221.2	8.1	33.4
P20774	Mimecan	138.1	5.4	33.9
P05388	60S acidic ribosomal protein P0	466.9	18.6	34.3
O75569	Interferon-inducible double-stranded RNA-dependent protein kinase activator A	121.5	9.6	34.4
P60891	Ribose-phosphate pyrophosphokinase 1	364.7	11.0	34.8
Q08257	Quinone oxidoreductase	126.9	29.2	35.2
P40926	Malate dehydrogenase, mitochondrial	630.2	36.7	35.5
P55735	Protein SEC13 homolog	227.5	13.4	35.5
Q9UBQ7	Glyoxylate reductase/hydroxypyruvate reductase	899.1	25.0	35.6
Q96CX2	BTB/POZ domain-containing protein KCTD12	304.6	11.7	35.7
P15121	Aldose reductase	615.7	24.7	35.8
P04406	Glyceraldehyde-3-phosphate dehydrogenase	2134.7	40.3	36.0
P01857	Ig gamma-1 chain C region	224.3	21.5	36.1
P05198	Eukaryotic translation initiation factor 2 subunit 1	76.0	17.1	36.1
P02649	Apolipoprotein E	1023.5	32.2	36.1
Q13642	Four and a half LIM domains protein 1	1797.7	30.3	36.2
P13716	Delta-aminolevulinic acid dehydratase	189.2	14.9	36.3
P40925	Malate dehydrogenase, cytoplasmic	581.7	19.5	36.4
P07195	L-lactate dehydrogenase B chain	250.7	11.1	36.6
P00338	L-lactate dehydrogenase A chain	455.7	18.4	36.7
Q04828	Aldo-keto reductase family 1 member C1	527.9	25.7	36.8
P31942	Heterogeneous nuclear ribonucleoprotein H3	224.0	9.5	36.9
P62140	Serine/threonine-protein phosphatase PP1-beta catalytic subunit	300.3	14.4	37.2
P62879	Guanine nucleotide-binding protein G(I)/G(S)/G(T) subunit beta-2	277.8	15.3	37.3
Q9UJ70	N-acetyl-D-glucosamine kinase	66.8	8.4	37.4
P62873	Guanine nucleotide-binding protein G(I)/G(S)/G(T) subunit beta-1	99.1	15.3	37.4
Q15365	Poly(rC)-binding protein 1	69.4	8.7	37.5
P21695	Glycerol-3-phosphate dehydrogenase [NAD(+)], cytoplasmic	567.2	13.5	37.5
Q9H2U2	Inorganic pyrophosphatase 2, mitochondrial	251.1	7.5	37.9
Q9Y394	Dehydrogenase/reductase SDR family member 7	617.5	23.3	38.3
Q14103	Heterogeneous nuclear ribonucleoprotein D0	46.4	6.8	38.4
P07355	Annexin A2	791.3	27.1	38.6
P04083	Annexin A1	1002.0	25.4	38.7
Q53GG5	PDZ and LIM domain protein 3	216.3	9.1	39.2
P11177	Pyruvate dehydrogenase E1 component subunit beta, mitochondrial	1311.7	31.5	39.2
P04075	Fructose-bisphosphate aldolase A	815.8	29.4	39.4
P50213	Isocitrate dehydrogenase [NAD] subunit alpha, mitochondrial	384.3	13.4	39.6
P11766	Alcohol dehydrogenase class-3	144.2	6.7	39.7
Q9GZV1	Ankyrin repeat domain-containing protein 2	339.3	11.7	39.8
P60712	Actin, cytoplasmic 1	1079.0	43.5	41.7
Q3ZC07	Actin, alpha cardiac muscle 1	2936.8	52.5	42.0
P68138	Actin, alpha skeletal muscle	2981.0	52.5	42.0
P12277	Creatine kinase B-type	204.6	16.3	42.6
P06732	Creatine kinase M-type	2246.9	34.1	43.1
Q9BXN1	Asporin	334.3	17.9	43.4
P51888	Prolargin	185.9	9.4	43.8
P00558	Phosphoglycerate kinase 1	469.0	21.3	44.6
P00738	Haptoglobin	96.7	9.1	45.2
O14979	Heterogeneous nuclear ribonucleoprotein D-like	42.3	6.2	46.4
P13929	Beta-enolase	584.8	21.7	47.0
O60664	Perilipin-3	125.1	6.7	47.0
P06733	Alpha-enolase	456.7	21.2	47.1
P17540	Creatine kinase S-type, mitochondrial	89.2	8.4	47.5
P01011	Alpha-1-antichymotrypsin	499.1	19.6	47.6
P15088	Mast cell carboxypeptidase A	69.2	5.5	48.6
P07437	Tubulin beta chain	539.4	16.4	49.6
Q9BQE3	Tubulin alpha-1C chain	213.9	10.9	49.9
P68104	Elongation factor 1-alpha 1	599.6	17.3	50.1
Q05639	Elongation factor 1-alpha 2	565.3	17.3	50.4
Q16181	Septin-7	113.3	5.3	50.6
P48735	Isocitrate dehydrogenase [NADP], mitochondrial	174.2	11.5	50.9
P02679	Fibrinogen gamma chain	78.5	4.9	51.5
P02533	Keratin, type I cytoskeletal 14	628.5	26.3	51.5
P10909	Clusterin	258.6	6.0	52.5
P17661	Desmin	1347.3	35.3	53.5
P08670	Vimentin	252.9	8.4	53.6

Q9UBF9	Myotilin	283.6	12.3	55.4
P02675	Fibrinogen beta chain	225.5	5.7	55.9
P06576	ATP synthase subunit beta, mitochondrial	227.7	13.4	56.5
P14618	Pyruvate kinase isozymes M1/M2	986.4	32.4	57.9
P13645	Keratin, type I cytoskeletal 10	2727.7	35.3	58.8
P25705	ATP synthase subunit alpha, mitochondrial	755.9	21.5	59.7
P02538	Keratin, type II cytoskeletal 6A	611.7	15.1	60.0
P04259	Keratin, type II cytoskeletal 6B	739.6	15.1	60.0
P36871	Phosphoglucomutase-1	245.2	7.1	61.4
P35527	Keratin, type I cytoskeletal 9	2093.9	54.6	62.0
P13647	Keratin, type II cytoskeletal 5	397.4	17.8	62.3
P35908	Keratin, type II cytoskeletal 2 epidermal	1760.7	35.7	65.4
P04264	Keratin, type II cytoskeletal 1	4829.7	45.7	66.0
P02768	Serum albumin	1711.7	21.0	69.3
P08107	Heat shock 70 kDa protein 1A/1B	168.6	12.0	70.0
P49748	Very long-chain specific acyl-CoA dehydrogenase, mitochondrial	509.7	12.7	70.3
P11142	Heat shock cognate 71 kDa protein	366.5	13.3	70.9
P08133	Annexin A6	341.4	8.0	75.8
O75112	LIM domain-binding protein 3	100.1	9.1	77.1
P40939	Trifunctional enzyme subunit alpha, mitochondrial	374.6	9.6	82.9
P08237	6-phosphofructokinase, muscle type	557.9	8.5	85.1
P55072	Transitional endoplasmic reticulum ATPase	83.4	3.7	89.3
Q15063	Periostin	230.2	9.9	93.3
P11217	Glycogen phosphorylase, muscle form	47.2	4.5	97.0
Q86TD4	Sarcalumenin	99.4	4.0	100.7
P55786	Puromycin-sensitive aminopeptidase	98.6	3.6	103.2
P35609	Alpha-actinin-2	3467.3	32.8	103.8
P12109	Collagen alpha-1(VI) chain	79.2	3.2	108.5
P12110	Collagen alpha-2(VI) chain	49.9	3.0	108.5
O14983	Sarcoplasmic/endoplasmic reticulum calcium ATPase 1	210.5	6.7	110.2
P18206	Vinculin	77.9	2.4	123.7
Q14324	Myosin-binding protein C, fast-type	186.0	3.1	128.0
Q00872	Myosin-binding protein C, slow-type	1336.0	12.5	128.2
P01024	Complement C3	102.1	3.4	187.0
P13535	Myosin-8	2607.3	15.6	222.6
Q9UKX2	Myosin-2	5471.4	26.8	222.9
P12883	Myosin-7	5865.7	30.9	223.0
P12882	Myosin-1	4122.9	19.8	223.0
P11055	Myosin-3	2767.9	12.5	223.8
Q14315	Filamin-C	171.0	2.2	290.8
P12111	Collagen alpha-3(VI) chain	1262.8	7.3	343.5
Q15149	Plectin	63.9	0.5	531.5
P20929	Nebulin	479.2	4.4	772.4
Q8WZ42	Titin	473.2	0.6	3813.7

Band 3:

Accession	Description	Score	Coverage	MW [kDa]
P01834	Ig kappa chain C region	427.7	32.1	11.6
P69905	Hemoglobin subunit alpha	827.1	25.4	15.2
P68871	Hemoglobin subunit beta	1934.2	70.8	16.0
P02144	Myoglobin	323.0	28.6	17.2
P08590	Myosin light chain 3	315.3	25.6	21.9
Q07955	Serine/arginine-rich splicing factor 1	182.5	19.8	27.7
P07451	Carbonic anhydrase 3	103.7	15.8	29.5
Q9NPC6	Myozenin-2	964.0	26.5	29.9
Q9Y277	Voltage-dependent anion-selective channel protein 3	350.0	8.1	30.6
P21796	Voltage-dependent anion-selective channel protein 1	4160.3	61.8	30.8
P29692	Elongation factor 1-delta	583.3	26.0	31.1
P47756	F-actin-capping protein subunit beta	879.4	25.3	31.3
P48739	Phosphatidylinositol transfer protein beta isoform	210.7	9.2	31.5
P45880	Voltage-dependent anion-selective channel protein 2	1179.2	39.5	31.5
Q9NP98	Myozenin-1	1642.3	41.1	31.7
P45378	Troponin T, fast skeletal muscle	2488.6	29.4	31.8
O43396	Thioredoxin-like protein 1	339.2	26.6	32.2
P09493	Tropomyosin alpha-1 chain	1228.3	29.9	32.7
P07951	Tropomyosin beta chain	1297.1	23.6	32.8
P13805	Troponin T, slow skeletal muscle	3101.0	26.3	32.9
P06753	Tropomyosin alpha-3 chain	816.4	26.3	32.9
P54920	Alpha-soluble NSF attachment protein	56.7	7.5	33.2
Q99623	Prohibitin-2	479.6	18.1	33.3
P20774	Mimecan	216.2	8.1	33.9
Q9UHQ9	NADH-cytochrome b5 reductase 1	352.8	12.5	34.1
P00387	NADH-cytochrome b5 reductase 3	975.6	29.9	34.2
Q16836	Hydroxyacyl-coenzyme A dehydrogenase, mitochondrial	78.7	6.1	34.3
O15144	Actin-related protein 2/3 complex subunit 2	163.8	8.7	34.3
O14579	Coatomer subunit epsilon	65.7	9.4	34.5
Q9HC38	Glyoxalase domain-containing protein 4	163.8	14.1	34.8
P63244	Guanine nucleotide-binding protein subunit beta-2-like 1	149.2	13.3	35.1
P13804	Electron transfer flavoprotein subunit alpha, mitochondrial	330.2	15.9	35.1
P40926	Malate dehydrogenase, mitochondrial	2869.9	47.0	35.5
O75208	Ubiquinone biosynthesis protein COQ9, mitochondrial	137.7	15.1	35.5
Q13011	Delta(3,5)-Delta(2,4)-dienoyl-CoA isomerase, mitochondrial	182.7	8.8	35.8
P09525	Annexin A4	1698.2	30.1	35.9
P08758	Annexin A5	838.6	33.1	35.9
P04406	Glyceraldehyde-3-phosphate dehydrogenase	1535.0	40.0	36.0
P02649	Apolipoprotein E	340.4	20.5	36.1
Q13642	Four and a half LIM domains protein 1	1982.8	19.8	36.2
P40925	Malate dehydrogenase, cytoplasmic	1474.4	24.6	36.4
P07195	L-lactate dehydrogenase B chain	2389.9	28.1	36.6
P00338	L-lactate dehydrogenase A chain	1881.4	25.6	36.7
Q9NUQ9	Protein FAM49B	107.1	10.2	36.7
P07355	Annexin A2	1229.7	32.2	38.6
P04083	Annexin A1	607.1	15.0	38.7
Q53GG5	PDZ and LIM domain protein 3	141.3	9.1	39.2
P04075	Fructose-bisphosphate aldolase A	542.8	22.3	39.4
P60712	Actin, cytoplasmic 1	2218.4	34.4	41.7
P68138	Actin, alpha skeletal muscle	5054.0	52.5	42.0
P06732	Creatine kinase M-type	1538.3	29.4	43.1
P00558	Phosphoglycerate kinase 1	121.4	11.3	44.6
P01009	Alpha-1-antitrypsin	73.3	6.7	46.7
P13929	Beta-enolase	180.2	5.8	47.0
P22695	Cytochrome b-c1 complex subunit 2, mitochondrial	425.8	14.4	48.4
P07437	Tubulin beta chain	840.0	21.0	49.6
Q9BQE3	Tubulin alpha-1C chain	154.7	14.5	49.9
P68104	Elongation factor 1-alpha 1	75.1	6.9	50.1
P48735	Isocitrate dehydrogenase [NADP], mitochondrial	404.5	13.9	50.9
P08779	Keratin, type I cytoskeletal 16	1057.1	18.6	51.2
P02679	Fibrinogen gamma chain	176.9	14.8	51.5
P02533	Keratin, type I cytoskeletal 14	1101.0	12.5	51.5
Q13203	Myosin-binding protein H	240.1	6.1	52.0
P17661	Desmin	1815.4	27.5	53.5
P08670	Vimentin	416.0	6.2	53.6
P06576	ATP synthase subunit beta, mitochondrial	238.3	12.9	56.5
P30101	Protein disulfide-isomerase A3	74.2	5.9	56.7
Q16851	UTP--glucose-1-phosphate uridylyltransferase	644.9	14.6	56.9
P14618	Pyruvate kinase isozymes M1/M2	111.4	6.8	57.9
P13645	Keratin, type I cytoskeletal 10	3311.7	33.2	58.8
P02538	Keratin, type II cytoskeletal 6A	315.2	9.9	60.0
P36871	Phosphoglucomutase-1	249.1	7.3	61.4
P35527	Keratin, type I cytoskeletal 9	1350.4	25.8	62.0
P13647	Keratin, type II cytoskeletal 5	211.9	8.5	62.3
P35908	Keratin, type II cytoskeletal 2 epidermal	2925.5	34.3	65.4
P04264	Keratin, type II cytoskeletal 1	5477.7	39.6	66.0
O60662	Kelch-like protein 41	326.0	5.8	68.0
P02768	Serum albumin	970.3	19.7	69.3
P08107	Heat shock 70 kDa protein 1A/1B	97.4	8.0	70.0
P11142	Heat shock cognate 71 kDa	155.9	8.5	70.9

	protein			
P08133	Annexin A6	37.4	2.8	75.8
O75112	LIM domain-binding protein 3	1495.2	14.2	77.1
P35609	Alpha-actinin-2	5535.4	33.7	103.8
O14983	Sarcoplasmic/endoplasmic reticulum calcium ATPase 1	844.2	9.7	110.2
Q00872	Myosin-binding protein C, slow-type	724.0	8.2	128.2
Q9UKX2	Myosin-2	5012.7	19.3	222.9
P12883	Myosin-7	4372.6	21.8	223.0
P12111	Collagen alpha-3(VI) chain	521.7	2.6	343.5
P20929	Nebulin	52.6	0.7	772.4
Q8WZ42	Titin	46.8	0.1	3813.7

Band 4:

Accession	Description	Score	Coverage	MW [kDa]
P81605	Dermcidin	136.1	20.0	11.3
P69905	Hemoglobin subunit alpha	111.4	19.0	15.2
P68871	Hemoglobin subunit beta	157.1	23.8	16.0
P02144	Myoglobin	170.9	32.5	17.2
P05976	Myosin light chain 1/3, skeletal muscle isoform	218.5	18.6	21.1
P08590	Myosin light chain 3	286.8	13.3	21.9
P45378	Troponin T, fast skeletal muscle	75.7	12.3	31.8
P09493	Tropomyosin alpha-1 chain	1047.5	19.0	32.7
P07951	Tropomyosin beta chain	2176.3	39.8	32.8
P13805	Troponin T, slow skeletal muscle	67.6	17.6	32.9
P06753	Tropomyosin alpha-3 chain	597.4	25.3	32.9
P12235	ADP/ATP translocase 1	98.2	7.1	33.0
P40926	Malate dehydrogenase, mitochondrial	50.9	5.9	35.5
P04406	Glyceraldehyde-3-phosphate dehydrogenase	662.6	37.9	36.0
Q13642	Four and a half LIM domains protein 1	1088.1	22.9	36.2
P00338	L-lactate dehydrogenase A chain	27.8	5.7	36.7
Q15365	Poly(rC)-binding protein 1	854.6	25.3	37.5
O94905	Erlin-2	370.3	11.5	37.8
Q9UJZ1	Stomatin-like protein 2, mitochondrial	293.1	13.5	38.5
A6NMY6	Putative annexin A2-like protein	138.8	9.1	38.6
Q53GG5	PDZ and LIM domain protein 3	1272.8	34.1	39.2
P04075	Fructose-bisphosphate aldolase A	11368.1	73.9	39.4
P09972	Fructose-bisphosphate aldolase C	3069.7	19.2	39.4
Q9GZV1	Ankyrin repeat domain-containing protein 2	724.6	31.7	39.8
P17612	cAMP-dependent protein kinase catalytic subunit alpha	45.3	9.7	40.6
O95299	NADH dehydrogenase [ubiquinone] 1 alpha subcomplex subunit 10, mitochondrial	224.7	13.2	40.7
P60712	Actin, cytoplasmic 1	6157.1	44.3	41.7
P68138	Actin, alpha skeletal muscle	16839.8	67.4	42.0
P30740	Leukocyte elastase inhibitor	67.7	6.3	42.7
P51553	Isocitrate dehydrogenase [NAD] subunit gamma, mitochondrial	142.1	7.9	42.8
Q9UNM6	26S proteasome non-ATPase regulatory subunit 13	85.6	5.3	42.9
P06732	Creatine kinase M-type	1980.5	38.6	43.1
P08559	Pyruvate dehydrogenase E1 component subunit alpha, somatic form, mitochondrial	230.6	6.7	43.3
P16219	Short-chain specific acyl-CoA dehydrogenase, mitochondrial	176.0	9.0	44.3
P00558	Phosphoglycerate kinase 1	156.8	13.9	44.6
Q16816	Phosphorylase b kinase gamma catalytic chain, skeletal muscle/heart isoform	373.1	19.4	45.0
O43813	LanC-like protein 1	165.5	12.5	45.3
P17174	Aspartate aminotransferase, cytoplasmic	105.9	6.8	46.2
P13929	Beta-enolase	855.4	20.1	47.0
P06733	Alpha-enolase	1097.4	23.0	47.1
P17540	Creatine kinase S-type, mitochondrial	277.0	11.9	47.5
P00505	Aspartate aminotransferase, mitochondrial	830.5	22.6	47.5
P48735	Isocitrate dehydrogenase [NADP], mitochondrial	351.0	11.5	50.9
P55084	Trifunctional enzyme subunit beta, mitochondrial	184.9	8.2	51.3
P02533	Keratin, type I cytoskeletal 14	1014.4	14.4	51.5
O75390	Citrate synthase, mitochondrial	164.2	5.8	51.7
O75306	NADH dehydrogenase [ubiquinone] iron-sulfur protein 2, mitochondrial	303.3	8.4	52.5
P31930	Cytochrome b-c1 complex subunit 1, mitochondrial	192.2	4.6	52.6
P17661	Desmin	1358.9	33.8	53.5
P14618	Pyruvate kinase isozymes M1/M2	1237.1	28.3	57.9
P13645	Keratin, type I cytoskeletal 10	2970.1	35.8	58.8
P25705	ATP synthase subunit alpha, mitochondrial	176.2	7.8	59.7
P36871	Phosphoglucomutase-1	55.6	4.5	61.4
P35527	Keratin, type I cytoskeletal 9	2064.1	40.6	62.0
P13647	Keratin, type II cytoskeletal 5	354.3	9.5	62.3
P06744	Glucose-6-phosphate isomerase	443.6	10.0	63.1
P35908	Keratin, type II cytoskeletal 2 epidermal	2729.1	52.9	65.4
P04264	Keratin, type II cytoskeletal 1	5431.7	49.1	66.0
P02768	Serum albumin	888.1	5.6	69.3
P08107	Heat shock 70 kDa protein 1A/1B	703.6	12.6	70.0
P11142	Heat shock cognate 71 kDa protein	869.5	20.6	70.9
O75112	LIM domain-binding protein 3	109.8	4.3	77.1
Q99798	Aconitate hydratase, mitochondrial	49.6	3.5	85.4
P23109	AMP deaminase 1	165.6	6.7	90.2
P11217	Glycogen phosphorylase, muscle form	1310.9	26.4	97.0
P35609	Alpha-actinin-2	2669.6	33.9	103.8
O14983	Sarcoplasmic/endoplasmic reticulum calcium ATPase 1	860.3	15.2	110.2
Q00872	Myosin-binding protein C, slow-type	182.5	4.3	128.2
O15061	Synemin	65.5	1.4	172.7
P52179	Myomesin-1	165.9	2.9	187.5
Q9UKX2	Myosin-2	5830.6	32.4	222.9
P12883	Myosin-7	5287.7	27.8	223.0
P12882	Myosin-1	4588.0	26.8	223.0
P20929	Nebulin	464.0	4.4	772.4
Q8WZ42	Titin	185.2	0.2	3813.7

Band 5:

Accession	Description	Score	Coverage	MW [kDa]
P81605	Dermcidin	162.8	22.7	11.3
P69905	Hemoglobin subunit alpha	143.9	19.0	15.2
P68871	Hemoglobin subunit beta	228.8	36.7	16.0
P02144	Myoglobin	76.2	19.5	17.2
P05976	Myosin light chain 1/3, skeletal muscle isoform	135.1	18.6	21.1
P08590	Myosin light chain 3	248.9	21.0	21.9
P07451	Carbonic anhydrase 3	42.9	7.7	29.5
P45378	Troponin T, fast skeletal muscle	217.8	15.2	31.8
P09493	Tropomyosin alpha-1 chain	1371.4	24.7	32.7
P07951	Tropomyosin beta chain	3086.8	36.6	32.8
P13805	Troponin T, slow skeletal muscle	328.8	20.9	32.9
P06753	Tropomyosin alpha-3 chain	892.8	31.6	32.9
P40926	Malate dehydrogenase, mitochondrial	72.9	5.9	35.5
P04406	Glyceraldehyde-3-phosphate dehydrogenase	895.1	35.2	36.0
Q13642	Four and a half LIM domains protein 1	425.5	19.8	36.2
P00338	L-lactate dehydrogenase A chain	151.5	12.7	36.7
O76003	Glutaredoxin-3	146.4	11.0	37.4
Q15365	Poly(rC)-binding protein 1	1004.8	35.1	37.5
Q9UDY4	DnaJ homolog subfamily B member 4	539.5	16.9	37.8
O94905	Erlin-2	166.0	7.1	37.8
Q14103	Heterogeneous nuclear ribonucleoprotein D0	143.1	6.8	38.4
Q9Y3F4	Serine-threonine kinase receptor-associated protein	112.6	8.9	38.4
Q8N8N7	Prostaglandin reductase 2	103.4	7.4	38.5
Q9UJZ1	Stomatin-like protein 2, mitochondrial	144.3	8.7	38.5
P07355	Annexin A2	223.3	20.9	38.6
P04083	Annexin A1	416.0	11.9	38.7
Q53GG5	PDZ and LIM domain protein 3	719.4	34.1	39.2

P04075	Fructose-bisphosphate aldolase A	7326.6	70.3	39.4
P09972	Fructose-bisphosphate aldolase C	1788.8	16.8	39.4
Q6IBS0	Twinfilin-2	71.4	10.9	39.5
P00325	Alcohol dehydrogenase 1B	72.7	5.9	39.8
Q9GZV1	Ankyrin repeat domain-containing protein 2	1379.2	48.3	39.8
Q8NDY3	[Protein ADP-ribosylarginine] hydrolase-like protein 1	204.7	6.2	40.1
P04899	Guanine nucleotide-binding protein G(i) subunit alpha-2	104.5	10.4	40.4
P17612	cAMP-dependent protein kinase catalytic subunit alpha	61.5	9.7	40.6
O95299	NADH dehydrogenase [ubiquinone] 1 alpha subcomplex subunit 10, mitochondrial	349.1	13.5	40.7
P60712	Actin, cytoplasmic 1	4651.3	45.9	41.7
Q562R1	Beta-actin-like protein 2	2557.4	19.4	42.0
Q3ZC07	Actin, alpha cardiac muscle 1	8902.4	64.2	42.0
P68138	Actin, alpha skeletal muscle	11463.5	64.2	42.0
P35237	Serpin B6	100.4	20.7	42.6
P51553	Isocitrate dehydrogenase [NAD] subunit gamma, mitochondrial	139.9	7.9	42.8
Q9UNM6	26S proteasome non-ATPase regulatory subunit 13	121.0	7.5	42.9
P06732	Creatine kinase M-type	1492.7	36.2	43.1
P08559	Pyruvate dehydrogenase E1 component subunit alpha, somatic form, mitochondrial	155.1	9.2	43.3
P16219	Short-chain specific acyl-CoA dehydrogenase, mitochondrial	304.7	13.8	44.3
P00558	Phosphoglycerate kinase 1	146.2	13.2	44.6
Q9BTV4	Transmembrane protein 43	89.2	7.8	44.8
Q16816	Phosphorylase b kinase gamma catalytic chain, skeletal muscle/heart isoform	485.8	22.0	45.0
Q9UKU7	Isobutyryl-CoA dehydrogenase, mitochondrial	51.5	5.8	45.0
O43813	LanC-like protein 1	240.3	11.8	45.3
P60842	Eukaryotic initiation factor 4A-I	169.4	6.7	46.1
P17174	Aspartate aminotransferase, cytoplasmic	161.9	13.1	46.2
P13929	Beta-enolase	701.5	21.4	47.0
O60664	Perilipin-3	57.1	6.7	47.0
P06733	Alpha-enolase	885.8	24.4	47.1
P17540	Creatine kinase S-type, mitochondrial	240.1	11.5	47.5
P00505	Aspartate aminotransferase, mitochondrial	313.2	9.8	47.5
P22695	Cytochrome b-c1 complex subunit 2, mitochondrial	200.3	7.7	48.4
P07437	Tubulin beta chain	218.9	12.6	49.6
P48735	Isocitrate dehydrogenase [NADP], mitochondrial	253.3	6.6	50.9
P55084	Trifunctional enzyme subunit beta, mitochondrial	138.0	6.3	51.3
P02533	Keratin, type I cytoskeletal 14	669.8	12.1	51.5
P31930	Cytochrome b-c1 complex subunit 1, mitochondrial	285.6	9.0	52.6
P17661	Desmin	1812.0	44.3	53.5
Q9UBF9	Myotilin	180.1	16.3	55.4
P06576	ATP synthase subunit beta, mitochondrial	120.5	9.8	56.5
Q9HCP6	Protein-cysteine N-palmitoyltransferase HHAT-like protein	226.8	4.8	56.7
P14618	Pyruvate kinase isozymes M1/M2	803.1	22.2	57.9
P13645	Keratin, type I cytoskeletal 10	2650.6	36.5	58.8
P25705	ATP synthase subunit alpha, mitochondrial	280.9	10.0	59.7
P04259	Keratin, type II cytoskeletal 6B	454.4	11.2	60.0
P35527	Keratin, type I cytoskeletal 9	1207.7	40.9	62.0
P13647	Keratin, type II cytoskeletal 5	270.1	7.6	62.3
P35908	Keratin, type II cytoskeletal 2 epidermal	1939.1	41.5	65.4
P04264	Keratin, type II cytoskeletal 1	3654.0	47.4	66.0
P03915	NADH-ubiquinone oxidoreductase chain 5	73.5	4.6	67.0
P02768	Serum albumin	530.1	8.4	69.3
P08107	Heat shock 70 kDa protein 1A/1B	638.5	14.2	70.0
P11142	Heat shock cognate 71 kDa protein	482.3	12.4	70.9
O75746	Calcium-binding mitochondrial carrier protein Aralar1	55.2	3.0	74.7
O75112	LIM domain-binding protein 3	136.0	4.8	77.1
Q99798	Aconitate hydratase, mitochondrial	67.9	5.3	85.4
P11217	Glycogen phosphorylase, muscle form	949.2	19.0	97.0
P35609	Alpha-actinin-2	2624.0	34.7	103.8
O14983	Sarcoplasmic/endoplasmic reticulum calcium ATPase 1	672.2	12.2	110.2
P16615	Sarcoplasmic/endoplasmic reticulum calcium ATPase 2	699.2	13.1	114.7
Q00872	Myosin-binding protein C, slow-type	148.4	3.4	128.2
O15061	Synemin	116.7	2.0	172.7
Q9UKX2	Myosin-2	3693.3	24.3	222.9
P12883	Myosin-7	5181.7	28.3	223.0
O75923	Dysferlin	185.2	1.2	237.1
Q14315	Filamin-C	52.7	1.2	290.8
P20929	Nebulin	607.2	5.8	772.4
Q8WZ42	Titin	119.4	0.4	3813.7

Band 6:

Accession	Description	Score	Coverage	MW [kDa]
P81605	Dermcidin	100.0	22.7	11.3
P68871	Hemoglobin subunit beta	390.9	44.9	16.0
P02144	Myoglobin	143.2	19.5	17.2
Q96A32	Myosin regulatory light chain 2, skeletal muscle isoform	38.9	13.6	19.0
P05976	Myosin light chain 1/3, skeletal muscle isoform	191.9	18.6	21.1
P08590	Myosin light chain 3	185.9	19.5	21.9
P67936	Tropomyosin alpha-4 chain	1365.2	24.2	28.5
O75822	Eukaryotic translation initiation factor 3 subunit J	60.0	8.5	29.0
Q14847	LIM and SH3 domain protein 1	116.6	10.3	29.7
P21796	Voltage-dependent anion-selective channel protein 1	61.9	11.7	30.8
Q13643	Four and a half LIM domains protein 3	81.0	7.1	31.2
P45880	Voltage-dependent anion-selective channel protein 2	276.2	26.5	31.5
Q9NP98	Myozenin-1	123.5	24.1	31.7
P45378	Troponin T, fast skeletal muscle	979.1	22.3	31.8
P09493	Tropomyosin alpha-1 chain	3418.2	43.0	32.7
P07951	Tropomyosin beta chain	2237.1	29.9	32.8
P08865	40S ribosomal protein SA	193.2	12.9	32.8
P52907	F-actin-capping protein subunit alpha-1	509.1	22.0	32.9
P13805	Troponin T, slow skeletal muscle	1971.5	26.3	32.9
P47755	F-actin-capping protein subunit alpha-2	1101.3	65.0	32.9
P06753	Tropomyosin alpha-3 chain	3222.2	47.4	32.9
P12235	ADP/ATP translocase 1	164.5	10.1	33.0
P53004	Biliverdin reductase A	168.3	12.8	33.4
P05388	60S acidic ribosomal protein P0	136.8	12.0	34.3
O75569	Interferon-inducible double-stranded RNA-dependent protein kinase activator A	57.8	9.6	34.4
P60891	Ribose-phosphate pyrophosphokinase 1	208.1	11.0	34.8
Q08257	Quinone oxidoreductase	148.0	14.0	35.2
P40926	Malate dehydrogenase, mitochondrial	575.0	33.1	35.5
Q9UBQ7	Glyoxylate reductase/hydroxypyruvate reductase	902.2	28.4	35.6
P15121	Aldose reductase	627.2	46.5	35.8
P04406	Glyceraldehyde-3-phosphate dehydrogenase	2064.7	40.3	36.0
P05198	Eukaryotic translation initiation factor 2 subunit 1	102.8	10.2	36.1
Q13642	Four and a half LIM domains protein 1	875.6	19.8	36.2
P40925	Malate dehydrogenase, cytoplasmic	504.8	22.2	36.4
P00338	L-lactate dehydrogenase A chain	336.9	19.9	36.7
O00757	Fructose-1,6-bisphosphatase isozyme 2	616.6	20.4	36.7
Q04828	Aldo-keto reductase family 1 member C1	561.7	25.7	36.8
P62140	Serine/threonine-protein phosphatase PP1-beta catalytic subunit	331.4	21.1	37.2
P62879	Guanine nucleotide-binding protein G(I)/G(S)/G(T) subunit beta-2	102.9	9.7	37.3
P52564	Dual specificity mitogen-	60.5	8.4	37.5

	activated protein kinase kinase 6			
P21695	Glycerol-3-phosphate dehydrogenase [NAD(+)], cytoplasmic	1195.6	37.5	37.5
Q9H2U2	Inorganic pyrophosphatase 2, mitochondrial	115.8	7.5	37.9
Q9Y394	Dehydrogenase/reductase SDR family member 7	251.2	10.3	38.3
Q8N335	Glycerol-3-phosphate dehydrogenase 1-like protein	755.0	28.5	38.4
Q15366	Poly(rC)-binding protein 2	79.4	9.3	38.6
P07355	Annexin A2	464.8	26.6	38.6
P04083	Annexin A1	140.4	7.8	38.7
Q53GG5	PDZ and LIM domain protein 3	210.9	9.1	39.2
P11177	Pyruvate dehydrogenase E1 component subunit beta, mitochondrial	1999.2	39.8	39.2
P04075	Fructose-bisphosphate aldolase A	1816.8	48.4	39.4
Q6IBS0	Twinfilin-2	269.9	15.2	39.5
O43488	Aflatoxin B1 aldehyde reductase member 2	164.8	8.6	39.6
P50213	Isocitrate dehydrogenase [NAD] subunit alpha, mitochondrial	490.8	16.1	39.6
P68138	Actin, alpha skeletal muscle	2510.0	52.5	42.0
Q16795	NADH dehydrogenase [ubiquinone] 1 alpha subcomplex subunit 9, mitochondrial	290.2	14.9	42.5
P06732	Creatine kinase M-type	1502.2	37.8	43.1
P00558	Phosphoglycerate kinase 1	427.7	23.3	44.6
P24752	Acetyl-CoA acetyltransferase, mitochondrial	70.7	5.9	45.2
P13929	Beta-enolase	794.6	24.0	47.0
P17540	Creatine kinase S-type, mitochondrial	816.9	21.2	47.5
P00505	Aspartate aminotransferase, mitochondrial	306.8	6.3	47.5
Q05639	Elongation factor 1-alpha 2	213.2	12.5	50.4
P48735	Isocitrate dehydrogenase [NADP], mitochondrial	241.8	11.5	50.9
Q13505	Metaxin-1	149.4	8.4	51.4
P02533	Keratin, type I cytoskeletal 14	655.6	10.2	51.5
P17661	Desmin	950.0	34.9	53.5
Q9UBF9	Myotilin	247.4	12.3	55.4
P06576	ATP synthase subunit beta, mitochondrial	594.1	18.9	56.5
P14618	Pyruvate kinase isozymes M1/M2	713.9	24.7	57.9
P13645	Keratin, type I cytoskeletal 10	2296.3	35.3	58.8
P25705	ATP synthase subunit alpha, mitochondrial	731.4	16.3	59.7
P36871	Phosphoglucomutase-1	729.4	15.8	61.4
P35527	Keratin, type I cytoskeletal 9	1198.4	31.6	62.0
P13647	Keratin, type II cytoskeletal 5	178.1	11.2	62.3
P35908	Keratin, type II cytoskeletal 2 epidermal	2084.8	36.8	65.4
P04264	Keratin, type II cytoskeletal 1	3234.3	47.5	66.0
O60662	Kelch-like protein 41	126.7	5.3	68.0
P02768	Serum albumin	121.3	10.3	69.3
P08107	Heat shock 70 kDa protein 1A/1B	152.0	6.2	70.0
P49748	Very long-chain specific acyl-CoA dehydrogenase, mitochondrial	457.3	15.9	70.3
P11142	Heat shock cognate 71 kDa protein	71.3	5.9	70.9
O75746	Calcium-binding mitochondrial carrier protein Aralar1	105.9	3.0	74.7
O75112	LIM domain-binding protein 3	58.5	6.2	77.1
P40939	Trifunctional enzyme subunit alpha, mitochondrial	138.7	4.7	82.9
P08237	6-phosphofructokinase, muscle type	602.8	8.9	85.1
Q99798	Aconitate hydratase, mitochondrial	42.6	3.3	85.4
P11217	Glycogen phosphorylase, muscle form	329.6	15.7	97.0
Q86TD4	Sarcalumenin	102.5	3.4	100.7
P35609	Alpha-actinin-2	1581.6	27.6	103.8
O14983	Sarcoplasmic/endoplasmic reticulum calcium ATPase 1	491.6	9.3	110.2
Q13423	NAD(P) transhydrogenase, mitochondrial	40.4	2.1	113.8
Q00872	Myosin-binding protein C, slow-type	967.2	11.8	128.2
P35573	Glycogen debranching enzyme	128.0	3.2	174.7
P52179	Myomesin-1	132.9	1.6	187.5
Q9UKX2	Myosin-2	3786.6	22.7	222.9
P12883	Myosin-7	4803.4	27.8	223.0
P20929	Nebulin	732.4	6.0	772.4
Q8WZ42	Titin	40.8	0.1	3813.7

Band 7:

Accession	Description	Score	Coverage	MW [kDa]
P81605	Dermcidin	173.4	22.7	11.3
P62805	Histone H4	169.7	17.5	11.4
P69905	Hemoglobin subunit alpha	82.9	19.0	15.2
P68871	Hemoglobin subunit beta	359.5	36.7	16.0
P02144	Myoglobin	84.1	19.5	17.2
Q96A32	Myosin regulatory light chain 2, skeletal muscle isoform	28.1	13.6	19.0
P05976	Myosin light chain 1/3, skeletal muscle isoform	213.6	18.6	21.1
P08590	Myosin light chain 3	230.1	31.3	21.9
P07451	Carbonic anhydrase 3	74.3	16.2	29.5
Q9NPC6	Myozenin-2	301.4	22.7	29.9
Q9Y277	Voltage-dependent anion-selective channel protein 3	280.2	9.2	30.6
P21796	Voltage-dependent anion-selective channel protein 1	3224.6	64.7	30.8
P29692	Elongation factor 1-delta	213.6	17.1	31.1
P47756	F-actin-capping protein subunit beta	572.2	25.6	31.3
P10768	S-formylglutathione hydrolase	163.6	9.6	31.4
P45880	Voltage-dependent anion-selective channel protein 2	931.0	46.6	31.5
Q9NP98	Myozenin-1	2498.9	51.2	31.7
P45378	Troponin T, fast skeletal muscle	1215.8	29.4	31.8
O43396	Thioredoxin-like protein 1	65.4	21.5	32.2
Q13326	Gamma-sarcoglycan	65.2	9.3	32.4
Q5SRE7	Phytanoyl-CoA dioxygenase domain-containing protein 1	156.2	10.3	32.4
P09493	Tropomyosin alpha-1 chain	1703.5	39.4	32.7
P07951	Tropomyosin beta chain	1242.5	29.9	32.8
P13805	Troponin T, slow skeletal muscle	1105.1	26.3	32.9
P06753	Tropomyosin alpha-3 chain	1457.1	40.0	32.9
P12235	ADP/ATP translocase 1	194.2	13.8	33.0
Q99623	Prohibitin-2	553.7	32.1	33.3
Q16762	Thiosulfate sulfurtransferase	106.0	14.5	33.4
Q9UHQ9	NADH-cytochrome b5 reductase 1	267.6	16.4	34.1
Q16836	Hydroxyacyl-coenzyme A dehydrogenase, mitochondrial	192.2	18.2	34.3
O14579	Coatomer subunit epsilon	35.4	9.4	34.5
Q9HC38	Glyoxalase domain-containing protein 4	101.1	7.7	34.8
P63244	Guanine nucleotide-binding protein subunit beta-2-like 1	62.1	11.0	35.1
P13804	Electron transfer flavoprotein subunit alpha, mitochondrial	495.2	28.5	35.1
P31937	3-hydroxyisobutyrate dehydrogenase, mitochondrial	247.5	19.6	35.3
P40926	Malate dehydrogenase, mitochondrial	2156.7	50.0	35.5
O75208	Ubiquinone biosynthesis protein COQ9, mitochondrial	295.7	20.1	35.5
P09525	Annexin A4	428.1	21.9	35.9
P08758	Annexin A5	282.9	17.5	35.9
P04406	Glyceraldehyde-3-phosphate dehydrogenase	1130.5	37.9	36.0
Q16698	2,4-dienoyl-CoA reductase, mitochondrial	67.0	7.2	36.0
P53597	Succinyl-CoA ligase [ADP/GDP-forming] subunit alpha, mitochondrial	219.3	15.9	36.2
Q13642	Four and a half LIM domains protein 1	754.2	19.8	36.2
P40925	Malate dehydrogenase, cytoplasmic	1085.2	29.0	36.4
P07195	L-lactate dehydrogenase B chain	1044.6	30.5	36.6
P00338	L-lactate dehydrogenase A chain	1301.7	32.8	36.7
O00757	Fructose-1,6-bisphosphatase isozyme 2	177.5	10.3	36.7
Q9NUQ9	Protein FAM49B	94.6	9.3	36.7
P36873	Serine/threonine-protein phosphatase PP1-gamma catalytic subunit	91.7	7.1	37.0
P21695	Glycerol-3-phosphate dehydrogenase [NAD(+)], cytoplasmic	115.3	6.9	37.5
Q9H2U2	Inorganic pyrophosphatase 2, mitochondrial	84.4	7.5	37.9
Q9H0P0	Cytosolic 5'-nucleotidase 3A	270.0	15.8	37.9
P07355	Annexin A2	349.6	21.2	38.6

P04083	Annexin A1	162.3	7.8	38.7
P11177	Pyruvate dehydrogenase E1 component subunit beta, mitochondrial	561.5	15.6	39.2
P04075	Fructose-bisphosphate aldolase A	1009.0	41.8	39.4
P60712	Actin, cytoplasmic 1	1127.3	25.3	41.7
P68138	Actin, alpha skeletal muscle	3005.9	50.4	42.0
P06732	Creatine kinase M-type	965.4	29.7	43.1
P00558	Phosphoglycerate kinase 1	95.2	14.6	44.6
P60842	Eukaryotic initiation factor 4A-I	30.1	5.9	46.1
Q14525	Keratin, type I cuticular Ha3-II	1794.4	24.3	46.2
P13929	Beta-enolase	233.3	9.9	47.0
Q15323	Keratin, type I cuticular Ha1	2737.6	28.4	47.2
P22695	Cytochrome b-c1 complex subunit 2, mitochondrial	759.6	26.5	48.4
O76011	Keratin, type I cuticular Ha4	1178.3	19.0	49.4
Q92764	Keratin, type I cuticular Ha5	956.3	17.6	50.3
P48735	Isocitrate dehydrogenase [NADP], mitochondrial	93.5	15.0	50.9
P02533	Keratin, type I cytoskeletal 14	237.9	8.1	51.5
O76013	Keratin, type I cuticular Ha6	907.8	14.8	52.2
P17661	Desmin	259.5	20.4	53.5
P78385	Keratin, type II cuticular Hb3	1596.8	26.8	54.2
P78386	Keratin, type II cuticular Hb5	1433.5	28.0	55.8
P06576	ATP synthase subunit beta, mitochondrial	164.4	14.0	56.5
Q9NSB4	Keratin, type II cuticular Hb2	336.0	7.8	56.6
Q16851	UTP--glucose-1-phosphate uridylyltransferase	214.5	9.3	56.9
P14618	Pyruvate kinase isozymes M1/M2	114.2	8.7	57.9
P13645	Keratin, type I cytoskeletal 10	1785.4	34.1	58.8
P25705	ATP synthase subunit alpha, mitochondrial	489.7	11.9	59.7
P36871	Phosphoglucomutase-1	507.6	12.5	61.4
P35527	Keratin, type I cytoskeletal 9	504.8	29.1	62.0
P13647	Keratin, type II cytoskeletal 5	59.2	8.6	62.3
P35908	Keratin, type II cytoskeletal 2 epidermal	1060.6	22.5	65.4
P04264	Keratin, type II cytoskeletal 1	2058.1	39.3	66.0
O60662	Kelch-like protein 41	115.9	5.8	68.0
P02768	Serum albumin	193.2	5.3	69.3
P11142	Heat shock cognate 71 kDa protein	311.4	11.9	70.9
O75112	LIM domain-binding protein 3	2768.8	17.5	77.1
P40939	Trifunctional enzyme subunit alpha, mitochondrial	155.2	3.4	82.9
P08237	6-phosphofructokinase, muscle type	98.5	5.1	85.1
P11217	Glycogen phosphorylase, muscle form	624.4	13.0	97.0
Q08043	Alpha-actinin-3	338.3	5.4	103.2
P35609	Alpha-actinin-2	2987.0	29.4	103.8
O14983	Sarcoplasmic/endoplasmic reticulum calcium ATPase 1	694.1	13.8	110.2
P16615	Sarcoplasmic/endoplasmic reticulum calcium ATPase 2	810.9	13.2	114.7
Q00872	Myosin-binding protein C, slow-type	617.8	9.0	128.2
P52179	Myomesin-1	47.6	2.1	187.5
Q9UKX2	Myosin-2	2295.2	16.2	222.9
P12883	Myosin-7	2684.7	24.4	223.0
P15924	Desmoplakin	57.7	0.7	331.6
P20929	Nebulin	266.2	2.1	772.4

Band 8:

Accession	Description	Score	Coverage	MW [kDa]
P81605	Dermcidin	71.3	20.0	11.3
P69905	Hemoglobin subunit alpha	75.3	19.0	15.2
P05976	Myosin light chain 1/3, skeletal muscle isoform	118.1	12.9	21.1
P07951	Tropomyosin beta chain	4540.7	29.2	32.8
P13805	Troponin T, slow skeletal muscle	72.6	6.8	32.9
P06753	Tropomyosin alpha-3 chain	764.5	27.4	32.9
Q13642	Four and a half LIM domains protein 1	2214.7	18.9	36.2
P00338	L-lactate dehydrogenase A chain	99.3	9.3	36.7
Q15365	Poly(rC)-binding protein 1	83.8	10.1	37.5
P04083	Annexin A1	208.1	6.4	38.7
P04075	Fructose-bisphosphate aldolase A	1894.5	38.5	39.4
Q8NDY3	[Protein ADP-ribosylarginine] hydrolase-like protein 1	68.7	6.2	40.1
O95299	NADH dehydrogenase [ubiquinone] 1 alpha subcomplex subunit 10, mitochondrial	102.7	7.3	40.7
P68138	Actin, alpha skeletal muscle	5262.5	45.1	42.0
P06732	Creatine kinase M-type	474.6	10.8	43.1
P60842	Eukaryotic initiation factor 4A-I	197.2	6.7	46.1
P13646	Keratin, type I cytoskeletal 13	235.0	13.1	49.6
P31930	Cytochrome b-c1 complex subunit 1, mitochondrial	188.6	4.6	52.6
P17661	Desmin	547.5	18.5	53.5
P13645	Keratin, type I cytoskeletal 10	747.4	19.5	58.8
P35527	Keratin, type I cytoskeletal 9	368.1	13.0	62.0
P35908	Keratin, type II cytoskeletal 2 epidermal	597.5	11.9	65.4
P04264	Keratin, type II cytoskeletal 1	535.4	17.2	66.0
P02768	Serum albumin	126.2	3.9	69.3
P08107	Heat shock 70 kDa protein 1A/1B	159.6	5.9	70.0
P11217	Glycogen phosphorylase, muscle form	357.4	16.3	97.0
P35609	Alpha-actinin-2	297.7	10.2	103.8
P16615	Sarcoplasmic/endoplasmic reticulum calcium ATPase 2	287.3	6.8	114.7
O15061	Synemin	66.9	1.8	172.7
P12883	Myosin-7	2097.8	11.4	223.0
P12882	Myosin-1	743.8	5.0	223.0
P20929	Nebulin	124.9	0.3	772.4
Q8WZ42	Titin	45.4	0.1	3813.7

Band 9:

Accession	Description	Score	Coverage	MW [kDa]
P81605	Dermcidin	82.2	12.7	11.3
P69905	Hemoglobin subunit alpha	175.2	19.0	15.2
P68871	Hemoglobin subunit beta	201.1	51.0	16.0
P05976	Myosin light chain 1/3, skeletal muscle isoform	55.3	12.9	21.1
P19237	Troponin I, slow skeletal muscle	25.2	9.6	21.7
P08590	Myosin light chain 3	225.2	32.8	21.9
O75822	Eukaryotic translation initiation factor 3 subunit J	42.4	8.5	29.0
P21796	Voltage-dependent anion-selective channel protein 1	114.4	19.4	30.8
P60174	Triosephosphate isomerase	85.2	7.7	30.8
P45880	Voltage-dependent anion-selective channel protein 2	242.7	22.1	31.5
Q9NP98	Myozenin-1	138.9	14.1	31.7
P45378	Troponin T, fast skeletal muscle	366.1	24.5	31.8
Q92629	Delta-sarcoglycan	145.8	9.3	32.1
P09493	Tropomyosin alpha-1 chain	2120.4	48.9	32.7
P07951	Tropomyosin beta chain	1520.2	43.7	32.8
P08865	40S ribosomal protein SA	322.8	21.4	32.8
P52907	F-actin-capping protein subunit alpha-1	333.6	27.3	32.9
P13805	Troponin T, slow skeletal muscle	955.4	20.9	32.9
P47755	F-actin-capping protein subunit alpha-2	516.4	47.6	32.9
P06753	Tropomyosin alpha-3 chain	2838.7	58.6	32.9
P53004	Biliverdin reductase A	145.8	15.5	33.4
Q14894	Ketimine reductase mu-crystallin	96.2	8.0	33.8
Q9UHQ9	NADH-cytochrome b5 reductase 1	72.5	9.8	34.1
P05388	60S acidic ribosomal protein P0	106.0	12.9	34.3
P60891	Ribose-phosphate pyrophosphokinase 1	146.8	8.8	34.8
Q9H0W9	Ester hydrolase C11orf54	203.8	12.4	35.1
Q9H479	Fructosamine-3-kinase	67.7	11.7	35.1
Q08257	Quinone oxidoreductase	100.2	31.6	35.2
P40926	Malate dehydrogenase, mitochondrial	423.2	21.9	35.5
P55735	Protein SEC13 homolog	49.3	8.7	35.5
Q9UBQ7	Glyoxylate reductase/hydroxypyruvate reductase	152.6	11.6	35.6
P15121	Aldose reductase	519.2	46.8	35.8
P04406	Glyceraldehyde-3-phosphate dehydrogenase	1271.0	41.5	36.0
P05198	Eukaryotic translation initiation factor 2 subunit 1	143.2	27.6	36.1
Q7L5N1	COP9 signalosome complex subunit 6	34.2	11.9	36.1
Q13642	Four and a half LIM domains	1096.9	34.7	36.2

	protein 1			
P40925	Malate dehydrogenase, cytoplasmic	228.9	20.7	36.4
P14550	Alcohol dehydrogenase [NADP(+)]	53.1	7.7	36.5
P00338	L-lactate dehydrogenase A chain	174.9	16.9	36.7
O00757	Fructose-1,6-bisphosphatase isozyme 2	369.4	20.4	36.7
Q04828	Aldo-keto reductase family 1 member C1	171.3	26.6	36.8
P62140	Serine/threonine-protein phosphatase PP1-beta catalytic subunit	215.2	15.6	37.2
P52564	Dual specificity mitogen-activated protein kinase kinase 6	158.0	17.1	37.5
P37837	Transaldolase	95.2	10.4	37.5
P21695	Glycerol-3-phosphate dehydrogenase [NAD(+)], cytoplasmic	772.2	45.3	37.5
Q92905	COP9 signalosome complex subunit 5	72.0	12.9	37.6
Q9Y394	Dehydrogenase/reductase SDR family member 7	291.5	23.3	38.3
Q8N335	Glycerol-3-phosphate dehydrogenase 1-like protein	369.8	30.8	38.4
Q15366	Poly(rC)-binding protein 2	114.4	18.4	38.6
P07355	Annexin A2	249.4	21.2	38.6
P04083	Annexin A1	93.1	7.8	38.7
Q53GG5	PDZ and LIM domain protein 3	133.7	9.1	39.2
P11177	Pyruvate dehydrogenase E1 component subunit beta, mitochondrial	580.7	21.5	39.2
P46734	Dual specificity mitogen-activated protein kinase kinase 3	39.5	8.7	39.3
P04075	Fructose-bisphosphate aldolase A	722.0	38.2	39.4
Q6IBS0	Twinfilin-2	102.1	14.6	39.5
P50213	Isocitrate dehydrogenase [NAD] subunit alpha, mitochondrial	237.4	10.7	39.6
P11766	Alcohol dehydrogenase class-3	40.5	6.4	39.7
P17612	cAMP-dependent protein kinase catalytic subunit alpha	59.6	11.4	40.6
P60712	Actin, cytoplasmic 1	536.9	25.3	41.7
P68138	Actin, alpha skeletal muscle	1754.9	57.6	42.0
Q16795	NADH dehydrogenase [ubiquinone] 1 alpha subcomplex subunit 9, mitochondrial	72.1	6.4	42.5
P12277	Creatine kinase B-type	53.8	9.5	42.6
P06732	Creatine kinase M-type	866.9	28.6	43.1
Q9BXN1	Asporin	76.4	9.7	43.4
P00558	Phosphoglycerate kinase 1	296.7	20.6	44.6
P31415	Calsequestrin-1	50.6	6.1	45.1
P13929	Beta-enolase	395.1	22.6	47.0
P06733	Alpha-enolase	147.9	10.6	47.1
P17540	Creatine kinase S-type, mitochondrial	378.7	21.2	47.5
P00505	Aspartate aminotransferase, mitochondrial	144.6	9.5	47.5
P22695	Cytochrome b-c1 complex subunit 2, mitochondrial	28.8	6.4	48.4
Q05639	Elongation factor 1-alpha 2	277.5	9.9	50.4
P48735	Isocitrate dehydrogenase [NADP], mitochondrial	258.1	12.4	50.9
P08779	Keratin, type I cytoskeletal 16	616.3	29.2	51.2
P55084	Trifunctional enzyme subunit beta, mitochondrial	164.2	7.0	51.3
P02533	Keratin, type I cytoskeletal 14	901.8	32.2	51.5
P10909	Clusterin	52.5	6.0	52.5
P31930	Cytochrome b-c1 complex subunit 1, mitochondrial	37.7	6.7	52.6
P20073	Annexin A7	244.0	6.4	52.7
P17661	Desmin	773.8	32.8	53.5
Q9UBF9	Myotilin	354.6	17.7	55.4
P06576	ATP synthase subunit beta, mitochondrial	827.3	26.1	56.5
Q8NB12	Histone-lysine N-methyltransferase SMYD1	51.9	10.4	56.6
Q9UHG3	Prenylcysteine oxidase 1	109.5	5.4	56.6
Q9HCP6	Protein-cysteine N-palmitoyltransferase HHAT-like protein	50.1	4.6	56.7
P14618	Pyruvate kinase isozymes M1/M2	580.0	26.6	57.9
P13645	Keratin, type I cytoskeletal 10	1516.7	33.7	58.8
P25705	ATP synthase subunit alpha, mitochondrial	595.4	13.6	59.7
P48668	Keratin, type II cytoskeletal 6C	366.4	21.6	60.0
P04259	Keratin, type II cytoskeletal 6B	392.5	21.6	60.0
P36871	Phosphoglucomutase-1	810.9	22.8	61.4
P35527	Keratin, type I cytoskeletal 9	1569.4	47.8	62.0
P13647	Keratin, type II cytoskeletal 5	406.5	21.5	62.3
O00499	Myc box-dependent-interacting protein 1	35.5	6.2	64.7
P35908	Keratin, type II cytoskeletal 2 epidermal	1632.6	39.0	65.4
P04264	Keratin, type II cytoskeletal 1	2681.4	48.5	66.0
O60662	Kelch-like protein 41	158.0	9.6	68.0
P02768	Serum albumin	421.4	20.5	69.3
P08107	Heat shock 70 kDa protein 1A/1B	221.9	12.2	70.0
P49748	Very long-chain specific acyl-CoA dehydrogenase, mitochondrial	236.9	14.8	70.3
P43155	Carnitine O-acetyltransferase	139.7	3.4	70.8
P11142	Heat shock cognate 71 kDa protein	181.5	9.1	70.9
Q8NI60	Atypical kinase ADCK3, mitochondrial	71.4	3.1	71.9
O75746	Calcium-binding mitochondrial carrier protein Aralar1	79.2	3.5	74.7
P08133	Annexin A6	72.9	3.9	75.8
O75112	LIM domain-binding protein 3	218.9	9.1	77.1
P40939	Trifunctional enzyme subunit alpha, mitochondrial	328.4	11.5	82.9
P08237	6-phosphofructokinase, muscle type	360.5	10.0	85.1
Q99798	Aconitate hydratase, mitochondrial	92.1	3.3	85.4
P11217	Glycogen phosphorylase, muscle form	505.6	16.4	97.0
Q86TD4	Sarcalumenin	255.4	10.2	100.7
Q08043	Alpha-actinin-3	494.7	12.1	103.2
P35609	Alpha-actinin-2	1258.8	32.8	103.8
O14983	Sarcoplasmic/endoplasmic reticulum calcium ATPase 1	439.7	15.0	110.2
Q13423	NAD(P) transhydrogenase, mitochondrial	128.6	4.2	113.8
P16615	Sarcoplasmic/endoplasmic reticulum calcium ATPase 2	629.9	14.7	114.7
Q00872	Myosin-binding protein C, slow-type	1100.9	18.1	128.2
P54296	Myomesin-2	96.8	4.9	164.8
P35573	Glycogen debranching enzyme	104.8	5.5	174.7
P52179	Myomesin-1	134.7	3.9	187.5
Q9UKX2	Myosin-2	2595.8	20.3	222.9
P12883	Myosin-7	3943.0	34.2	223.0
P12882	Myosin-1	2261.8	17.3	223.0
Q14315	Filamin-C	121.8	1.9	290.8
Q15149	Plectin	128.0	1.3	531.5
P20929	Nebulin	1649.1	12.3	772.4
Q8WZ42	Titin	767.0	1.1	3813.7

Band 10:

Accession	Description	Score	Coverage	MW [kDa]
P81605	Dermcidin	103.9	20.0	11.3
P69905	Hemoglobin subunit alpha	129.8	19.0	15.2
P68871	Hemoglobin subunit beta	310.5	53.7	16.0
P02144	Myoglobin	110.0	28.6	17.2
P05976	Myosin light chain 1/3, skeletal muscle isoform	70.2	12.9	21.1
P08590	Myosin light chain 3	246.2	27.2	21.9
P07451	Carbonic anhydrase 3	169.9	24.6	29.5
Q9NPC6	Myozenin-2	486.7	22.7	29.9
Q9Y277	Voltage-dependent anion-selective channel protein 3	196.2	12.0	30.6
P21796	Voltage-dependent anion-selective channel protein 1	1923.9	64.7	30.8
P60174	Triosephosphate isomerase	79.5	8.7	30.8
P29692	Elongation factor 1-delta	80.0	12.8	31.1
Q13643	Four and a half LIM domains protein 3	38.5	7.1	31.2
P47756	F-actin-capping protein subunit beta	671.9	33.2	31.3
P10768	S-formylglutathione hydrolase	160.3	17.4	31.4
P45880	Voltage-dependent anion-selective channel protein 2	429.4	35.7	31.5
Q9NP98	Myozenin-1	1518.6	47.8	31.7
P45378	Troponin T, fast skeletal muscle	406.7	21.6	31.8
O43396	Thioredoxin-like protein 1	257.7	17.7	32.2
Q13326	Gamma-sarcoglycan	50.1	9.3	32.4
Q5SRE7	Phytanoyl-CoA dioxygenase domain-containing protein 1	229.2	10.3	32.4

P09493	Tropomyosin alpha-1 chain	294.6	31.7	32.7
P07951	Tropomyosin beta chain	430.7	20.1	32.8
P13805	Troponin T, slow skeletal muscle	773.5	20.9	32.9
P06753	Tropomyosin alpha-3 chain	272.8	31.2	32.9
P12235	ADP/ATP translocase 1	146.4	10.7	33.0
Q99623	Prohibitin-2	406.2	31.4	33.3
Q16762	Thiosulfate sulfurtransferase	41.2	10.4	33.4
Q6P1N9	Putative deoxyribonuclease TATDN1	69.8	12.1	33.6
Q9UHQ9	NADH-cytochrome b5 reductase 1	433.0	25.6	34.1
P00387	NADH-cytochrome b5 reductase 3	379.0	29.9	34.2
Q16836	Hydroxyacyl-coenzyme A dehydrogenase, mitochondrial	126.4	13.7	34.3
Q9HC38	Glyoxalase domain-containing protein 4	87.9	7.7	34.8
P13804	Electron transfer flavoprotein subunit alpha, mitochondrial	204.0	15.9	35.1
P31937	3-hydroxyisobutyrate dehydrogenase, mitochondrial	234.4	15.8	35.3
P40926	Malate dehydrogenase, mitochondrial	889.6	43.8	35.5
O75208	Ubiquinone biosynthesis protein COQ9, mitochondrial	374.0	15.1	35.5
Q13011	Delta(3,5)-Delta(2,4)-dienoyl-CoA isomerase, mitochondrial	325.2	15.2	35.8
P09525	Annexin A4	367.3	21.3	35.9
P08758	Annexin A5	469.0	25.6	35.9
P04406	Glyceraldehyde-3-phosphate dehydrogenase	718.2	26.6	36.0
Q16698	2,4-dienoyl-CoA reductase, mitochondrial	83.0	17.0	36.0
P53597	Succinyl-CoA ligase [ADP/GDP-forming] subunit alpha, mitochondrial	180.4	9.0	36.2
Q13642	Four and a half LIM domains protein 1	1155.1	26.6	36.2
P40925	Malate dehydrogenase, cytoplasmic	393.9	26.7	36.4
P07195	L-lactate dehydrogenase B chain	879.0	28.7	36.6
P00338	L-lactate dehydrogenase A chain	658.9	28.6	36.7
O00757	Fructose-1,6-bisphosphatase isozyme 2	103.9	9.7	36.7
Q9NUQ9	Protein FAM49B	79.9	7.7	36.7
Q5HYK3	2-methoxy-6-polyprenyl-1,4-benzoquinol methylase, mitochondrial	73.4	8.0	37.1
Q9H2U2	Inorganic pyrophosphatase 2, mitochondrial	68.0	7.5	37.9
Q9H0P0	Cytosolic 5'-nucleotidase 3A	79.8	9.2	37.9
P07355	Annexin A2	362.9	27.1	38.6
Q53GG5	PDZ and LIM domain protein 3	145.4	9.1	39.2
P11177	Pyruvate dehydrogenase E1 component subunit beta, mitochondrial	164.0	11.1	39.2
P04075	Fructose-bisphosphate aldolase A	930.9	41.8	39.4
Q9NZU5	LIM and cysteine-rich domains protein 1	104.7	8.5	40.8
P60712	Actin, cytoplasmic 1	1379.4	34.4	41.7
P68138	Actin, alpha skeletal muscle	3170.4	56.0	42.0
P06732	Creatine kinase M-type	624.9	24.4	43.1
P00558	Phosphoglycerate kinase 1	199.8	18.5	44.6
P01009	Alpha-1-antitrypsin	38.7	6.0	46.7
P13929	Beta-enolase	306.6	18.9	47.0
P17540	Creatine kinase S-type, mitochondrial	134.2	8.4	47.5
P22695	Cytochrome b-c1 complex subunit 2, mitochondrial	590.1	25.2	48.4
P07437	Tubulin beta chain	135.2	13.3	49.6
P68366	Tubulin alpha-4A chain	21.5	6.3	49.9
P68104	Elongation factor 1-alpha 1	103.1	7.4	50.1
Q9P2R7	Succinyl-CoA ligase [ADP-forming] subunit beta, mitochondrial	97.1	7.1	50.3
P48735	Isocitrate dehydrogenase [NADP], mitochondrial	368.5	19.3	50.9
P02533	Keratin, type I cytoskeletal 14	260.4	9.3	51.5
P17661	Desmin	590.2	30.9	53.5
P50995	Annexin A11	76.6	5.0	54.4
Q9UBF9	Myotilin	107.3	12.3	55.4
P06576	ATP synthase subunit beta, mitochondrial	128.5	11.3	56.5
Q16851	UTP--glucose-1-phosphate uridylyltransferase	480.3	14.0	56.9
P14618	Pyruvate kinase isozymes M1/M2	206.4	12.8	57.9
P13645	Keratin, type I cytoskeletal 10	865.1	31.3	58.8
P25705	ATP synthase subunit alpha, mitochondrial	152.3	6.9	59.7
P36871	Phosphoglucomutase-1	830.5	23.7	61.4
P35527	Keratin, type I cytoskeletal 9	1746.8	54.4	62.0
P13647	Keratin, type II cytoskeletal 5	81.4	8.0	62.3
Q96HC4	PDZ and LIM domain protein 5	68.0	8.4	63.9
P35908	Keratin, type II cytoskeletal 2 epidermal	738.2	22.9	65.4
P04264	Keratin, type II cytoskeletal 1	2582.8	46.9	66.0
O60662	Kelch-like protein 41	93.9	5.8	68.0
P02768	Serum albumin	222.0	9.7	69.3
P08107	Heat shock 70 kDa protein 1A/1B	431.0	16.9	70.0
P49748	Very long-chain specific acyl-CoA dehydrogenase, mitochondrial	64.6	3.4	70.3
P11142	Heat shock cognate 71 kDa protein	422.5	14.6	70.9
O75112	LIM domain-binding protein 3	2046.1	19.8	77.1
P48147	Prolyl endopeptidase	52.2	5.5	80.6
P40939	Trifunctional enzyme subunit alpha, mitochondrial	263.0	4.1	82.9
P08237	6-phosphofructokinase, muscle type	51.7	4.0	85.1
P11217	Glycogen phosphorylase, muscle form	709.7	16.0	97.0
Q08043	Alpha-actinin-3	704.2	14.2	103.2
P35609	Alpha-actinin-2	3254.8	35.6	103.8
O14983	Sarcoplasmic/endoplasmic reticulum calcium ATPase 1	583.9	11.5	110.2
P16615	Sarcoplasmic/endoplasmic reticulum calcium ATPase 2	821.6	13.6	114.7
Q00872	Myosin-binding protein C, slow-type	879.4	9.8	128.2
Q5VTT5	Myomesin-3	71.2	2.2	162.1
P54296	Myomesin-2	76.8	3.5	164.8
Q9UKX2	Myosin-2	1943.7	17.7	222.9
P12883	Myosin-7	4281.9	28.6	223.0
P12882	Myosin-1	1730.0	14.5	223.0
P20929	Nebulin	707.1	6.3	772.4
Q8WZ42	Titin	453.2	0.5	3813.7

Band 11:

Accession	Description	Score	Coverage	MW [kDa]
P81605	Dermcidin	104.3	20.0	11.3
P01834	Ig kappa chain C region	297.9	32.1	11.6
P69905	Hemoglobin subunit alpha	186.6	19.0	15.2
P68871	Hemoglobin subunit beta	462.5	64.6	16.0
P02144	Myoglobin	101.2	28.6	17.2
P05976	Myosin light chain 1/3, skeletal muscle isoform	91.8	17.0	21.1
P08590	Myosin light chain 3	250.9	21.0	21.9
P45378	Troponin T, fast skeletal muscle	224.7	22.3	31.8
P06748	Nucleophosmin	131.2	19.1	32.6
P09493	Tropomyosin alpha-1 chain	1465.9	32.4	32.7
P07951	Tropomyosin beta chain	2735.7	45.8	32.8
P13805	Troponin T, slow skeletal muscle	349.0	17.6	32.9
P06753	Tropomyosin alpha-3 chain	1526.3	43.9	32.9
P07910	Heterogeneous nuclear ribonucleoproteins C1/C2	116.7	8.5	33.6
P20774	Mimecan	259.3	11.4	33.9
P40926	Malate dehydrogenase, mitochondrial	114.7	10.4	35.5
P04406	Glyceraldehyde-3-phosphate dehydrogenase	997.7	29.9	36.0
O00151	PDZ and LIM domain protein 1	203.4	11.3	36.0
P01857	Ig gamma-1 chain C region	432.9	22.7	36.1
Q13642	Four and a half LIM domains protein 1	976.2	22.9	36.2
P14550	Alcohol dehydrogenase [NADP(+)]	26.8	5.9	36.5
P00338	L-lactate dehydrogenase A chain	85.9	9.3	36.7
Q15365	Poly(rC)-binding protein 1	266.5	22.2	37.5
P37837	Transaldolase	308.5	23.4	37.5
Q9NZL9	Methionine adenosyltransferase 2 subunit beta	144.7	13.5	37.5
P21695	Glycerol-3-phosphate dehydrogenase [NAD(+)], cytoplasmic	964.0	40.1	37.5
Q9Y5K5	Ubiquitin carboxyl-terminal hydrolase isozyme L5	71.1	6.7	37.6
Q03591	Complement factor H-related protein 1	28.9	7.3	37.6

Q96C23	Aldose 1-epimerase	160.5	11.4	37.7
Q9UDY4	DnaJ homolog subfamily B member 4	388.4	17.5	37.8
O75436	Vacuolar protein sorting-associated protein 26A	71.1	13.2	38.1
P51884	Lumican	105.1	5.6	38.4
Q8N8N7	Prostaglandin reductase 2	103.2	10.3	38.5
P07355	Annexin A2	2324.4	45.1	38.6
P04083	Annexin A1	1654.6	41.9	38.7
Q9NX46	Poly(ADP-ribose) glycohydrolase ARH3	72.0	11.6	38.9
P04075	Fructose-bisphosphate aldolase A	1052.4	44.0	39.4
P07585	Decorin	192.2	10.3	39.7
P00325	Alcohol dehydrogenase 1B	207.9	10.1	39.8
Q8NDY3	[Protein ADP-ribosylarginine] hydrolase-like protein 1	99.1	5.9	40.1
P04899	Guanine nucleotide-binding protein G(i) subunit alpha-2	459.5	28.7	40.4
O95299	NADH dehydrogenase [ubiquinone] 1 alpha subcomplex subunit 10, mitochondrial	146.0	9.9	40.7
P50502	Hsc70-interacting protein	394.2	13.3	41.3
P21810	Biglycan	51.3	7.6	41.6
P60712	Actin, cytoplasmic 1	2550.4	46.1	41.7
Q562R1	Beta-actin-like protein 2	889.3	19.4	42.0
Q3ZC07	Actin, alpha cardiac muscle 1	3436.2	53.3	42.0
P68138	Actin, alpha skeletal muscle	3984.9	53.3	42.0
Q9NVD7	Alpha-parvin	180.5	8.1	42.2
P06732	Creatine kinase M-type	872.8	28.1	43.1
Q9BXN1	Asporin	744.0	21.8	43.4
Q6NVY1	3-hydroxyisobutyryl-CoA hydrolase, mitochondrial	97.7	9.1	43.5
P51888	Prolargin	305.9	21.7	43.8
O15382	Branched-chain-amino-acid aminotransferase, mitochondrial	74.6	15.1	44.3
P00558	Phosphoglycerate kinase 1	130.0	20.6	44.6
Q13510	Acid ceramidase	72.7	5.3	44.6
Q9UKU7	Isobutyryl-CoA dehydrogenase, mitochondrial	152.5	14.0	45.0
P00738	Haptoglobin	208.3	11.8	45.2
P06727	Apolipoprotein A-IV	77.1	5.1	45.4
P60842	Eukaryotic initiation factor 4A-I	398.2	11.8	46.1
Q14240	Eukaryotic initiation factor 4A-II	381.2	15.5	46.4
P13929	Beta-enolase	282.8	12.7	47.0
P06733	Alpha-enolase	497.8	20.7	47.1
P49411	Elongation factor Tu, mitochondrial	102.3	8.2	49.5
P07437	Tubulin beta chain	217.2	9.7	49.6
Q9BQE3	Tubulin alpha-1C chain	216.1	9.1	49.9
P26641	Elongation factor 1-gamma	99.0	8.0	50.1
P68104	Elongation factor 1-alpha 1	409.0	15.2	50.1
P48735	Isocitrate dehydrogenase [NADP], mitochondrial	197.9	7.7	50.9
P02533	Keratin, type I cytoskeletal 14	757.7	27.3	51.5
P31930	Cytochrome b-c1 complex subunit 1, mitochondrial	155.8	10.6	52.6
Q6ZMU5	Tripartite motif-containing protein 72	38.5	4.6	52.7
P40123	Adenylyl cyclase-associated protein 2	215.0	9.6	52.8
P34896	Serine hydroxymethyltransferase, cytosolic	133.1	6.2	53.0
P52209	6-phosphogluconate dehydrogenase, decarboxylating	105.6	8.1	53.1
Q6NUK1	Calcium-binding mitochondrial carrier protein SCaMC-1	138.7	6.7	53.3
P17661	Desmin	2195.8	46.0	53.5
P08670	Vimentin	1108.0	34.1	53.6
Q9UBF9	Myotilin	214.1	16.1	55.4
P02675	Fibrinogen beta chain	620.1	32.8	55.9
O60240	Perilipin-1	381.4	14.2	56.0
P05091	Aldehyde dehydrogenase, mitochondrial	81.4	7.4	56.3
P06576	ATP synthase subunit beta, mitochondrial	197.7	13.4	56.5
Q9HCP6	Protein-cysteine N-palmitoyltransferase HHAT-like protein	79.6	4.6	56.7
Q02252	Methylmalonate-semialdehyde dehydrogenase [acylating], mitochondrial	35.3	3.4	57.8
P14618	Pyruvate kinase isozymes M1/M2	74.1	3.8	57.9
P13645	Keratin, type I cytoskeletal 10	2488.3	35.3	58.8
P25705	ATP synthase subunit alpha, mitochondrial	127.4	11.2	59.7
P04040	Catalase	231.6	13.5	59.7
P10809	60 kDa heat shock protein, mitochondrial	54.1	3.0	61.0
Q9NZN4	EH domain-containing protein 2	82.1	3.7	61.1
P36871	Phosphoglucomutase-1	137.6	8.5	61.4
P35527	Keratin, type I cytoskeletal 9	2335.2	53.8	62.0
P13647	Keratin, type II cytoskeletal 5	441.2	21.4	62.3
P06744	Glucose-6-phosphate isomerase	287.7	10.0	63.1
P35908	Keratin, type II cytoskeletal 2 epidermal	2851.7	54.2	65.4
P04264	Keratin, type II cytoskeletal 1	4015.5	49.2	66.0
O75083	WD repeat-containing protein 1	280.5	5.3	66.2
O60662	Kelch-like protein 41	139.5	3.8	68.0
P04843	Dolichyl-diphosphooligosaccharide--protein glycosyltransferase subunit 1	76.6	3.6	68.5
P02768	Serum albumin	1044.1	32.8	69.3
P08107	Heat shock 70 kDa protein 1A/1B	787.4	20.0	70.0
P11142	Heat shock cognate 71 kDa protein	299.1	10.7	70.9
P02545	Prelamin-A/C	43.7	3.0	74.1
Q9Y2J8	Protein-arginine deiminase type-2	94.2	5.6	75.5
P08133	Annexin A6	265.1	11.3	75.8
O75112	LIM domain-binding protein 3	82.2	5.4	77.1
P33121	Long-chain-fatty-acid--CoA ligase 1	84.6	3.3	77.9
P07384	Calpain-1 catalytic subunit	81.1	4.2	81.8
P08237	6-phosphofructokinase, muscle type	64.3	5.4	85.1
Q99798	Aconitate hydratase, mitochondrial	178.4	5.6	85.4
P06396	Gelsolin	505.6	12.8	85.6
Q14BN4	Sarcolemmal membrane-associated protein	308.1	9.3	95.1
P11217	Glycogen phosphorylase, muscle form	434.0	15.1	97.0
Q86TD4	Sarcalumenin	56.4	3.2	100.7
P02730	Band 3 anion transport protein	85.2	4.5	101.7
P35609	Alpha-actinin-2	1222.4	29.9	103.8
P12110	Collagen alpha-2(VI) chain	63.7	2.0	108.5
P16615	Sarcoplasmic/endoplasmic reticulum calcium ATPase 2	773.6	12.8	114.7
P22314	Ubiquitin-like modifier-activating enzyme 1	137.7	2.8	117.8
O00159	Unconventional myosin-Ic	33.8	2.7	121.6
P18206	Vinculin	74.5	2.4	123.7
Q00872	Myosin-binding protein C, slow-type	317.5	8.5	128.2
Q96Q06	Perilipin-4	553.4	8.0	134.3
P01023	Alpha-2-macroglobulin	177.5	1.8	163.2
O15061	Synemin	165.6	4.0	172.7
P48681	Nestin	37.1	1.4	177.3
Q9HBL0	Tensin-1	53.2	1.4	185.6
P01024	Complement C3	172.2	1.7	187.0
Q9UKX2	Myosin-2	2052.4	17.8	222.9
P12883	Myosin-7	5223.0	36.1	223.0
P35579	Myosin-9	173.6	3.1	226.4
Q14315	Filamin-C	92.1	1.7	290.8
P12111	Collagen alpha-3(VI) chain	866.5	6.0	343.5
Q15149	Plectin	292.7	1.7	531.5
Q09666	Neuroblast differentiation-associated protein AHNAK	133.4	4.8	628.7
P20929	Nebulin	469.2	4.0	772.4
Q8WZ42	Titin	935.2	1.2	3813.7

Band 12:

Accession	Description	Score	Coverage	MW [kDa]
P81605	Dermcidin	166.4	22.7	11.3
P62805	Histone H4	46.5	17.5	11.4
P01834	Ig kappa chain C region	268.4	32.1	11.6
P69905	Hemoglobin subunit alpha	233.2	30.3	15.2
P68871	Hemoglobin subunit beta	456.2	70.8	16.0
P02144	Myoglobin	108.0	28.6	17.2
P05976	Myosin light chain 1/3, skeletal muscle isoform	149.6	18.6	21.1
P08590	Myosin light chain 3	219.6	31.3	21.9
P51858	Hepatoma-derived growth factor	102.7	19.6	26.8

Q969G5	Protein kinase C delta-binding protein	163.1	19.2	27.7
O75822	Eukaryotic translation initiation factor 3 subunit J	39.8	8.5	29.0
Q14847	LIM and SH3 domain protein 1	85.9	10.3	29.7
P45880	Voltage-dependent anion-selective channel protein 2	48.9	10.5	31.5
P45378	Troponin T, fast skeletal muscle	234.9	22.3	31.8
Q92629	Delta-sarcoglycan	257.2	14.9	32.1
P06748	Nucleophosmin	165.6	23.5	32.6
P09493	Tropomyosin alpha-1 chain	1702.3	42.3	32.7
P07951	Tropomyosin beta chain	1055.2	29.9	32.8
P08865	40S ribosomal protein SA	411.8	26.8	32.8
P52907	F-actin-capping protein subunit alpha-1	763.7	50.0	32.9
P13805	Troponin T, slow skeletal muscle	540.6	23.0	32.9
P47755	F-actin-capping protein subunit alpha-2	770.4	59.1	32.9
P06753	Tropomyosin alpha-3 chain	2018.8	46.7	32.9
P53004	Biliverdin reductase A	182.3	19.6	33.4
P20774	Mimecan	357.1	11.4	33.9
P05388	60S acidic ribosomal protein P0	186.7	15.1	34.3
O75569	Interferon-inducible double-stranded RNA-dependent protein kinase activator A	114.4	8.0	34.4
P60891	Ribose-phosphate pyrophosphokinase 1	294.2	12.9	34.8
O00764	Pyridoxal kinase	106.7	11.9	35.1
Q9H0W9	Ester hydrolase C11orf54	275.1	11.8	35.1
Q9H479	Fructosamine-3-kinase	31.6	7.1	35.1
Q08257	Quinone oxidoreductase	109.2	21.9	35.2
P40926	Malate dehydrogenase, mitochondrial	230.3	24.9	35.5
P55735	Protein SEC13 homolog	250.7	16.8	35.5
Q9UBQ7	Glyoxylate reductase/hydroxypyruvate reductase	518.0	35.4	35.6
Q96CX2	BTB/POZ domain-containing protein KCTD12	363.3	16.6	35.7
P45381	Aspartoacylase	58.3	6.1	35.7
P15121	Aldose reductase	648.1	45.9	35.8
P04406	Glyceraldehyde-3-phosphate dehydrogenase	904.5	36.1	36.0
P01857	Ig gamma-1 chain C region	323.3	18.5	36.1
P05198	Eukaryotic translation initiation factor 2 subunit 1	231.0	24.1	36.1
P02649	Apolipoprotein E	701.7	32.2	36.1
Q13642	Four and a half LIM domains protein 1	876.2	33.4	36.2
P13716	Delta-aminolevulinic acid dehydratase	135.1	20.6	36.3
P40925	Malate dehydrogenase, cytoplasmic	304.3	18.3	36.4
P07195	L-lactate dehydrogenase B chain	158.8	14.4	36.6
P00338	L-lactate dehydrogenase A chain	154.3	9.3	36.7
Q04828	Aldo-keto reductase family 1 member C1	1053.5	32.2	36.8
P31942	Heterogeneous nuclear ribonucleoprotein H3	122.4	15.0	36.9
P62140	Serine/threonine-protein phosphatase PP1-beta catalytic subunit	369.3	22.9	37.2
P62873	Guanine nucleotide-binding protein G(I)/G(S)/G(T) subunit beta-1	302.6	23.8	37.4
P52564	Dual specificity mitogen-activated protein kinase kinase 6	38.4	8.4	37.5
P62136	Serine/threonine-protein phosphatase PP1-alpha catalytic subunit	296.6	21.2	37.5
P37837	Transaldolase	218.4	11.0	37.5
P21695	Glycerol-3-phosphate dehydrogenase [NAD(+)], cytoplasmic	1666.1	50.7	37.5
Q9H2U2	Inorganic pyrophosphatase 2, mitochondrial	83.8	7.5	37.9
Q9Y394	Dehydrogenase/reductase SDR family member 7	373.9	15.9	38.3
Q8N335	Glycerol-3-phosphate dehydrogenase 1-like protein	441.3	28.2	38.4
P51884	Lumican	70.3	5.6	38.4
P07355	Annexin A2	668.0	35.1	38.6
P04083	Annexin A1	530.0	22.0	38.7
P11177	Pyruvate dehydrogenase E1 component subunit beta, mitochondrial	556.2	23.7	39.2
P46734	Dual specificity mitogen-activated protein kinase kinase 3	78.4	8.7	39.3
P04075	Fructose-bisphosphate aldolase A	285.0	20.3	39.4
Q6IBS0	Twinfilin-2	164.4	10.9	39.5
P50213	Isocitrate dehydrogenase [NAD] subunit alpha, mitochondrial	308.0	13.4	39.6
P11766	Alcohol dehydrogenase class-3	84.4	6.7	39.7
P07585	Decorin	214.3	17.0	39.7
P00325	Alcohol dehydrogenase 1B	240.0	18.4	39.8
P04899	Guanine nucleotide-binding protein G(i) subunit alpha-2	68.1	7.3	40.4
P17612	cAMP-dependent protein kinase catalytic subunit alpha	34.3	5.4	40.6
P60712	Actin, cytoplasmic 1	865.5	37.6	41.7
Q3ZC07	Actin, alpha cardiac muscle 1	1924.8	45.1	42.0
P68138	Actin, alpha skeletal muscle	2029.8	45.1	42.0
P12277	Creatine kinase B-type	247.5	15.8	42.6
P06732	Creatine kinase M-type	1334.0	36.0	43.1
Q9BXN1	Asporin	954.3	24.2	43.4
Q6NZI2	Polymerase I and transcript release factor	171.0	6.7	43.4
P51888	Prolargin	201.0	16.0	43.8
P00558	Phosphoglycerate kinase 1	446.7	26.4	44.6
P00738	Haptoglobin	52.3	4.7	45.2
P36955	Pigment epithelium-derived factor	73.8	7.9	46.3
P01009	Alpha-1-antitrypsin	37.7	6.2	46.7
P13929	Beta-enolase	548.1	13.4	47.0
P06733	Alpha-enolase	498.6	18.2	47.1
P17540	Creatine kinase S-type, mitochondrial	482.4	20.3	47.5
P15088	Mast cell carboxypeptidase A	118.5	7.7	48.6
P07437	Tubulin beta chain	159.5	10.8	49.6
P68104	Elongation factor 1-alpha 1	479.0	19.9	50.1
P68363	Tubulin alpha-1B chain	110.4	14.4	50.1
Q05639	Elongation factor 1-alpha 2	415.0	16.2	50.4
Q16181	Septin-7	126.1	5.5	50.6
P48735	Isocitrate dehydrogenase [NADP], mitochondrial	185.7	6.6	50.9
P02679	Fibrinogen gamma chain	50.8	15.0	51.5
P02533	Keratin, type I cytoskeletal 14	741.2	22.3	51.5
Q01518	Adenylyl cyclase-associated protein 1	100.2	8.6	51.9
Q13203	Myosin-binding protein H	182.4	9.2	52.0
P10909	Clusterin	143.0	11.1	52.5
P20073	Annexin A7	134.1	4.9	52.7
P02774	Vitamin D-binding protein	58.5	7.4	52.9
P17661	Desmin	685.8	31.7	53.5
P08670	Vimentin	332.3	16.7	53.6
P30566	Adenylosuccinate lyase	32.6	4.6	54.9
P05155	Plasma protease C1 inhibitor	101.9	5.4	55.1
Q9UBF9	Myotilin	287.6	23.5	55.4
P02675	Fibrinogen beta chain	323.2	12.4	55.9
O60240	Perilipin-1	115.4	5.0	56.0
P54578	Ubiquitin carboxyl-terminal hydrolase 14	209.5	8.1	56.0
P05091	Aldehyde dehydrogenase, mitochondrial	113.5	4.8	56.3
P06576	ATP synthase subunit beta, mitochondrial	789.7	26.1	56.5
Q9UHG3	Prenylcysteine oxidase 1	467.9	12.5	56.6
P14618	Pyruvate kinase isozymes M1/M2	319.1	19.0	57.9
P13645	Keratin, type I cytoskeletal 10	2321.5	38.9	58.8
Q99832	T-complex protein 1 subunit eta	346.2	7.9	59.3
P25705	ATP synthase subunit alpha, mitochondrial	249.2	12.3	59.7
P04040	Catalase	196.9	4.7	59.7
P49368	T-complex protein 1 subunit gamma	150.3	6.2	60.5
Q9NZN4	EH domain-containing protein 2	119.6	3.3	61.1
P36871	Phosphoglucomutase-1	508.7	14.1	61.4
Q14195	Dihydropyrimidinase-related protein 3	214.0	4.0	61.9
P35527	Keratin, type I cytoskeletal 9	3369.8	54.4	62.0
P13647	Keratin, type II cytoskeletal 5	270.8	15.1	62.3
P23141	Liver carboxylesterase 1	159.4	7.9	62.5
O00499	Myc box-dependent-interacting protein 1	23.2	4.7	64.7
P35908	Keratin, type II cytoskeletal 2 epidermal	2452.8	48.4	65.4
P04264	Keratin, type II cytoskeletal 1	4620.4	53.0	66.0
O60662	Kelch-like protein 41	154.6	10.4	68.0
P02768	Serum albumin	1115.9	37.0	69.3
P08107	Heat shock 70 kDa protein 1A/1B	555.9	18.3	70.0

P49748	Very long-chain specific acyl-CoA dehydrogenase, mitochondrial	347.0	18.9	70.3
P11142	Heat shock cognate 71 kDa protein	378.3	14.6	70.9
P02545	Prelamin-A/C	44.3	3.0	74.1
Q15582	Transforming growth factor-beta-induced protein ig-h3	85.5	3.2	74.6
P08133	Annexin A6	427.3	15.3	75.8
O75112	LIM domain-binding protein 3	116.0	4.8	77.1
P40939	Trifunctional enzyme subunit alpha, mitochondrial	389.2	14.3	82.9
P08237	6-phosphofructokinase, muscle type	474.0	11.2	85.1
Q99798	Aconitate hydratase, mitochondrial	59.2	3.9	85.4
P06396	Gelsolin	232.1	5.9	85.6
P11217	Glycogen phosphorylase, muscle form	120.0	7.5	97.0
Q86TD4	Sarcalumenin	154.6	4.7	100.7
P35606	Coatomer subunit beta'	36.2	2.5	102.4
P35609	Alpha-actinin-2	1213.6	28.3	103.8
Q14697	Neutral alpha-glucosidase AB	95.1	2.2	106.8
O60763	General vesicular transport factor p115	30.0	4.2	107.8
P12110	Collagen alpha-2(VI) chain	36.4	2.0	108.5
Q02413	Desmoglein-1	49.7	3.2	113.7
Q13423	NAD(P) transhydrogenase, mitochondrial	91.0	4.3	113.8
P16615	Sarcoplasmic/endoplasmic reticulum calcium ATPase 2	518.8	9.1	114.7
P22314	Ubiquitin-like modifier-activating enzyme 1	148.2	4.3	117.8
Q00872	Myosin-binding protein C, slow-type	1075.3	16.6	128.2
Q9NQC3	Reticulon-4	170.8	2.4	129.9
Q96Q06	Perilipin-4	582.8	5.5	134.3
P01023	Alpha-2-macroglobulin	57.8	1.8	163.2
P54296	Myomesin-2	48.4	3.3	164.8
P35573	Glycogen debranching enzyme	145.7	2.4	174.7
Q9HBL0	Tensin-1	104.0	2.7	185.6
P01024	Complement C3	873.9	12.9	187.0
Q9UKX2	Myosin-2	2108.4	19.4	222.9
P12883	Myosin-7	4520.0	33.2	223.0
P35579	Myosin-9	96.0	2.5	226.4
P49327	Fatty acid synthase	130.7	1.0	273.3
Q86YZ3	Hornerin	239.0	2.5	282.2
Q14315	Filamin-C	53.2	1.2	290.8
P15924	Desmoplakin	110.7	0.7	331.6
P12111	Collagen alpha-3(VI) chain	655.6	5.7	343.5
Q15149	Plectin	151.3	1.9	531.5
Q09666	Neuroblast differentiation-associated protein AHNAK	74.1	3.5	628.7
P20929	Nebulin	668.9	5.7	772.4
Q8WZ42	Titin	615.2	0.7	3813.7

Band 13:

Accession	Description	Score	Coverage	MW [kDa]
P81605	Dermcidin	213.9	22.7	11.3
P01834	Ig kappa chain C region	331.8	32.1	11.6
P69905	Hemoglobin subunit alpha	230.3	19.0	15.2
P68871	Hemoglobin subunit beta	436.4	68.0	16.0
P02144	Myoglobin	137.8	28.6	17.2
P05976	Myosin light chain 1/3, skeletal muscle isoform	112.3	18.6	21.1
P08590	Myosin light chain 3	261.6	31.3	21.9
P07451	Carbonic anhydrase 3	86.0	20.8	29.5
P21796	Voltage-dependent anion-selective channel protein 1	220.0	33.6	30.8
O94760	N(G),N(G)-dimethylarginine dimethylaminohydrolase 1	110.7	13.0	31.1
P29692	Elongation factor 1-delta	398.9	36.3	31.1
Q13643	Four and a half LIM domains protein 3	29.0	7.1	31.2
P45880	Voltage-dependent anion-selective channel protein 2	468.9	32.3	31.5
Q9NP98	Myozenin-1	365.6	30.8	31.7
P45378	Troponin T, fast skeletal muscle	383.6	24.5	31.8
Q92629	Delta-sarcoglycan	317.6	15.9	32.1
O43396	Thioredoxin-like protein 1	101.7	11.1	32.2
Q15181	Inorganic pyrophosphatase	247.4	12.5	32.6
P09493	Tropomyosin alpha-1 chain	279.5	26.4	32.7
P07951	Tropomyosin beta chain	406.2	16.6	32.8
P13805	Troponin T, slow skeletal muscle	909.6	23.0	32.9
P06753	Tropomyosin alpha-3 chain	408.4	33.7	32.9
Q99623	Prohibitin-2	37.9	6.0	33.3
P20774	Mimecan	375.5	11.4	33.9
A6NDG6	Phosphoglycolate phosphatase	41.3	8.7	34.0
P50224	Sulfotransferase 1A3/1A4	35.6	6.1	34.2
P00387	NADH-cytochrome b5 reductase 3	84.2	8.0	34.2
Q16836	Hydroxyacyl-coenzyme A dehydrogenase, mitochondrial	205.6	30.6	34.3
P63244	Guanine nucleotide-binding protein subunit beta-2-like 1	296.3	17.4	35.1
P13804	Electron transfer flavoprotein subunit alpha, mitochondrial	377.1	31.5	35.1
Q9Y315	Putative deoxyribose-phosphate aldolase	182.3	21.7	35.2
P40926	Malate dehydrogenase, mitochondrial	1614.9	46.8	35.5
Q53FA7	Quinone oxidoreductase PIG3	67.8	8.7	35.5
P27695	DNA-(apurinic or apyrimidinic site) lyase	147.7	8.8	35.5
P67775	Serine/threonine-protein phosphatase 2A catalytic subunit alpha isoform	406.3	27.8	35.6
Q9UBQ7	Glyoxylate reductase/hydroxypyruvate reductase	53.6	8.2	35.6
P15121	Aldose reductase	68.1	6.0	35.8
P09525	Annexin A4	485.7	24.1	35.9
P08758	Annexin A5	35.7	5.9	35.9
P04406	Glyceraldehyde-3-phosphate dehydrogenase	429.2	26.6	36.0
P01857	Ig gamma-1 chain C region	103.0	18.5	36.1
P02649	Apolipoprotein E	929.4	36.6	36.1
P53597	Succinyl-CoA ligase [ADP/GDP-forming] subunit alpha, mitochondrial	222.4	22.8	36.2
Q13642	Four and a half LIM domains protein 1	1375.1	33.4	36.2
P13716	Delta-aminolevulinic acid dehydratase	164.7	25.5	36.3
P40925	Malate dehydrogenase, cytoplasmic	1251.8	35.0	36.4
P07195	L-lactate dehydrogenase B chain	402.0	25.2	36.6
P00338	L-lactate dehydrogenase A chain	577.3	28.6	36.7
Q9NUQ9	Protein FAM49B	187.8	23.5	36.7
Q04828	Aldo-keto reductase family 1 member C1	357.7	22.9	36.8
P36873	Serine/threonine-protein phosphatase PP1-gamma catalytic subunit	69.0	7.1	37.0
P62879	Guanine nucleotide-binding protein G(I)/G(S)/G(T) subunit beta-2	127.2	9.7	37.3
Q9UJ70	N-acetyl-D-glucosamine kinase	179.6	16.9	37.4
P21695	Glycerol-3-phosphate dehydrogenase [NAD(+)], cytoplasmic	306.7	14.6	37.5
Q9H2U2	Inorganic pyrophosphatase 2, mitochondrial	160.4	7.5	37.9
Q9H0P0	Cytosolic 5'-nucleotidase 3A	138.0	17.6	37.9
P07355	Annexin A2	1293.7	37.5	38.6
P04083	Annexin A1	1509.3	41.9	38.7
P04075	Fructose-bisphosphate aldolase A	906.2	37.9	39.4
O43488	Aflatoxin B1 aldehyde reductase member 2	139.7	8.6	39.6
P00325	Alcohol dehydrogenase 1B	387.5	21.3	39.8
Q9NZU5	LIM and cysteine-rich domains protein 1	198.6	15.3	40.8
P60712	Actin, cytoplasmic 1	1738.4	34.4	41.7
P68138	Actin, alpha skeletal muscle	3146.2	65.5	42.0
Q9NVD7	Alpha-parvin	299.5	11.8	42.2
P12277	Creatine kinase B-type	127.6	8.1	42.6
P06732	Creatine kinase M-type	699.7	29.7	43.1
Q9BXN1	Asporin	415.8	21.6	43.4
P51888	Prolargin	130.6	12.6	43.8
P00558	Phosphoglycerate kinase 1	60.5	7.2	44.6
P01009	Alpha-1-antitrypsin	74.5	7.4	46.7
P13929	Beta-enolase	165.8	10.1	47.0
P06733	Alpha-enolase	169.2	13.6	47.1
P22695	Cytochrome b-c1 complex subunit 2, mitochondrial	376.6	21.6	48.4
P15088	Mast cell carboxypeptidase A	129.1	5.5	48.6
P07437	Tubulin beta chain	121.6	8.8	49.6

Q9BQE3	Tubulin alpha-1C chain	147.6	18.0	49.9
P68104	Elongation factor 1-alpha 1	92.5	11.5	50.1
Q16181	Septin-7	87.8	8.5	50.6
P55084	Trifunctional enzyme subunit beta, mitochondrial	93.1	4.9	51.3
P02533	Keratin, type I cytoskeletal 14	2217.2	36.0	51.5
Q13203	Myosin-binding protein H	44.9	6.1	52.0
P17661	Desmin	638.9	28.7	53.5
O94919	Endonuclease domain-containing 1 protein	115.2	4.8	55.0
Q9UBF9	Myotilin	33.2	5.0	55.4
P02675	Fibrinogen beta chain	111.0	5.7	55.9
O60240	Perilipin-1	238.3	11.7	56.0
P30101	Protein disulfide-isomerase A3	312.3	8.3	56.7
Q16851	UTP--glucose-1-phosphate uridylyltransferase	76.9	6.9	56.9
P13645	Keratin, type I cytoskeletal 10	3898.1	38.9	58.8
P25705	ATP synthase subunit alpha, mitochondrial	123.1	6.0	59.7
P02538	Keratin, type II cytoskeletal 6A	415.1	21.6	60.0
Q9NZN4	EH domain-containing protein 2	116.3	3.7	61.1
P36871	Phosphoglucomutase-1	577.0	21.4	61.4
P35527	Keratin, type I cytoskeletal 9	3619.0	53.3	62.0
P13647	Keratin, type II cytoskeletal 5	826.6	32.2	62.3
Q5T749	Keratinocyte proline-rich protein	40.9	5.7	64.1
P35908	Keratin, type II cytoskeletal 2 epidermal	4151.5	54.3	65.4
P04264	Keratin, type II cytoskeletal 1	5439.2	52.6	66.0
O60662	Kelch-like protein 41	117.3	7.3	68.0
P02768	Serum albumin	766.0	27.4	69.3
P34931	Heat shock 70 kDa protein 1-like	229.1	10.6	70.3
P11142	Heat shock cognate 71 kDa protein	278.3	12.1	70.9
P11021	78 kDa glucose-regulated protein	248.4	12.2	72.3
P08133	Annexin A6	198.4	16.9	75.8
O75112	LIM domain-binding protein 3	681.8	15.3	77.1
P40939	Trifunctional enzyme subunit alpha, mitochondrial	459.1	8.4	82.9
P11217	Glycogen phosphorylase, muscle form	61.2	4.3	97.0
P02730	Band 3 anion transport protein	181.7	6.7	101.7
P12814	Alpha-actinin-1	519.2	12.2	103.0
P55786	Puromycin-sensitive aminopeptidase	45.1	2.3	103.2
P35609	Alpha-actinin-2	1253.5	29.9	103.8
O43707	Alpha-actinin-4	447.4	13.0	104.8
Q02413	Desmoglein-1	60.1	4.4	113.7
P16615	Sarcoplasmic/endoplasmic reticulum calcium ATPase 2	528.6	12.5	114.7
Q02218	2-oxoglutarate dehydrogenase, mitochondrial	30.0	2.5	115.9
Q00872	Myosin-binding protein C, slow-type	595.5	8.0	128.2
Q9NQC3	Reticulon-4	248.3	2.4	129.9
Q96Q06	Perilipin-4	253.9	3.5	134.3
P01023	Alpha-2-macroglobulin	113.1	4.8	163.2
P54296	Myomesin-2	115.4	1.4	164.8
Q9HBL0	Tensin-1	154.2	1.9	185.6
Q9UKX2	Myosin-2	1453.3	14.7	222.9
P12883	Myosin-7	3094.6	28.9	223.0
P15924	Desmoplakin	183.8	1.7	331.6
P12111	Collagen alpha-3(VI) chain	469.7	3.6	343.5
P20929	Nebulin	339.7	3.0	772.4
Q8WZ42	Titin	249.4	0.5	3813.7

Band 14:

Accession	Description	Score	Coverage	MW [kDa]
P81605	Dermcidin	109.8	20.0	11.3
P62805	Histone H4	51.0	17.5	11.4
P01834	Ig kappa chain C region	314.2	32.1	11.6
P69905	Hemoglobin subunit alpha	236.9	19.0	15.2
P68871	Hemoglobin subunit beta	443.1	53.7	16.0
P08590	Myosin light chain 3	192.4	19.5	21.9
P55083	Microfibril-associated glycoprotein 4	35.5	4.7	28.6
P00915	Carbonic anhydrase 1	155.0	8.8	28.9
P07451	Carbonic anhydrase 3	71.2	11.9	29.5
O15400	Syntaxin-7	135.2	9.6	29.8
Q9NPC6	Myozenin-2	451.5	35.6	29.9
Q9Y277	Voltage-dependent anion-selective channel protein 3	140.0	7.4	30.6
P21796	Voltage-dependent anion-selective channel protein 1	1619.4	61.8	30.8
P60174	Triosephosphate isomerase	49.5	8.7	30.8
P29692	Elongation factor 1-delta	41.2	12.8	31.1
P47756	F-actin-capping protein subunit beta	615.4	30.0	31.3
P10768	S-formylglutathione hydrolase	271.1	17.4	31.4
P48739	Phosphatidylinositol transfer protein beta isoform	77.9	14.0	31.5
P45880	Voltage-dependent anion-selective channel protein 2	184.5	32.3	31.5
Q9NP98	Myozenin-1	657.5	41.1	31.7
Q00169	Phosphatidylinositol transfer protein alpha isoform	34.8	11.9	31.8
P45378	Troponin T, fast skeletal muscle	218.8	15.2	31.8
O43396	Thioredoxin-like protein 1	77.7	12.8	32.2
P07951	Tropomyosin beta chain	152.5	12.7	32.8
P13805	Troponin T, slow skeletal muscle	895.3	26.3	32.9
P06753	Tropomyosin alpha-3 chain	148.1	11.6	32.9
P36542	ATP synthase subunit gamma, mitochondrial	69.2	7.4	33.0
P54920	Alpha-soluble NSF attachment protein	33.1	7.5	33.2
Q99623	Prohibitin-2	166.2	11.7	33.3
P20774	Mimecan	149.9	9.1	33.9
Q9UHQ9	NADH-cytochrome b5 reductase 1	472.0	25.6	34.1
P00387	NADH-cytochrome b5 reductase 3	884.3	31.9	34.2
O15144	Actin-related protein 2/3 complex subunit 2	25.9	8.0	34.3
P31937	3-hydroxyisobutyrate dehydrogenase, mitochondrial	212.7	19.6	35.3
P40926	Malate dehydrogenase, mitochondrial	182.0	13.6	35.5
O75208	Ubiquinone biosynthesis protein COQ9, mitochondrial	28.7	9.4	35.5
Q13011	Delta(3,5)-Delta(2,4)-dienoyl-CoA isomerase, mitochondrial	368.9	15.2	35.8
P09525	Annexin A4	611.1	16.9	35.9
P08758	Annexin A5	967.8	33.4	35.9
P04406	Glyceraldehyde-3-phosphate dehydrogenase	489.1	26.6	36.0
Q16698	2,4-dienoyl-CoA reductase, mitochondrial	87.5	13.7	36.0
Q13642	Four and a half LIM domains protein 1	690.3	22.9	36.2
P40925	Malate dehydrogenase, cytoplasmic	76.9	8.1	36.4
P07195	L-lactate dehydrogenase B chain	914.2	28.7	36.6
P00338	L-lactate dehydrogenase A chain	386.6	9.3	36.7
P21695	Glycerol-3-phosphate dehydrogenase [NAD(+)], cytoplasmic	54.9	6.9	37.5
P07355	Annexin A2	669.8	24.5	38.6
P04083	Annexin A1	195.8	12.7	38.7
Q53GG5	PDZ and LIM domain protein 3	119.4	9.1	39.2
P11177	Pyruvate dehydrogenase E1 component subunit beta, mitochondrial	67.9	7.5	39.2
P04075	Fructose-bisphosphate aldolase A	567.1	31.3	39.4
P60712	Actin, cytoplasmic 1	736.0	31.5	41.7
Q99536	Synaptic vesicle membrane protein VAT-1 homolog	44.7	8.1	41.9
P68138	Actin, alpha skeletal muscle	1776.3	49.6	42.0
P06732	Creatine kinase M-type	741.3	24.7	43.1
Q9BXN1	Asporin	377.0	16.8	43.4
P51888	Prolargin	69.3	6.5	43.8
P00558	Phosphoglycerate kinase 1	154.3	14.6	44.6
P31415	Calsequestrin-1	123.1	9.3	45.1
P01009	Alpha-1-antitrypsin	181.8	14.1	46.7
P13929	Beta-enolase	193.9	13.4	47.0
Q04695	Keratin, type I cytoskeletal 17	480.5	14.1	48.1
P22695	Cytochrome b-c1 complex subunit 2, mitochondrial	356.6	26.5	48.4
P07437	Tubulin beta chain	290.8	13.3	49.6
P68104	Elongation factor 1-alpha 1	85.9	11.9	50.1
Q9P2R7	Succinyl-CoA ligase [ADP-forming] subunit beta, mitochondrial	73.3	6.3	50.3
P48735	Isocitrate dehydrogenase [NADP], mitochondrial	85.3	8.6	50.9
P08779	Keratin, type I cytoskeletal 16	1171.5	40.4	51.2
P02679	Fibrinogen gamma chain	85.1	17.0	51.5

P02533	Keratin, type I cytoskeletal 14	1383.4	34.1	51.5
Q13203	Myosin-binding protein H	350.9	18.7	52.0
P17661	Desmin	219.2	12.6	53.5
P06576	ATP synthase subunit beta, mitochondrial	86.3	9.1	56.5
Q16851	UTP--glucose-1-phosphate uridylyltransferase	687.8	15.9	56.9
P13645	Keratin, type I cytoskeletal 10	2476.5	32.2	58.8
P02538	Keratin, type II cytoskeletal 6A	1006.9	31.6	60.0
P04259	Keratin, type II cytoskeletal 6B	1100.0	29.8	60.0
P36871	Phosphoglucomutase-1	117.8	10.1	61.4
P35527	Keratin, type I cytoskeletal 9	1115.7	33.9	62.0
P13647	Keratin, type II cytoskeletal 5	449.1	23.4	62.3
P35908	Keratin, type II cytoskeletal 2 epidermal	2518.1	44.9	65.4
P04264	Keratin, type II cytoskeletal 1	3573.9	44.1	66.0
P02768	Serum albumin	400.5	15.3	69.3
P08107	Heat shock 70 kDa protein 1A/1B	293.6	16.7	70.0
P11142	Heat shock cognate 71 kDa protein	213.0	12.1	70.9
O75112	LIM domain-binding protein 3	535.9	14.2	77.1
P40939	Trifunctional enzyme subunit alpha, mitochondrial	166.5	6.2	82.9
P11217	Glycogen phosphorylase, muscle form	80.3	3.4	97.0
P35609	Alpha-actinin-2	1476.9	22.7	103.8
P16615	Sarcoplasmic/endoplasmic reticulum calcium ATPase 2	390.3	8.9	114.7
Q00872	Myosin-binding protein C, slow-type	86.7	2.5	128.2
Q96Q06	Perilipin-4	422.4	4.1	134.3
P54296	Myomesin-2	69.5	1.7	164.8
Q9UKX2	Myosin-2	1031.0	9.7	222.9
P12883	Myosin-7	2534.8	22.5	223.0
P12111	Collagen alpha-3(VI) chain	209.2	2.4	343.5
P20929	Nebulin	98.7	1.9	772.4
Q8WZ42	Titin	85.1	0.1	3813.7

Band 15:

Accession	Description	Score	Coverage	MW [kDa]
P35609	Alpha-actinin-2	1889,67	25,95	103,8
Q14697	Neutral alpha-glucosidase AB	79,55	2,22	106,8
P81605	Dermcidin	174,10	20,00	11,3
Q02413	Desmoglein-1	87,76	3,15	113,7
Q13423	NAD(P) transhydrogenase, mitochondrial	212,96	7,55	113,8
Q02218	2-oxoglutarate dehydrogenase, mitochondrial	153,22	4,79	115,9
Q14896	Myosin-binding protein C, cardiac-type	837,77	13,50	140,7
P61626	Lysozyme C	186,43	14,19	16,5
P54296	Myomesin-2	280,34	4,64	164,8
P52179	Myomesin-1	480,42	4,09	187,5
P12883	Myosin-7	10084,34	41,29	223,0
Q5D862	Filaggrin-2	339,51	2,97	247,9
Q86YZ3	Hornerin	411,26	13,75	282,2
Q14315	Filamin-C	673,25	4,33	290,8
P15924	Desmoplakin	65,58	1,81	331,6
P12111	Collagen alpha-3(VI) chain	45,75	1,23	343,5
P01876	Ig alpha-1 chain C region	430,80	16,43	37,6
Q8WZ42	Titin	2173,28	2,04	3813,7
P62739	Actin, aortic smooth muscle	435,37	29,44	42,0
P06732	Creatine kinase M-type	90,96	12,34	43,1
O95810	Serum deprivation-response protein	92,39	7,76	47,1
P01011	Alpha-1-antichymotrypsin	520,67	17,73	47,6
P48735	Isocitrate dehydrogenase [NADP], mitochondrial	138,16	6,64	50,9
P08779	Keratin, type I cytoskeletal 16	1039,58	23,68	51,2
P02533	Keratin, type I cytoskeletal 14	1220,21	32,63	51,5
P17661	Desmin	212,09	10,00	53,5
P08670	Vimentin	525,25	7,94	53,6
P06576	ATP synthase subunit beta, mitochondrial	61,14	7,37	56,5
P14618	Pyruvate kinase isozymes M1/M2	210,48	12,24	57,9
P13645	Keratin, type I cytoskeletal 10	4135,41	39,55	58,8
P21397	Amine oxidase [flavin-containing] A	160,35	14,23	59,6
P02538	Keratin, type II cytoskeletal 6A	546,42	23,58	60,0
P10809	60 kDa heat shock protein, mitochondrial	1549,85	32,29	61,0
Q9NZN4	EH domain-containing protein 2	85,81	6,08	61,1
Q9H223	EH domain-containing protein 4	76,42	4,44	61,1
P36871	Phosphoglucomutase-1	764,97	18,33	61,4
Q7Z794	Keratin, type II cytoskeletal 1b	621,38	7,09	61,9
P35527	Keratin, type I cytoskeletal 9	2201,57	39,33	62,0
Q15124	Phosphoglucomutase-like protein 5	86,34	4,76	62,2
P13647	Keratin, type II cytoskeletal 5	930,89	28,64	62,3
Q16555	Dihydropyrimidinase-related protein 2	111,23	4,55	62,3
P35908	Keratin, type II cytoskeletal 2 epidermal	4698,95	48,67	65,4
P04264	Keratin, type II cytoskeletal 1	5558,35	46,89	66,0
Q7Z3D6	UPF0317 protein C14orf159, mitochondrial	565,16	11,69	66,4
O95831	Apoptosis-inducing factor 1, mitochondrial	141,02	12,07	66,9
P27824	Calnexin	455,98	10,47	67,5
P26038	Moesin	34,76	4,85	67,8
Q16134	Electron transfer flavoprotein-ubiquinone oxidoreductase, mitochondrial	331,55	9,24	68,5
P02768	Serum albumin	1729,59	16,09	69,3
P08107	Heat shock 70 kDa protein 1A/1B	156,06	8,58	70,0
P49748	Very long-chain specific acyl-CoA dehydrogenase, mitochondrial	1622,59	37,40	70,3
P38646	Stress-70 protein, mitochondrial	299,22	12,52	73,6
P02545	Prelamin-A/C	71,67	4,22	74,1
P21980	Protein-glutamine gamma-glutamyltransferase 2	82,31	4,95	77,3
P14923	Junction plakoglobin	173,68	6,58	81,7
P40939	Trifunctional enzyme subunit alpha, mitochondrial	459,10	11,01	82,9
P08238	Heat shock protein HSP 90-beta	386,83	11,74	83,2
Q99798	Aconitate hydratase, mitochondrial	668,43	11,92	85,4
Q9Y4W6	AFG3-like protein 2	86,68	2,38	88,5

Validation of semiautomated strain analysis

Strain measurements can be done by TDI or speckle tracking as outlined in section 2.2.4. Speckle tracking is a newer technique, has the advantage of better reproducibility and needs only a small fraction of time compared to TDI strain analysis, which is rather cumbersome because it requires manual placement of a region of interest and manual correction over the cardiac cycle. However, speckle tracking requires high quality grey scale images that were not acquired in the baseline examination, whereas TDI data was obtained. This prompted the use of a semiautomatic approach, which would facilitate TDI strain data acquisition. This method had to be newly adapted using an existing function of the EchoPAC software (GE Healthcare, Chicago, USA) (**Supplementary figure 7**). Feasibility and comparability of this method (TDI-ST) was proven by reanalysing TDI recordings with existing manual analysis (TDI-manual).[38]

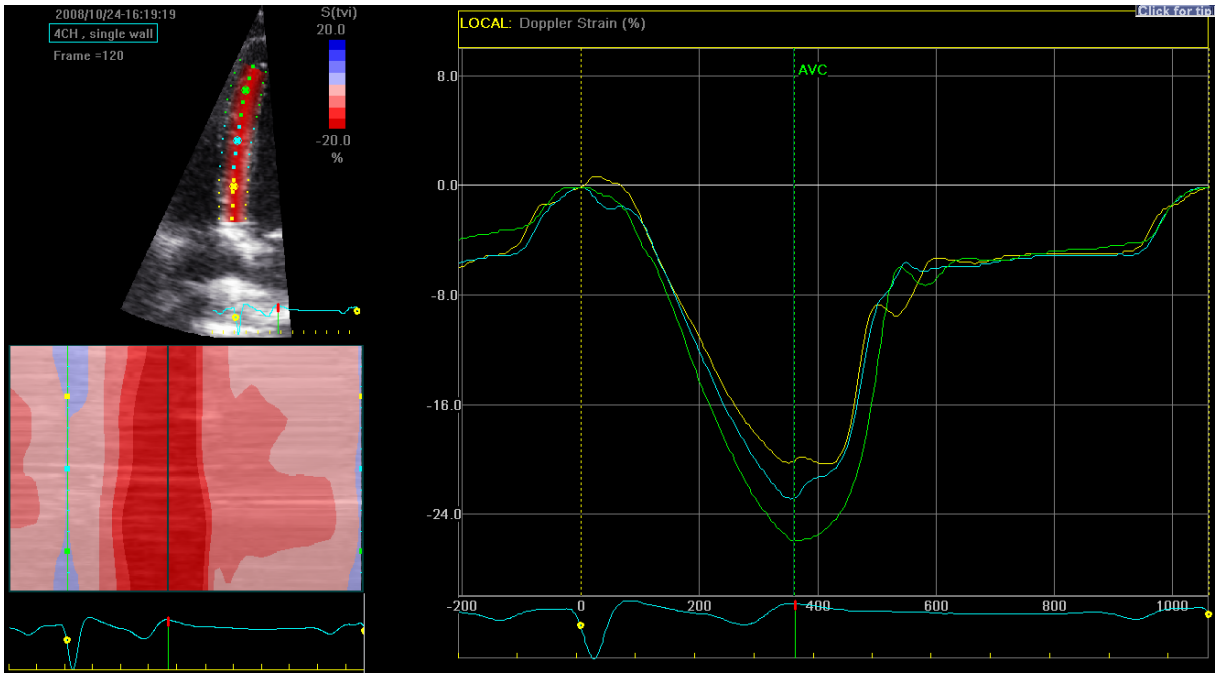

Supplementary figure 7: EchoPAC user interface, TDI-ST strain analysis. Each myocardial wall was analysed separately to enable a narrow sector and higher frame rate.

Forty healthy subjects (mean age 38.3±12.8 years) and 16 patients with FHL1 cardiomyopathy (CMP) (36.8±14.2 years) were analysed with TDI-manual and TDI-ST. TDI-ST was performed with commercial software (EchoPAC, GE Healthcare, Chicago, US), using speckle-tracking for myocardial tracking and TDI information to derive longitudinal strain and SR from high frame rate TDI recordings. Measurements of longitudinal systolic

strain (S) and global S (GLS) made with the two methods were compared with Bland Altman plots and Deming regression.

Mean S was -20.11±4.85% (healthy) and -16.12±4.44% (CMP) with TDI-ST and -21.15±5.68% (healthy) and -16.27±6.44 (CMP) with TDI-manual (**Supplementary table 2**). Using all measured segments, mean bias was 0.78 % strain towards less negative S with TDI-ST (**Supplementary figure 8**); Deming regression slope was 0.7 for S and 0.9 for GLS (**Supplementary figure 9**). Intra- and inter-observer CVs were 5.4% and 7.0%, respectively.

Overall parameters showed acceptable comparability, and especially GLS was well comparable between the two methods.

Supplementary table 2: Mean ± standard deviation of TDI-ST and TDI-manual derived parameters. Differences between methods including all segments of healthy subjects were statistically significant ($p<0.05$) for all parameters. S, peak systolic S; SR_S, peak systolic SR; SR_E, early diastolic SR; SR_A, late diastolic SR; n, number of segments. (Reproduced from [38] with permission of publisher)

	TDI-ST				TDI-manual			
	S (%)	**SR_S (1/s)**	**SR_E (1/s)**	**SR_A (1/s)**	**S (%)**	**SR_S (1/s)**	**SR_E (1/s)**	**SR_A (1/s)**
Healthy (n = 602)	-20.11 ±4.85	-1.19 ±0.37	2.27 ±0.96	1.40 ±0.62	-21.15 ±5.68	-1.27 ±0.45	1.99 ±0.92	1.28 ±0.68
Basal	-19.82 ±4.93	-1.26 ±0.41	2.52 ±1.08	1.38 ±0.62	-20.98 ±5.82	-1.31 ±0.42	2.13 ±1.05	1.33 ±0.69
Mid	-19.54 ±4.39	-1.09 ±0.33	1.99 ±0.78	1.27 ±0.53	-20.40 ±5.08	-1.16 ±0.40	1.78 ±0.76	1.14 ±0.62
Apical	-21.02 ±5.12	-1.22 ±0.36	2.33 ±0.94	1.57 ±0.67	-22.14 ±6.04	-1.36 ±0.49	2.09 ±0.90	1.36 ±0.72
FHL1-CMP (n=244)	-16.12 ±4.44	-1.03 ±0.30	1.46 ±0.64	1.06 ±0.48	-16.27 ±6.44	-1.08 ±0.46	1.39 ±0.79	0.97 ±0.57

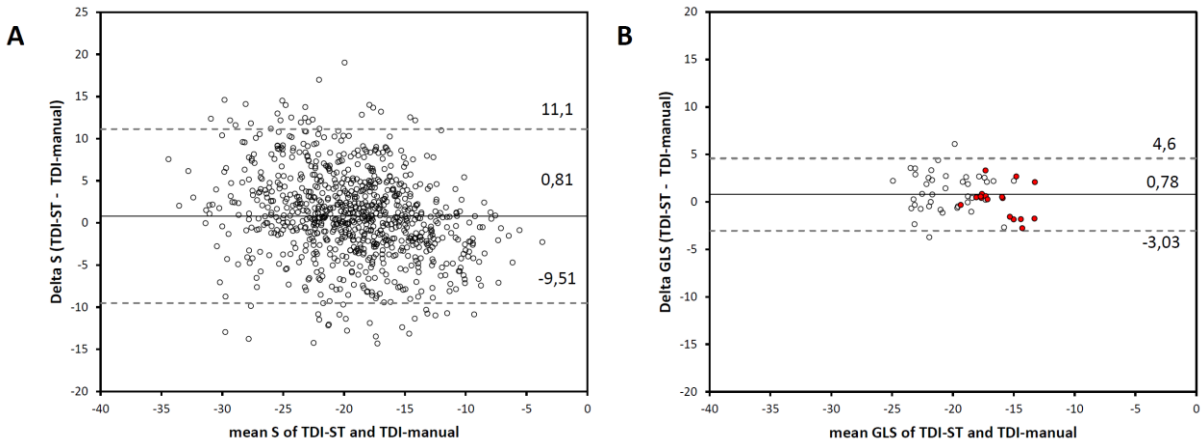

Supplementary figure 8: Bland Altman plots showing mean and difference of TDI-ST and TDI-manual S for each measured segment (**A**) and GLS for each patient (**B**). Filled dots show mutation carriers. Mean difference and 95%-interval are shown as horizontal lines. (Reproduced from [38] with permission of publisher)

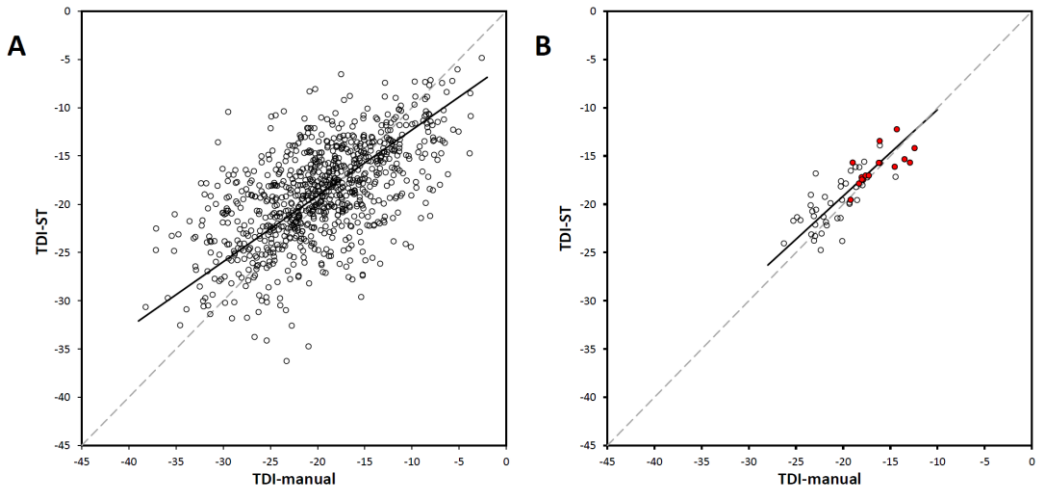

Supplementary figure 9: Scatterplots comparing S by TDI-ST and TDI-manual for each measured segment (**A**) and GLS for each patient (**B**). Filled dots show mutation carriers. Deming regression lines (A: slope=0.7, intercept=-5.4; B: slope=0.9, intercept=-1.2) and a dashed 45° line are shown. (Reproduced from [38] with permission of publisher)